

TREATMENT VERIFICATION IN RADIATION ONCOLOGY

PORTAL IMAGING IN CLINICAL PRACTICE

Uitgeverij Eburon
Postbus 2867, 2601 CW Delft
info@eburon.nl

ISBN 90 5166 6489

Copyright: C.L. Creutzberg, 1998

All rights reserved. No part of this publication may be reproduced, stored in a retrieval system, or transmitted, in any form or by any means, electronic, mechanical, photocopying, recording, or otherwise, without the prior written permission of the author.

TREATMENT VERIFICATION IN RADIATION ONCOLOGY

PORTAL IMAGING IN CLINICAL PRACTICE

VERIFICATIE VAN DE BEHANDELING IN DE RADIOTHERAPIE

KLINISCHE TOEPASSING VAN MEGAVOLTAFBEELDINGEN

PROEFSCHRIFT

ter verkrijging van de graad van doctor
aan de Erasmus Universiteit Rotterdam
op gezag van de Rector Magnificus
Prof. dr P.W.C. Akkermans M.A.
en volgens besluit van het College voor Promoties.
De openbare verdediging zal plaatsvinden op
vrijdag 2 oktober 1998 om 13.30 uur

door

Caroline Laurette Creutzberg

geboren te Leiderdorp

PROMOTIECOMMISSIE

Promotor Prof. dr P.C. Levendag

Co-promotor Dr A.G. Visser

Overige leden	Prof. dr J.J. Broerse
	Prof. dr B. Löwenberg
	Prof. dr W. De Neve

CONTENTS

1	Quality control and treatment verification in radiotherapy	3
1.1	Introduction	5
1.2	Quality assurance in radiotherapy	8
1.3	Consequences of dose variations in the target volume	9
1.4	Clinical consequences of underdosing in the field margins	12
1.5	The reproducibility of patient positioning	13
1.6	Types of errors and interpretation of error rates	15
1.7	From portal films to electronic portal imaging devices	16
2	Accuracy of patient positioning in mantle field irradiation	21
3	Quality assurance using portal imaging: the accuracy of patient positioning in irradiation of breast cancer	37
4	A quality control study of the accuracy of patient positioning in irradiation of pelvic fields	61
5	High-precision prostate cancer irradiation by clinical application of an off-line patient setup verification procedure, using portal imaging	87
6	General discussion, conclusions and implications for future work	115
6.1.	Patient positioning studies	117
6.2.	Implications for clinical practice	122
6.3.	Recent developments and present EPI use in the DDHCC	133
6.4.	Drawbacks in the introduction and use of EPID	134
6.5.	Conclusions and recommendations	138
	Bibliography	141
	Summary	157
	Samenvatting	161
	Dankwoord	167
	Curriculum vitae	169

CHAPTER 1

QUALITY CONTROL AND TREATMENT VERIFICATION IN RADIOTHERAPY

1.1. Introduction

In radiation oncology, the treatment aims include cure of cancer (curative radiotherapy), a prolongation of the progression- or symptom free interval, and/or the palliation of symptoms (palliative radiotherapy). In the curative setting, the purpose of radiotherapy is to eradicate a patient's cancer, while preserving normal anatomy and function. Ideally, this would be achieved by treating the tumor volume to a radiation dose offering a maximum probability of tumor control, without causing damage to the surrounding healthy tissue. Realistically, however, the dose level will be chosen as a result of balancing the probability of tumor control and the risk of serious complications, thus accepting a certain level of minor complaints and a small risk of major complications.

The radiation oncologist defines the target volume to be irradiated from the known tumor extension and/or the tissues at risk of containing tumor cells (subclinical disease), which is called the clinical target volume (CTV) (61). A margin is then added to compensate for the effects of organ and patient movement and inaccuracies in beam and patient setup: the planning target volume (PTV). The radiotherapy treatment fields are planned tightly around the PTV, in order to ensure treatment of the PTV to a high dose, while reducing the dose delivered to the surrounding normal tissues. The volume in the patient which will receive $\geq 95\%$ of the prescribed dose is called the treated volume, which ideally matches the PTV closely. The volume which will receive a dose that is considered significant in relation to normal tissue tolerance is called the irradiated volume (61). Often the 20% or 30% dose level is chosen to represent the irradiated volume.

The radiation which is delivered to a target volume in a patient causes damage to the DNA in the constituent cells of the tissues within the target volume. The DNA contains the genetic information of the cells. Prior to a cell division, the DNA of the cell is duplicated. If the DNA is damaged, its duplication is impeded, and cell death ensues at a subsequent cell division. This is particularly the case for damage inflicted to both strands of the DNA helix, so-called double strand breaks. Normal tissues are able to repair most of the sublethal damage inflicted to its DNA, while delaying cell division until the DNA is repaired. In general, the repair capacity of tumors is less than that of most normal tissues. To make use of the differences between normal tissues and tumors, the total

radiation dose is usually given in a so-called fractionated treatment: a course of radiotherapy, consisting of a large number of short daily treatments delivering a small radiation dose, conventionally with a 24 hour interval between the treatments. Such fractionation spares normal tissues because of repair of sublethal damage in the interval between the treatment fractions. At the same time fractionation can result in higher tumor cell kill because of reoxygenation and redistribution of cells into radiosensitive phases of the cell cycle (49). The differences in radiation sensitivity and fractionation sensitivity between the tumor and its surrounding normal tissues determine if the dose, required for tumor control, can be safely delivered.

In practice, the radiation oncologist designs a treatment plan for a patient based on the characteristics of the patient and the specific tumor type, the tumor site, and additional factors such as preceding treatment (e.g. surgery), the pathology report, radiological findings, etc. Usually, a curative radiation treatment consists of 25-35 daily fractions. In the preparatory phase, the treatment fields are simulated and treatment planning is carried out. A simple treatment plan consists, for example, of two parallel opposed beams. More often, multiple beams are used to restrict the high dose area to the area immediately surrounding the tumor. Modern computer planning systems enable three-dimensional (3D) treatment planning using computed tomography (CT) scans to design individually shaped treatment fields tightly planned around the PTV. This treatment technique, using individually shaped fields conformed to the specific tumor volume with maximum sparing of the surrounding normal tissues, is called conformal therapy. Its benefits can be used in two ways: either to reduce the risk of normal tissue complications without reduction of the tumor control probability, or to escalate the dose to increase cure rates, without increasing complication rates.

At the time of simulation, the position of the treatment fields is defined and radiographs are taken of the treatment fields for documentation. The isocenter of the fields is marked onto the patient's skin, as well as longitudinal and lateral reference lines for precise positioning. Depending on the treatment technique chosen, simulation either precedes or follows treatment planning. In case of CT scan planning, in some instances digitally reconstructed radiographs (DRR) of the treatment fields can be produced which obviate the need for physical simulation (so-called virtual simulation; see also Chapter 6, section 6.2). In that

case, definitive isocenter marking is carried out at the CT unit. All individual treatment data (including the treatment field characteristics such as field width and length, gantry angle, and wedges, as well as the details of patient positioning such as the immobilization device used) are noted on the patient treatment chart and entered into the patient's computer file. At the treatment unit, the daily radiation treatments are given. After careful patient setup, the prescribed fraction dose is delivered, which takes only a few minutes. These 25-35 daily treatments are usually given on weekdays during five to seven weeks (Fig. 1).

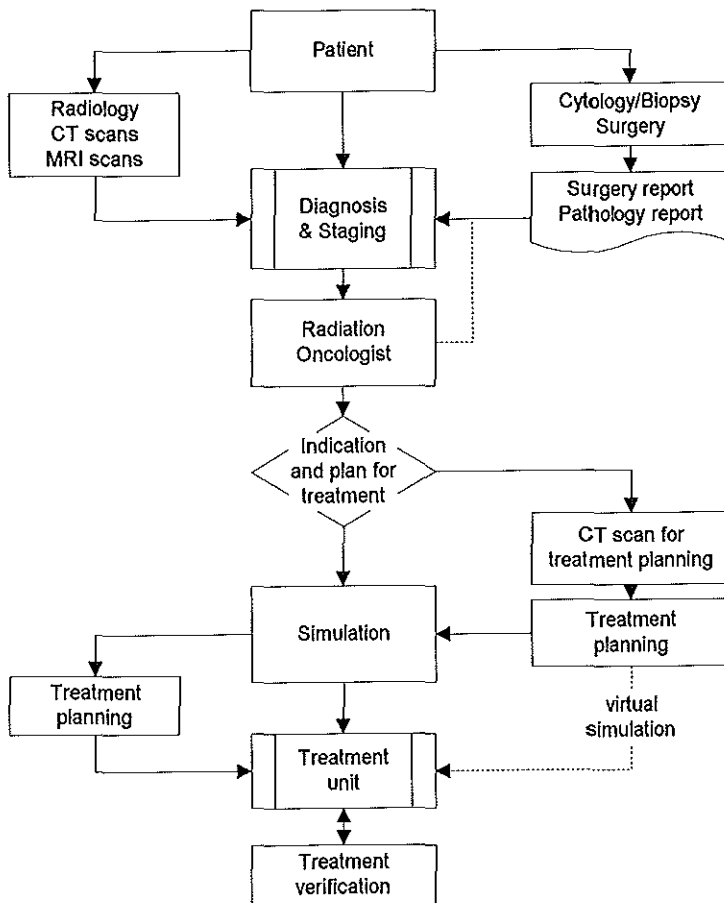


Figure 1. The process of radiotherapy. The radiation oncologist decides on the indication for treatment and designs a treatment plan. Treatment simulation and planning is carried out, followed by the daily delivery of radiation treatments at the treatment unit.

1.2. Quality assurance in radiotherapy

In today's practice of radiotherapy it is essential to have a quality assurance program monitoring all steps in the chain between the first patient contact to the last treatment session. It is common practice to have regular quality control procedures for the treatment units and simulators. The verification of daily patient treatment includes the monitoring of the accuracy of the delivered dose (in vivo dosimetry) and of the accuracy of patient positioning.

In Dutreix's noteworthy lecture "When and how can we improve precision in radiotherapy?" (33) the various stages of the radiotherapy planning and treatment procedure are described, together with the responsible specialists, the sources of errors in each stage of the process and the level of accuracy to achieve. It is clear that the achievement of accuracy in radiotherapy requires a multidisciplinary effort which can best be accomplished by a dedicated team of radiation oncologists, physicists, and radiotherapy technicians. The prescription of the dose to be delivered and the determination of the target volume to be treated are responsibilities of the radiation oncologist. The exact delivery of that dose to a reference point, the homogeneity of the dose distribution, the number of monitor units to set for each field, and the day-to-day reproducibility of patient setup are to a great extent the shared responsibility of radiation oncologists, physicists and technicians.

The introduction of computers into radiotherapy planning and treatment has enabled precise monitoring of many aspects of the daily delivery of radiation treatment. For example, the calculation of dose distributions for complicated treatment plans has become reproducible within narrow and known limits. Record-and-verify systems ensure the precise monitoring of machine parameters such as couch position, gantry angle and collimator rotation. At the same time, 3D computer planning systems and linear accelerators equipped with multileaf collimators have become available which enable conformal therapy. The development of conformal therapy has led to the design of treatment schedules using dose escalation, aimed at the improvement of cure rates without increasing the complication rates. It is obvious that for such schedules, exact daily patient positioning is an absolute prerequisite. Thus, the verification of patient setup has rapidly become an area of clinical importance.

1.3. Consequences of dose variations in the target volume

Wambersie *et al.* (127,128) and Herring and Compton (52) set the level of accuracy required in the dose delivered in radiotherapy at 5% (1 SD). Brahme (19) stated that the relative standard variation of the mean dose in the target volume should be less than 5%, and preferably 3%. Mijnheer *et al.* (84) proposed a standard requirement that the uncertainty in absorbed dose should not exceed 3.5% (1 SD). What is the biological basis of the requirement of this level of precision?

The relationship between the surviving fraction of cells after irradiation, and the radiation dose delivered, is described by the cell survival curve. Such a survival curve shows a logarithmic reduction of cells in response to a (linear) increase in dose. From the survival curve of its constituent cells, the response of a tumor or an organ to irradiation (the dose response curve) can be estimated. The survival curve of the cells in experimental conditions represents an over-estimation of the tumor response to a certain radiation dose in the patient: in treatment conditions, many factors influence the response, such as the number of proliferative and quiescent cells, the presence of hypoxic areas in the tumor, accelerated repopulation, etc. The probability of complete tumor cell kill after a given radiation dose is called the tumor control probability (TCP). In the steep part of the dose response curve, i.e. from about 20-70% TCP, the response is an almost linear function of the total absorbed dose. The slope of this function - the response gradient γ - describes the expected increase in tumor control probability for a given relative increase in absorbed dose. A dose increase of 1% on the linear part of the dose response curve (i.e. at the dose level where a TCP of 50% is obtained) will result in an increase in tumor control probability of γ %. The steeper the slope, the more effect a minor dose variation will have on the tumor control probability. Many authors have estimated dose response curves for the probability of tumor control for various tumor types. Usually, they found steep dose response curves (4,84). However, these dose response curves were mostly determined for small patient groups. In practice, the dose response curves turn out to be much more shallow, due to factors such as overall treatment time, inter- and intratumoral variation of intrinsic radiation sensitivity, and other sources of heterogeneity in larger patient groups. Okunieff *et al.* (90) gave an excellent overview of the dose response data which are available in the

literature. A wide range of values for γ was found. Most gamma values were in the range of 0.5 - 4.5, with a median of around 1. They concluded that the slope of the dose response curve calculated from combined clinical data is shallow, with typical γ values of approximately 1. Such shallow dose response curves were also found in studies conducted at the DDHCC¹ in head and neck tumor sites. Levendag *et al.* (55,69-72) found that significant dose response relations could only be obtained if a correction for treatment related factors was applied. A corrected biological effective dose (BEDcor₁₀) was used instead of the absolute dose, taking into account factors such as the overall treatment time, the dose per fraction and the number of fractions, while making assumptions for the potential doubling time of the tumor cells (T_{pot}) and the α/β ratio (the fractionation sensitivity of the tumor). The dose response curves thus obtained were shallow, with γ ranging from 0.6 to 1.

The steepness of the dose response curve reflects the consequences that dose variations in the target volume may have on treatment outcome. This is illustrated by the findings of Goitein and Busse (44). They calculated the potential reduction in tumor control probability resulting from treatment errors for carcinoma of the supraglottic larynx (steep dose response curve) and for Hodgkin's disease (rather shallow dose response curve). Immobilization errors (IE) were defined as displacements of the treatment fields relative to the intended treatment volume, resulting in a reduction of the total dose delivered to the margins of the field. The consequences of IE, in terms of the reduction of the TCP, turned out to depend strongly on the steepness of the dose response curve at the dose level applied. For supraglottic cancer, 36% random IE of 5 mm at a dose level of 66 Gy were estimated to result in a reduction of TCP of 12%. For 74 Gy the TCP reduction would be 10%. In contrast, for Hodgkin's disease 36% IE of 1 cm would cause a reduction of TCP of only 0.3%. This is due to the shallow dose response curve for Hodgkin's disease, and the fact that the considered dose (44 Gy) is already in the very shallow most upper portion of the dose response curve.

The effect of the actual (nonuniform) dose distribution in a target volume on

¹ Since the merger of the Daniel den Hoed Cancer Center and the University Hospital Rotterdam in 1995, its full name is University Hospital Rotterdam/Daniel den Hoed Cancer Center. Throughout this thesis it will in short be referred to as DDHCC.

the response of tumors was investigated by Brahme (19), Goitein (43) and Niemierko (89). An effective dose D_{eff} was defined which, for a given γ , if delivered uniformly to the target volume, would result in the same TCP as the actual nonuniform dose distribution. For modest nonuniformities of dose, D_{eff} would be closely approximated by the average dose, being in fact somewhat less than the average dose, as D_{eff} is a function of the average dose, its standard deviation and γ (19,43). The larger the dose variations in the target volume and the steeper the dose effect curve, the lower D_{eff} and, consequently, the TCP will be. For this reason, Brahme concluded that the relative standard deviation of the mean dose in the target volume should be less than 5%, and even as small as 3% in cases where the dose response curve is very steep ($\gamma > 3$). Niemierko (89) introduced the concept of Effective Uniform Dose (EUD), which uses the cellular radiation sensitivity (represented by the fraction of clonogens surviving a dose of 2 Gy) instead of γ to calculate an equivalent dose. The (retrospective) application of the EUD concept to a clinical dataset revealed a significant variation in the doses actually delivered as compared to the prescribed doses. This shows that prescribed doses do not always represent the doses actually (and radiobiologically) delivered, which may be one of the causes of the flattening of dose-response curves in clinical studies.

Dose effect curves for normal tissue complications are generally reported to be steeper than those for tumor control (84). The probability for most normal tissue reactions raises from 25 to 50% for a relative dose increase varying between 4 and 10%, implying γ values ranging from 2.5 to 6. Based on these facts, Mijnheer *et al.* (84) stated that unacceptable risks of complications will be introduced if the overall uncertainty in the absorbed dose value exceeds 7% (2 SD). They therefore proposed a standard requirement that the combined uncertainty in dose delivery should not exceed 3.5% (1 SD).

Clinical examples of the consequences of systematic underdosing or overdosing of the target volume have been described by Flamant *et al.* (37) and Chassagne *et al.* (22). In the study by Flamant *et al.* (37), patients with carcinoma of the tonsil were randomized to receive radiation therapy with either photons or electrons. A significant difference in tumor regression appeared between the groups, which had been treated with nominally identical doses. The electron treatment was significantly less effective. Later on, recalibration of the dosimeters used showed that there had been a 7% difference between the doses

of electrons and photons. This could, at least in part, explain the difference observed in tumor regression. Chassagne *et al.* (22) described an investigation which had been carried out after the radiation oncologist in charge of the gynaecological patients had reported a clinically evident increase in toxicity of the routine 50 Gy treatment of pelvic fields in these patients. Careful checking of the accelerator revealed an error in the calibration factors of the monitor chamber, which had been leading to a systematic 10% overdosage.

It can thus be concluded that dose variations of 5-10% in the target volume may have a significant impact on both tumor control probability and normal tissue complication probability. The steepness of the dose response curves for tumor control and normal tissue complications, as well as many other tumor and treatment related factors, determine the actual impact of such dose variations. Unfortunately, for many tumor types and normal tissues only limited data is available with regard to clinically established dose response relationships.

1.4. Clinical consequences of underdosing in the field margins

Variations in daily patient setup as well as patient movement during treatment lead to an enlargement of the penumbra region in the periphery of the treatment field. If these variations are random, the actual dose delivered to the margins of the field is lower than the intended dose. In the case of systematic displacement of the patient, the dose in the margin of the field is either lower or higher, thus risking a decreased tumor control probability or increased toxicity. That underdosing of parts of the target volume may indeed lead to a clinically apparent decrease in local control rates or even survival rates has been shown by several authors (64,91,130).

Kinzie *et al.* (64) published the results of a Patterns of Care Study on treatment practice of Hodgkin's disease. A survey was conducted on 181 patient records from four facilities with a large experience in treating Hodgkin's disease. Portal films were analyzed for adequacy at the margins. If a shielding block consistently touched or overlapped the edge of known tumor, or if blocks covered nodal areas uninvolved by Hodgkin's disease but included in the target volume, the portals were labeled inadequate. Thirty-six percent of the portals was considered inadequate. Those patients having adequate portal margins had

significantly fewer relapses of any type (15% vs. 50%, $P = 0.0001$), and significantly fewer infield or marginal recurrences (8% vs. 32%, $P = 0.001$). For patients treated with radiation therapy alone, these differences were even more striking. Planned chemotherapy diluted the effect of technically inadequate margins: in the group of 26 patients who received chemotherapy as part of their initial treatment, there was no significant increase in relapse rate when the margins were judged inadequate.

White *et al.* (130) conducted a radiation therapy quality control analysis in 140 patients with limited small cell lung cancer. Treatment consisted of chemotherapy and radiation therapy. A major radiation therapy protocol variation (MPV) included a 5-10% underdosage of any involved area, a $\geq 10\%$ underdosage of any area, or a $\geq 10\%$ overdosage of any critical structure. A total of 102 MPV in 44 patients was found, and were mostly related to field shaping or shielding. The overall and median survivals were significantly ($p = 0.02$) longer for patients with no or minor protocol variations than for those who had an MPV. Only performance status and radiation evaluation ($p = 0.0001$) were significant predictors of survival. Perez *et al.* (91) conducted a radiotherapy quality control survey of the treatment of 301 non small cell lung cancer patients, randomized to one of four definitive radiation regimens. Patients treated with full compliance ($n = 277$) had an intrathoracic recurrence rate of 46%, compared to a recurrence rate of 54% in 39 patients treated with major protocol variations. This difference did, however, not reach statistical significance.

1.5. The reproducibility of patient positioning

As variations in day-to-day patient positioning may cause under- or overdosage in the margins of the treatment field, the verification of daily patient positioning is an indispensable aspect of radiotherapy quality control. The first publication mentioning various possible errors in radiation therapy was the 1962 ICRU Clinical Dosimetry Report 10d (60), its last recommendation being: "Some method of immobilising the patient and of checking the patient's position during treatment should be used". This publication was followed by a decade of silence which lasted until the mid 1970s, in which the first clinical studies measuring

actual setup accuracy in daily practice appeared. True pioneers in this field were Marks and Haus. In 1974 they reported a survey of localization errors (LE: shielding of an area with known or potential disease) in the treatment of a variety of tumors in 173 patients (75). An LE rate of 27% was found. They also published a report on extended mantle fields: for 902 portal films in 99 patients the LE rate was 36% (77). In 2 of 10 patients with local recurrence, a correlation with repeated errors at that site (which could mean a dose reduction of 7.5% to 15%) could be made. The axillae were the sites of most frequent LE (50%) and of repeated errors; they were also the most frequent sites of local recurrence. They proposed a margin of 1 cm between the lung shielding blocks and the chest wall at the axillary border, and recommended frequent portal film checks. In 1976, a follow-up study of extended mantle fields was published (78), showing an LE reduction from 36% to 15%. For head and neck cancer, Marks and Haus showed that adequate immobilization and supine (instead of lateral) positioning reduced LE (in this study defined as a shift of the margins of the treatment field of ≥ 1 cm) rates from 16% to 1% (76).

Byhardt *et al.* (in 1978), and Rabinowitz *et al.* (in 1985) were also among the first authors to publish surveys of treatment accuracy for various treatment sites. Byhardt *et al.* (20) emphasized the importance of establishing a baseline rate of field placement errors (FPE) that may be expected in the delivery of radiation therapy to specific treatment sites at a specific institution. They reviewed 1221 portal films and 447 simulation films of 228 patients and defined deviations of ≥ 5 mm as FPE. The overall FPE rate was 15%, and 10% if the error limit was set at ≥ 1 cm. Highest FPE rates were recorded in the pelvic region (26%), followed by the abdomen (20%), and the ENT region (17%). The observed displacements ranged from 5 mm to 4 cm (average 1.2 cm). It was recommended to take portal films at least once a week, and every 2-3 days in setups identified to be prone to FPE.

Rabinowitz *et al.* (97) reported on the accuracy of radiation field alignment for several treatment sites in 71 patients. For each treatment field anatomical landmarks were selected, the distance of each landmark to an appropriate field margin was measured. For each distance the difference between the portal film and the simulator film was calculated. The results were characterized by calculating both the average of all the differences, and the largest difference ("worst case discrepancy", WCD). If more portals were available, the average standard

deviation (SD) was calculated: the treatment-to-treatment variability. For all sites combined, the average SD was 3.3 mm. Comparison of simulation films and portal films showed an average discrepancy of 5.1 mm and a mean WCD of 7.7 mm. The thorax and the pelvis were the sites having the largest errors (mean WCD of 9.2 and 8.4 mm, respectively). Rabinowitz *et al.* considered the average 3 mm treatment-to-treatment variability gratifyingly small. They suggested therefore that the differences between simulation and portal films were caused by systematic errors rather than random uncertainties in treatment setup.

The studies cited above provided invaluable information on treatment accuracy in daily practice, and showed which treatment sites were the most error prone. Moreover, they established a baseline rate of positioning variations, which stimulated others to undertake similar studies, and to which further data could be compared. An increasing number of authors began to conduct studies on treatment accuracy and immobilization techniques, often for specific treatment sites. These will be discussed in the subsequent chapters.

1.6. Types of errors and interpretation of error rates

The three major types of errors are systematic errors, random errors and accidental mistakes. The distinction between these is not always unequivocal. Usually, systematic errors are considered to be deviations from the intended standard which repeatedly occur in the same fashion, causing a nonrandom reduction or increase in dose. Examples are a mistake in a computer algorithm (causing a systematic over- or underdosage), or a discrepancy between the light field at a simulator and the radiation beam of the linac (causing, for example, a narrower field with, consequently, an underdosage in the margins of the field). Random errors are considered to be uncertainties in the application of procedures, resulting in a distribution of deviations with respect to the intended standard, for example the daily variation in positioning of a 70-year-old gentleman with aching hip joints on the treatment couch. Random errors are expected to result in a uniform dose reduction in the margins of the field. Accidental mistakes are incidentally occurring, possibly large deviations from the standard, for example the misplacement of a block or use of the wrong wedge.

It should be stressed that comparison of the error rates as reported by the various authors is extremely difficult: some (e.g. Rabinowitz *et al.* (97), Byhardt *et al.* (20)) define errors as shifts of the treatment field as compared to the simulation field (being the "gold standard"), while others (e.g. Marks *et al.* (75,77,78), Kinzie *et al.* (64)) judge the accuracy of field *design* according to the extent of disease, as well as the field placement itself, and report these together as errors. Furthermore, some authors take the maximum deviation of a field margin or an anatomical structure in a treatment field as the representative error, disregarding other errors in the same field, while others take several errors in one field (e.g. field margin shift and block misplacement) as separate errors in the calculation of error rates. It is evident that the failure to appreciate the correct extent of disease and to design adequate treatment fields is a very different type of error as compared to variations in field placement. In Table 1 an overview of the results of several studies (20,31,50,53,56,58,76,86,97) on positioning accuracy in treatment of head and neck cancer is presented. It is apparent that comparison of the results of these studies is difficult.

1.7. From portal films to electronic portal imaging devices

It has been argued (97) that the quality of megavolt films is a major factor in discerning and correcting discrepancies in the treatment field. As megavolt films are usually of very poor quality, and magnification factors are uncertain, tools are needed to aid the radiation oncologist in the quantitative comparison of portal and simulation films. Apart from the poor contrast resolution, other disadvantages of megavolt films are the time involved with the processing of the films, the space needed for archiving, and the fact that only one image can be obtained per fraction, so that on-line verification is not feasible.

These limitations of megavolt films prompted the development of electronic portal imaging devices (EPID). Since 1985, several groups have developed various types of electronic imaging systems (18,80,132). These can be divided into two major classes: (1) fluoroscopic systems, consisting of a luminescent device (fluorescent screen) producing photons in the visible range, in combination with imaging optics and a camera system, and (2) systems using arrays of radiation detectors, comprising a 2-dimensional array of ionization chambers, or

a one-dimensional array of diodes which scans the radiation field, or an array of scintillator detectors coupled to photodiodes (18). The system used in the DDHCC belongs to the class of fluoroscopic devices and has been described by Visser *et al.* (123) and Althof *et al.* (2). A schematic diagram of the system is presented in Fig. 2.

Table 1. Results of studies on the accuracy of patient positioning in treatment of head and neck cancer. Note the differences in definition of errors, and in the presentation of the results

Author	Immobilization	Error type	Results
Marks (1976)	no yes (bite block)	shift > 1 cm	16% 1%
Byhardt (1978)	yes (head mask)	shift > 0.5 mm shift > 1 cm	17% 9.6%
Rabinowitz (1985)	yes (head cup and neck roll)	average and worst case discrepancy; shift > 5 mm shift > 10 mm	2.5 mm av. 3.5 mm worst 17% > 5 mm 0% > 10 mm
Huizenga (1988)	yes (head mask)	SIM-MV differences (median and 1 SD)	5 mm median 1 SD 5 mm
Halverson (1991)	yes (head mask)	separation of the 0-100% and the 20-80% block overlap contours	9 mm 0-100% 5 mm 20-80%
Mitine (1991)	yes (head mask)	SIM-MV differences (1 SD) and shift > 5 mm	1 SD 4 mm 20% > 5 mm
Dunscombe (1993)	yes (head mask)	SIM-MV differences (median and 95th percentile)	4.4 mm median 8.9 mm 95%
Hunt (1993)	yes (head mask)	average SIM-MV translations average distance SIM-MV isocenters	1.5 - 3 mm 5 mm
Hess (1995)	yes (head mask)	SIM-MV differences (mean and 1 SD)	mean 0-3 mm 1 SD 3-5 mm 5% > 1 cm

The introduction and clinical development of the EPIDs prompted many studies. Methods were developed for the interpretation and comparison of the images, field placement variations were quantified, and the accuracy of various patient positioning and fixation techniques was determined. This interest in the verification of patient positioning, and potential correction thereof, was strongly influenced by the concurrent introduction of conformal therapy. As precise patient positioning is a prerequisite for conformal therapy and, even more strongly, for dose escalation, many studies were directed at off-line and/or on-line verification and correction of the patient setup.

The possibilities of EPIDs for transmission dose measurements (in vivo dosimetry) have been studied as well. EPIDs might, in future, be used for the simultaneous verification of patient setup and dose delivery. Their dosimetric application is, however, outside the scope of this thesis.

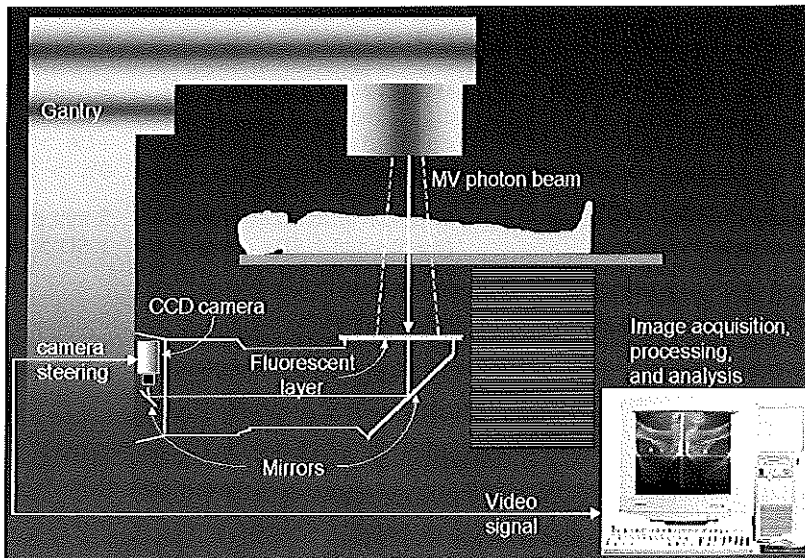


Figure 2

Diagram of the electronic portal imaging system developed in the DDHCC. The detector assembly (the fluorescent screen and a mirror) is housed in a lightweight structure which can be easily coupled to and removed from the gantry, and functions at all gantry angles. The CCD (charge coupled device) camera is mounted on the gantry, and connected to a microcomputer via dedicated electronics. Image acquisition, enhancement and display is carried out within a few seconds.

The purposes of this thesis were to introduce electronic portal imaging into clinical practice, to investigate and improve the accuracy of patient positioning in various treatment techniques, and to develop strategies for the verification and correction of patient setup as an indispensable aspect of conformal therapy.

Chapters 2 and 3 describe quality control studies which were carried out to establish the accuracy of daily patient positioning, both in a complex positioning technique such as mantle field irradiation (Chapter 2) and in a "routine" technique such as the treatment of breast cancer (Chapter 3). In these chapters, the interpretation and consequences of positioning errors are discussed. The improvement of immobilization and/or positioning techniques on the basis of such studies is described in Chapter 4, which comprises a set of studies on patient positioning accuracy in urological and gynaecological treatments. The use of data on organ motion and patient setup variations for the calculation of margins for a specific treatment site is also discussed in Chapter 4.

In recent years, many groups have worked on the sophistication of methods for the on-line and off-line analysis of portal images, and comparison to the simulation images. This resulted in the use of portal imaging to minimize random variations, and to correct systematic errors early in the treatment series. In Chapter 5, the joint clinical testing by three centres of an off-line verification and correction protocol in the treatment of prostate cancer is described. The general discussion (Chapter 6) summarizes the main findings of the studies described in this thesis, and discusses the implications of these and other studies for clinical practice. In particular, the present and future developments in portal imaging, the interpretation of patient positioning errors, and the place of verification and correction strategies both in routine and in sophisticated (high-precision high-dose) treatments are put into clinical perspective.

CHAPTER 2

ACCURACY OF PATIENT POSITIONING IN MANTLE FIELD IRRADIATION

C.L. Creutzberg, A.G. Visser, P.M.Z.R. De Porre, J.H. Meerwaldt,
V.G.M. Althof, P.C. Levendag

Radiotherapy and Oncology 23: 257-264, 1992

Summary

A prospective study of the accuracy of patient positioning in mantle field irradiation was carried out in 13 lymphoma patients treated with curative radiotherapy. Patients were treated in the supine and prone position for anterior and posterior fields, respectively. Individually shaped divergent shielding blocks were placed in a fixed position in a template which was positioned on a tray above the patient. A total number of 94 megavoltage portal films (MV) was analyzed and compared to 26 simulation films (SIM). MV-SIM differences were larger for posterior fields than for anterior fields. Regarding the position of the lung shielding blocks, mean MV-SIM differences ranged from 1.3 to 4.4 mm and errors exceeding 1 cm were found in 7.2% of cases. Most discrepancies appeared to be randomly distributed. A 4-5 mm systematic cranial shift of patients in the posterior treatment position was noted. Discrepancies in the position of the laryngeal block, spinal cord shielding block and humerus blocks were small with mean MV-SIM differences ranging from 0.3 to 2.7 mm. Differences between simulation setup and treatment setup were modest as compared to error rates reported in the literature. Shielding of tumor bearing areas did not occur. It was concluded that the present standardised technique of patient positioning and the design of treatment fields result in acceptable error rates. Attention should be directed towards increasing the stability of patients in the prone treatment position in order to further reduce both systematic and random error rates.

Introduction

Treatment of patients with stage I and II supradiaphragmatic Hodgkin's disease usually includes radiation therapy, resulting in high cure rates (80-90% relapse-free survival) (42). Depending on the presence of prognostic factors such as B-symptoms, bulky disease, age, and sex, treatment either consists of subtotal nodal irradiation or of a combination of chemotherapy and radiation therapy. The aim of subtotal nodal irradiation is to treat in continuity the lymphatic chains that are involved or likely to be involved with Hodgkin's disease. This is achieved by the combination of the so-called mantle field and a subdiaphrag-

matic field including the spleen and paraaortic nodes. The mantle field includes the cervical nodes, supraclavicular and infraclavicular nodes, axillary nodes, the mediastinum, and the hilar nodes.

An important feature of the mantle field technique is the individualization of radiation fields conformed to the patient's anatomy in the treatment position. The use of individually shaped blocks ensures adequate treatment of lymphoid tissue while sparing lung tissue, spinal cord, larynx, heart and the humerus. However, the complex shape of these extended fields makes precision in radiotherapy setup difficult to achieve (77,112). Discrepancies in daily treatment positioning and differences between localization setup and treatment setup could result either in an underdosage in the field margins, which might lead to a clinically relevant geographical miss, or in an overdosage to normal tissues.

Underdosage in the field margins, due to either uncaredful planning of radiotherapy setup or to localization errors, has been shown to result in higher in-field or marginal recurrence rates (64). For this reason, treatment fields should be designed carefully and should include regions of known and potential disease with adequate margins, while protecting normal tissues. The amount of margin that should be left around the target volume is directly related to the precision of radiotherapy setup and the reliability of day-to-day treatment positioning. Quality control regarding precision of treatment positioning enables the radiation oncologist to use small but reliable margins around the intended target volume, and could therefore be of importance in reducing relapse rates and in preventing radiation damage.

In our institute, a series of prospective quality control studies regarding the accuracy of patient positioning for various treatment sites and immobilization techniques has been started. In a previous study (56) the accuracy of radiation field alignment in head and neck cancer was ascertained, showing an average error due to the transition from simulation to treatment of 3 mm in a random fashion, and treatment-to-treatment variations, also random, of 3 mm, contributing together to an overall error (1 SD) of 5 mm. However, these patients were immobilized using plastic fixation casts and were therefore felt to be subject to minimal positioning errors. Because of the nonrigid patient fixation in mantle field irradiation, the complexity of the treatment setup, and in view of the impact positioning errors may have on treatment outcome, a study was set up to investigate the accuracy of patient positioning in mantle field irradiation.

Patients and Methods

During a 7-month period (November 1987 through May 1988) 13 consecutive lymphoma patients treated with radiation therapy using the mantle field technique were entered into this study. The group comprised 12 patients with stage I or II Hodgkin's disease and 1 patient with non-Hodgkin's lymphoma. Positioning and treatment of patients were carried out according to a standardized technique as described below.

The patient is positioned on the treatment couch on a cross-shaped board (a so-called Hodgkin board) with arms extended. A marker line on both arm rests is matched to the patient's middle finger. For the anterior (AP) field, the patient is positioned in the supine position using a head support and nose-strap to ensure exact positioning of the head in hyperextension; for the posterior (PA) field the patient is lying prone with the head supported in a head-chin rest (Fig. 1). Simulation films are taken of all regions of the target volume in both the supine and the prone treatment position, after which the radiation oncologist draws the outlines of the AP and PA treatment fields on the respective simulation films. Divergent lead shot shielding blocks are shaped to conform to AP and PA contours and are placed in a styrofoam template, which is positioned on a tray above the patient. The field centre and the horizontal and vertical axes are marked on the template. After positioning the patient on the treatment couch, the central axes of the lightbeam of the linac are matched with 5 points tattooed on the patient during simulation, marking the field centre and the horizontal and vertical axes. The marker cross on the template is then matched with the central axes of the lightbeam. Control films are taken with the shielding blocks in position and, if necessary, adjustments are made.

Both AP and PA fields are treated daily, five times a week, to a total dose of 40 Gy in 2 Gy fractions. Dose levels are specified at the midplane of the region of the treatment field with the smallest patient diameter (usually the neck region) and are calculated for the other parts of the treatment volume (axillae, supraclavicular region, mediastinum, lower mediastinal border). When in a particular part a dose level of 40 Gy has been reached, this part is shielded until a dose of 40 Gy has been delivered to all parts of the treatment volume.

For this study, megavolt portal films (Kodak X-omat V2) of both AP and PA fields were obtained at the first treatment, at a dose level of 20 Gy and at the

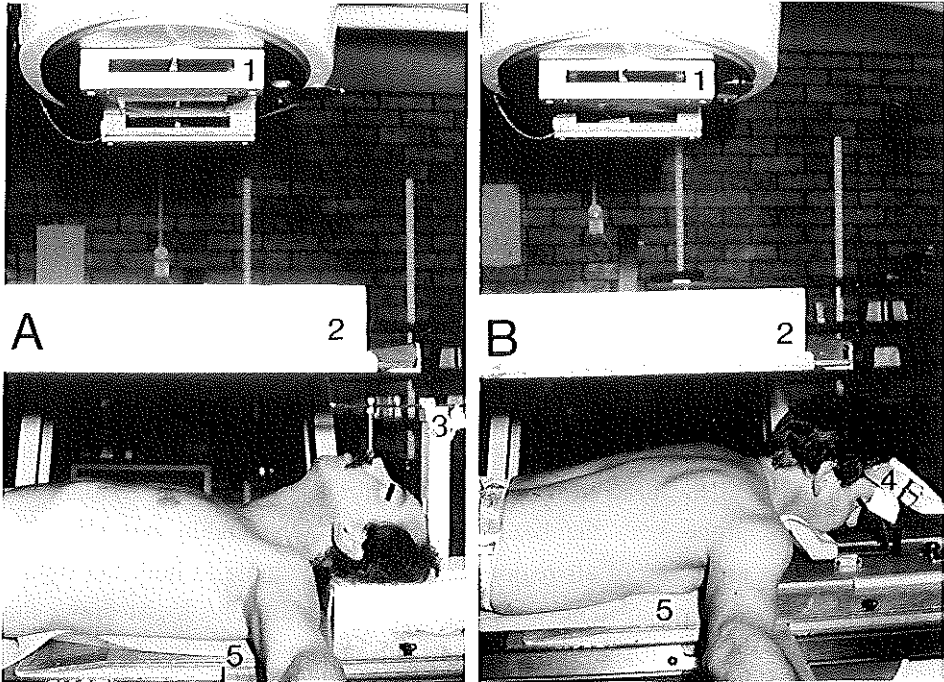


Figure 1

Supine (A) and prone (B) position of the patient in mantle field irradiation. (1) collimator; (2) template with shielding blocks; (3) head support with nose-strap; (4) head-chin rest; (5) treatment couch with Hodgkin board.

final fraction of the radiotherapy series. In five randomly chosen patients, megavolt portal films were taken more often, at least once a week. However, one patient refused further treatment after the sixth radiotherapy fraction and two sets (AP and PA) of portal films had to be discarded because of shielding at the final fraction of those parts of the treatment volume in which the 40 Gy dose level had already been reached. Thus, a total number of 94 megavolt portal (MV) films was obtained in addition to 26 simulation (SIM) films, yielding an average number of 3.6 portal films per field. Daily patient positioning was carried out as described above. Patients were treated with 4 MV photons from a linear accelerator at a focus-to-table distance of 127.5 cm and a tray-to-table distance of 40.5 cm.

To compare simulation films to portal films and to assess day-to-day variations in the portal images, a number of relevant anatomical points, as well as points related to the field margins were identified and distances between these points were measured (Fig. 2). Appropriate points were chosen in order to be able to assess discrepancies caused by lateral shift, cranio-caudal shift, or rotation, respectively. Distances between the anatomical points and/or field points were corrected for magnification (i.e. transformed to distances in the patient's midplane) and corresponding distances on the SIM films and MV films were compared. This method of analysis was chosen as opposed to the method used in a previous study (56), in which individual points were marked and digitised and subsequently the coordinate system of the megavolt film was transformed by rotation and translation to obtain the best match with anatomical landmarks on the simulation film. The latter method has the advantage of greater flexibility in

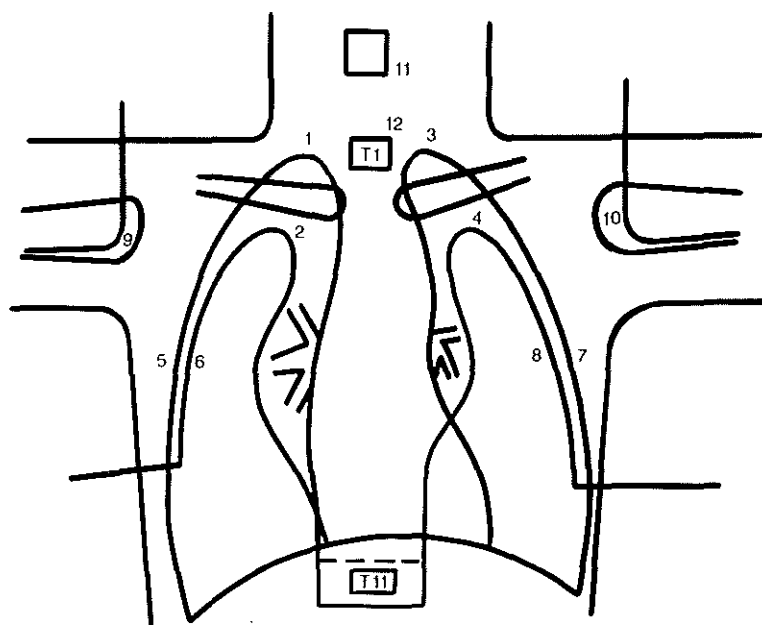


Figure 2

Diagram of the points indicated on the simulation films and megavolt films: anatomical points (1,3,5,7,12) and shielding block points (2,4,6,8,9,10,11).

distinguishing between types of errors and in detecting incorrectly marked points. In this study, however, simulation and megavolt films often consisted of two separate films, each covering part of the treatment field, thus preventing the use of a single coordinate system per treatment field. It was therefore decided to use the present method of determining distances on the simulation and treatment films and of comparing corresponding distances.

Differences between the distances measured on MV and SIM films were calculated and averaged over all patients; of each mean MV-SIM difference the standard deviation and range of extremes were calculated. If a large difference between corresponding distances was found (> 10 mm), the indication of the points on the films was checked. In 8% of the MV films an initially found large discrepancy appeared to be caused by an incorrect indication and a correction was applied. Specific anatomical landmarks which most often required corrections were the lung tops and points on the thoracic spine. With regard to the indication of these points it should be kept in mind that for simulation films contrast depends on both differences in tissue density and atomic number, as opposed to megavolt images, where contrast only depends on variations in density and hence air volumes are more prominent. Indication of the edges of Th1 and especially of Th10 were occasionally hampered because of lack of contrast. For this reason, measurements related to these points have been interpreted with caution.

Results

Position of lung shielding blocks

In general, discrepancies between corresponding distances on simulation and megavolt portal films were larger for PA fields than for AP fields. Correlation between measurements of the position of the lung blocks at the left and right sides was good ($r = 0,65$), so both sides were taken together.

Analysis of the distances between the lung tops and lung shielding blocks showed a mean difference between SIM and MV films of 1.3 mm (standard deviation 4.5 mm) for AP fields and 4.4 mm (± 5.6 mm) for PA fields with a maximum difference of 18 mm (Table 1 and Fig. 3). In 7.6% of the films an

error exceeding 1 cm was recorded. As shown in Table 1, the frequency of errors > 1 cm was larger for PA fields than for AP fields.

On PA films a general trend towards a slight (4-5 mm) cranial shift of the patients was noted (distances between lung tops and lung blocks on MV films larger than on SIM films, Fig. 3); this shift in cranial direction was confirmed by measurements of distances between the lung tops and upper field margins and between Th10 and the lower field margins.

Table 1. Mean values, standard deviations, range of extremes for the differences [MV-SIM]^a and frequency of differences [MV-SIM] ≥ 10 mm

Distance	Field	Mean [MV-SIM] (mm)	S.D. (mm)	Range [MV-Sim] min-max	Freq.diff. [MV-SIM] ≥ 10 mm
Lung top to block (cranio-caudal) left and right	AP	1.3	4.5	-10 +16	5.3 %
Lung top to block (cranio-caudal) left and right	PA	4.4	5.6	-11 +18	11.1 %
Chest wall to block (lateral) left and right	AP	1.3	3.5	-6 +11	2.1 %
Chest wall to block (lateral) left and right	PA	3.9	5.1	-8 +20	11.6 %

^a difference [MV-SIM]: the difference between a distance measured on the megavolt film and the corresponding distance as measured on the simulation film; a positive value indicates a larger distance on the MV film as compared to the SIM film.

The position of the lung blocks in the lateral direction was analysed by measurements of the distances between the outer margin of the lung block and the outer aspect of the lateral chest wall at a level 10 cm below the level of the lung top. Again MV-SIM differences were larger in the PA position with mean differences of 1.3 mm (± 3.5 mm) for AP fields and 3.9 mm (± 5.1 mm) for

PA fields and a maximum difference of 20 mm (Table 1 and Fig. 4). In 6.7% of films an error of > 1 cm was found. Usually, when designing treatment fields a routine margin of 0.5-1 cm is left between the lung block and the inner aspect of the chest wall in order to prevent shielding of axillary lymph nodes close to the rib cage (45,77). Thus, the distance between the lung block and the outer edge of the rib cage appears to be 1.5-2.0 cm. As a result, shielding of axillary tissues did not occur. In two instances the lateral margin of the lung block just covered the rib cage completely; in both cases a smaller margin (< 0.5 cm) had been left between the lung block and the chest wall at simulation.

On most MV films a larger distance between the lateral chest wall and the lung block was measured on both left and right sides as compared to the SIM films; this was especially the case for PA fields. As the blocks are in a fixed position in the template, an increase in chest wall-block distance at one side might be expected to be accompanied by a decrease at the opposite side. The larger chest wall-block distance found on both sides therefore reflects a larger total chest width on MV films. Fig. 5 shows the inverse correlation between measurements of chest wall-block distance at the left and right sides for AP and PA fields, respectively. However, an increased chest wall-block distance on both sides is indicated, representing an increase in total chest width of a few millimeters on MV films as compared to SIM films.

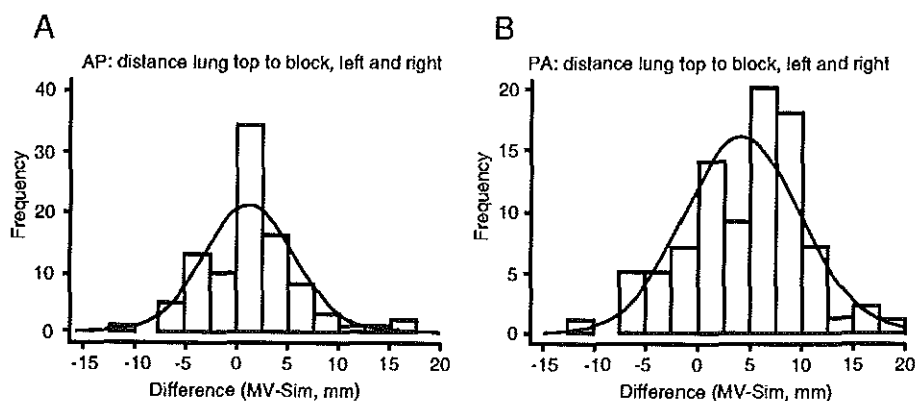


Figure 3

Histograms of the differences (MV-SIM) between corresponding distances on megavolt and simulation films for the distance between the lung tops and the lung shielding blocks (1-2 and 3-4 in Fig. 2) on (A) anterior and (B) posterior films. The curve shows a Gaussian profile fitted to the data.

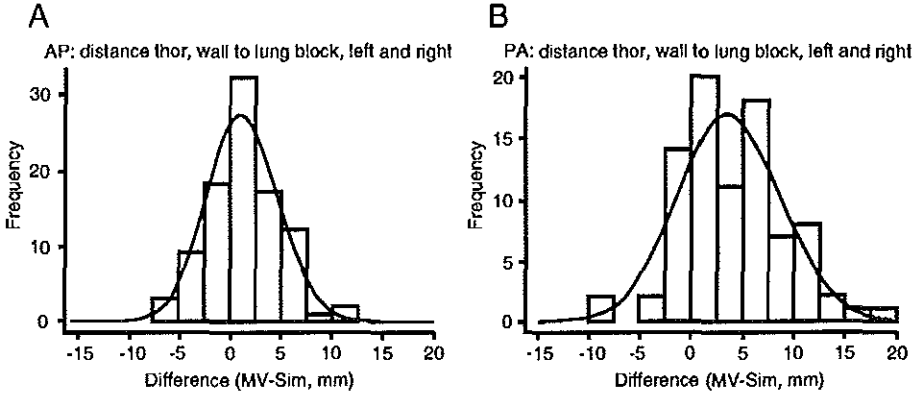


Figure 4

Histograms of the differences (MV-SIM) between corresponding distances on megavolt and simulation films for the distance between the lung block and the chest wall (5-6 and 7-8 in Fig. 2) on (A) anterior and (B) posterior films. The curve shows a Gaussian profile fitted to the data.

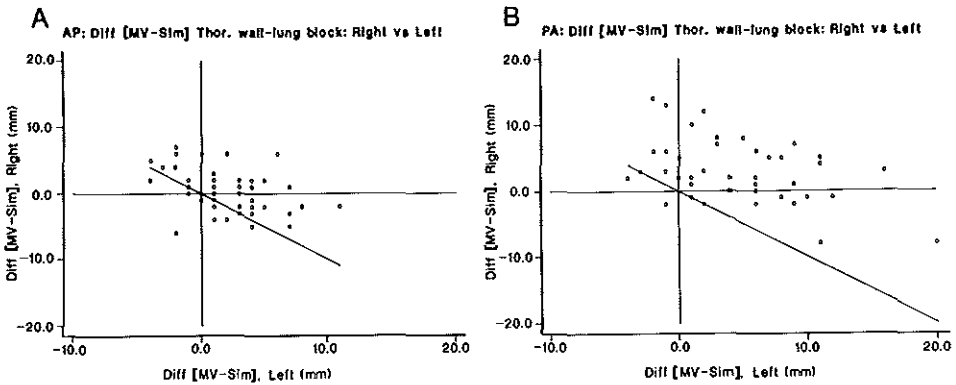


Figure 5

Inverse correlation between the differences (MV-SIM) in the chest wall to block distances at the left side (horizontal axis) and the corresponding differences at the right side (vertical axis) on (A) anterior and (B) posterior films.

Except for the small systematic cranial shift found on PA films, the discrepancies in position of the lung shielding blocks appeared to be randomly distributed. This is reflected by the fact that the mean values of the MV-SIM differences are close to zero, while standard deviations of the mean are relatively large (Table 1).

Position of laryngeal block, spinal cord shielding block and humerus blocks

Discrepancies in the position of the laryngeal shielding block, the spinal cord shielding block and the humerus blocks were modest with mean differences ranging from 0.3 to 2.7 mm and 0 to 5.9% of errors exceeding 1 cm (Table 2). Again, differences are mainly randomly distributed with standard errors of the mean ranging from 4 to 6 mm.

Table 2. Mean values, standard deviations, range of extremes for the differences [MV-SIM]^a and frequency of differences [MV-SIM] ≥ 10 mm

Distance	Field	Mean [MV-SIM] (mm)	S.D. (mm)	Range [MV-Sim] min-max	Freq.diff. [MV-SIM] ≥ 10 mm
Laryngeal block (cranio-caudal)	AP	0.3	4.0	-12 +6	5.7%
Laryngeal block (lateral)	AP	2.7	4.9	-8 +12	5.9%
Spinal cord block (cranio-caudal)	PA	1.7	5.6	-19 +8	6.6%
Spinal cord block (lateral)	PA	0.1	3.4	-8 +9	0%
Humerus blocks (lateral) left and right	AP/PA	1.5	4.4	-12 +12	4.5%

^a difference [MV-SIM]: the difference between a distance measured on the megavolt film and the corresponding distance as measured on the simulation film; a positive value indicates a larger distance on the MV film as compared to the SIM film.

Discussion

The accuracy of patient positioning in mantle field irradiation has been the subject of various investigations (47,57,64,77,78,112) because of the complexity of the treatment setup and in view of the possible consequences of localization errors in terms of geographical miss and recurrence rate. In their 1974 review of

902 treatment verification films of mantle fields, Marks and Haus (77) found an incidence of localization errors (LE, shielding of an area with disease or potential disease) of 36%. In 17 patients a so-called clustering of errors (three or more errors at one site) was observed, which resulted in a dose reduction at the specific site. In two out of 10 patients with local recurrence, enough localization errors had been found at the site of recurrence to account for a dose reduction sufficient to explain the recurrence. In 1976, Marks and Haus (78) once again carried out a review of mantle fields (451 verification films made between 1973 and 1974). They found a decreased error rate (15% LE vs. 36% in the 1974 review), due both to increased attention of radiation oncologists to leaving adequate margins around the target volume, and to increased use of verification films. Taylor *et al.* (112) likewise observed a reduction in number of deviations and unacceptable set-ups due to technical improvements as well as increased alertness. In their analysis of daily treatment films of 28 patients, 15% of films contained a minor deviation (deviation of more than 0.5 cm but no tumor or prophylactic area shielded) and 1% of fields were considered unacceptable, compared to 29% and 5% in a previous study.

Griffiths and Pearcey (47) studied 171 verification films of 19 patients treated with full or partial mantle fields. They reported a field placement error rate (shielding of the intended treatment volume by more than 1 cm) of 21%. In 11% of cases the areas shielded contained known disease. In an analysis by Hulshof *et al.* (57) of 216 treatment setups of mantle field irradiation, verification films showed a localization error of over 1 cm in 13% of cases, leading to a critical margin between a shielding block and the tumor bearing area in 9% of treatment setups.

Rabinowitz *et al.* (97) and Byhardt *et al.* (20) reported field placement error rates for several treatment sites. Rabinowitz found the highest error rates in the chest region with an average discrepancy of 5.8 mm and a mean worst case discrepancy (WCD) of 9.2 mm; 32% of fields exceeded a WCD of 1 cm (as compared to 23% of fields exceeding a WCD of 1 cm for all sites combined). Byhardt, however, found highest error rates in the pelvic region (23% error of > 1 cm); for the chest region the error rate was 8%.

Using the 1 cm limit set by some authors (20,47), field placement error rates reported for mantle field irradiation range from 8% to 32%; error rates based on qualitative reviews range from 15% to 36% (Table 3). In the present analysis,

discrepancies between simulation set-up and treatment set-up were modest as compared to the error rates reported in the literature. Regarding the position of the lung shielding blocks, mean displacements ranged from 1.3 to 4.4 mm and errors exceeding 1 cm were found in 7.2% of cases. It should, however, be kept in mind that as an average of 3.6 portal films per field was sampled, the error rate of 7.2% could be an underestimate. Radiotherapy technicians might be more careful and thus technical setups might be more accurate on the days that films are taken.

Table 3. Error rates reported in literature (errors exceeding 0.5 cm, errors exceeding 1.0 cm and error rates based on qualitative reviews).

Author (ref.)	fields studied	error rate > 0.5 cm	error rate > 1 cm	error rate (qual.)
Marks (77)	mantle fields			36%
Marks (78)	mantle fields			15%
Byhardt (20)	chest region (lung, esophagus)	13%	8%	
Griffiths (47)	mantle fields		21%	
Hulshof (57)	mantle fields	50%	13%	
Taylor (112)	mantle fields	16%		
Rabinowitz (97)	chest region (unspecified)	77%	32%	
Kinzie (64)	mantle fields			36%
present study	mantle fields		8%	

Error rates were higher for PA fields (prone position of the patient) than for AP fields, a finding which has been reported by Hulshof (57) as well. Shielding of tumor bearing areas did not occur; this may be due to the standardized technique of patient positioning used, along with guidelines for design of treatment fields ensuring adequate margins around the target volume. The use of a template with the shielding blocks in fixed position both facilitates daily patient

positioning and reduces positioning errors. The laborious task of placing each individual block in its correct position is time consuming and, as observed by Pötter (93, and personal communication), may yield higher error rates as each block can be a separate source of positioning errors.

A 4-5 mm cranial shift of patients in the PA treatment position was noted. In order to rule out errors in indication of the lung tops on the MV films as a possible cause, a review of these measurements was conducted. After correction of some incorrectly marked points this observation could be confirmed. A possible explanation of this small cranial shift of patients in the prone treatment position might be a relaxation of the patient in the head-chin rest during the course of treatment, thus putting more weight on the head with a consequent slight shift in cranial direction. The fact that no shoulder support was used, thus allowing forward movement of the shoulders onto the treatment couch, may also have contributed to a cranial shift and higher error rates in the prone position.

Analysis of the lateral position of the lung blocks on the MV films revealed a systematically larger distance between the chest wall and the lung block on both sides as compared to the SIM films, reflecting an increased total chest width on the MV films. This was especially the case for PA treatment fields (Table 1). The cause of this small increase in total chest width is not quite clear. One explanation might be a difference in respiratory situation between simulation and treatment. In the prone treatment position, chest movements are impeded by the external pressure on the chest. In the course of the treatment the patient may tend to breathe more freely in the prone position than during simulation, resulting in an increased total chest width on MV films. Another factor might be the systematic cranial shift of patients found on PA films: as the distance between chest wall and lung block was measured at a fixed distance of 10 cm below the level of the lung tops, the level of measurement of the chest width shifted cranially as well, and thus a 1-2 mm larger distance could be found incorrectly.

Most reports on patient positioning in mantle field irradiation are restricted to an analysis of the position of the lung blocks. In this study attention was paid to the positioning of laryngeal blocks, spinal cord shielding blocks and humerus blocks as well. The modest discrepancies found comply with a correct position of the patient in both cranio-caudal and lateral directions and absence of rotation

or torsion. However, random errors do occur, as reflected by the relatively high standard errors of the mean.

In conclusion, the present standardised technique of patient positioning and design of treatment fields, ensuring adequate margins around the target volume, seems to result in acceptable error rates. Shielding of tumor bearing areas did not occur. The small systematic cranial shift of patients in the prone position causes irradiation of a somewhat larger volume of lung than intended. In the future, attention will have to be directed towards increasing the stability of patient support in the prone position in order to further reduce both systematic and random error rates. As also stated by Marks (77,78) and Taylor (112), continuous attention to the accuracy of patient positioning is very important in keeping error rates as low as possible. In this institute verification of day-to-day patient positioning is presently carried out using an on-line megavolt portal imaging system (123). Megavolt images can be displayed on a monitor together with the digitised simulation image, thus enabling immediate verification. The on-line contrast enhancement performed by the system ensures a good image quality. Patient positioning studies are facilitated by the fixed coordinate system of both megavolt and digitised simulation images, thus allowing identification of anatomical landmarks and field edge points of both types of images in a common coordinate system. In order to evaluate the accuracy of present patient positioning and fixation techniques and to assess for which treatment sites very frequent verification will be necessary to ensure optimal treatment precision, patient positioning studies of various treatment sites are being conducted.

Acknowledgements

The authors wish to thank B. Göbel for his assistance in performing measurements on the radiographs, W.L.J. van Putten for his statistical advice and H. Huizenga for valuable discussions on study design and data analysis and for comments on the manuscript. The manuscript was skilfully prepared by Ms. I. Dijkstra. The cooperation of the radiation oncologists W.H.M. Eijkenboom and B.A. Reichgelt, and of the technicians is gratefully acknowledged.

CHAPTER 3

QUALITY ASSURANCE USING PORTAL IMAGING: THE ACCURACY OF PATIENT POSITIONING IN IRRADIATION OF BREAST CANCER

C.L. Creutzberg, M.D., V.G.M. Althof, M.Sc., H. Huizenga, Ph.D.,
A.G. Visser, Ph.D., P.C. Levendag, M.D., Ph.D.

International Journal of Radiation Oncology, Biology, Physics 25: 529-539, 1993

Abstract

Purpose To study the accuracy of patient positioning in irradiation of breast cancer.

Methods and materials Megavolt portal images were obtained using a fast electronic megavoltage radiotherapy imaging system in 17 breast cancer patients immobilized with plastic fixation masks on a flat board with arm support and in 14 patients positioned without a mask on either a flat or a wedge-shaped board. Quantitative analysis of 510 megavolt portal images and comparison to 66 digitized simulation films was performed. Differences between the positioning techniques were evaluated.

Results For the position of the patient in the field, standard deviations of the difference between simulation and treatment images were 3.2 mm and 4.6 mm for irradiation with and without masks, respectively. Larger standard deviations were found for the field width and length (5-7 mm), for collimator rotation (1.5-2°), and for the position of the lung shielding block for patients positioned on the flat board (10-16 mm). The changes in field size and collimator rotation appeared to be largely due to the inclination of the radiotherapy technicians to slightly adapt fields in order to obtain a seemingly better congruity of the field with the skin or mask markings. Comparison of the accuracy of patient positioning with and without masks yielded similar error rates; standard deviations and extremes tended to be somewhat larger in positioning without a mask. The wedge-shaped board was preferred because of the ease of patient setup and because the use of a lung block is avoided. The transition from simulation to treatment setup yielded larger deviations than repeated treatment setups.

Conclusion These results emphasize again the continuous need for focusing attention on the accuracy of patient positioning in order to achieve maximal precision in radiotherapy. The electronic portal imaging system is very suitable for both quick on-line treatment verification and off-line analyses.

Introduction

Quality control in radiotherapy has become a significant issue. The process of planning and daily delivery of radiation therapy involves a long chain of technical procedures. Quality control programs address inaccuracies in each step of this process, as small inaccuracies might accumulate into major deviations. Quality control regarding dosimetry calibration, dose calculation, treatment planning systems, and simulator and treatment unit parameters has been improved over the past decades. More recently, the possible impact of patient setup inaccuracies has attracted attention as well. The availability of modern diagnostic devices such as magnetic resonance imaging and computerized tomography has led to a more precise definition of target volume. The development of highly sophisticated (three-dimensional) planning systems and radiotherapy equipment enables high precision conformal radiotherapy to the target volume. To ensure adequate covering of the target volume in high precision radiotherapy, accuracy and reproducibility of day-to-day patient positioning are prerequisites and might well turn out to be the limiting factors. Knowledge of the accuracy of the patient positioning techniques currently used and the possibility of (on-line) verification and correction of patient setup have thus become increasingly important.

In the Daniel den Hoed Cancer Center (DDHCC) a series of prospective quality control studies of current positioning techniques for various tumor sites is being carried out. In previous studies of the accuracy of patient positioning in head and neck cancer (56) and in mantle field irradiation (26) megavolt portal films were used. In the past few years, a number of research groups started the development of fast on-line electronic imaging systems. In 1985 a project was initiated to develop a fluoroscopic imaging system in the DDHCC in collaboration with Philips Medical Systems Radiotherapy and the Laboratory of Space Research Leiden. After a prototype phase, the product type was installed on a linear accelerator² in 1989. The characteristics of this system, the Philips SRI-100, have been described in previous publications (1,123). Major advantages of these electronic imaging devices are the speed and ease of imaging

² Philips SL-75/10.

with automatic on-line contrast enhancement, thus enabling immediate comparison with the digitized simulation image.

At present, the preferred treatment for a large majority of patients with early breast cancer is breast conserving therapy. Treatment consists of lumpectomy (excision of the tumor with 1-2 cm margin) and axillary dissection, followed by postoperative radiotherapy to the breast. Radiotherapy to the breast is carried out using lateral and medial tangential beams. In our department, patients used to be positioned on a flat board with arm-support using a plastic fixation mask for immobilization of the chest and neck. Recently, a wedge-shaped board with an adjustable slope angle has been introduced which enables a quick patient positioning without a mask and without use of a lung shielding block. The present study was carried out in order to evaluate the accuracy of field alignment in irradiation of breast cancer patients using tangential fields, and to compare the different patient positioning techniques in order to determine if the use of a fixation cast is necessary in terms of positioning accuracy.

Methods and Materials

The imaging system

The Philips SRI-100 electronic portal imaging system consists of a detector, that is, a metal plate/fluorescent screen combination producing photons in the visible range, in combination with imaging optics and a CCD camera system. The detector assembly (the fluorescent screen and a mirror) is housed in a lightweight structure which may be easily coupled to and removed from the gantry (Fig. 1). The shielded CCD camera is mounted on the gantry of the linear accelerator and functions at all gantry angles. The camera is connected to a microcomputer (PC-AT) via dedicated electronics. The microcomputer, the video monitor, and a videographic printer are situated next to the accelerator control console. Image acquisition and handling, as well as system control, are performed with a dedicated user interface requiring a minimum of known therapy data. A digitization station for simulation films allows an easy recording of simulation images and simultaneous display of simulation (SIM) and megavolt (MV) images on the same monitor.

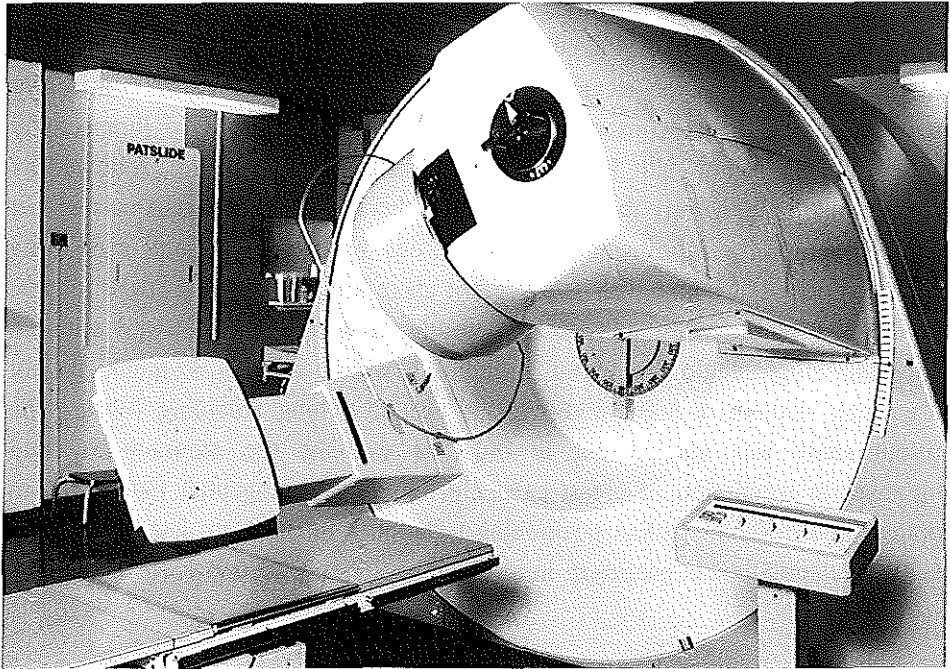


Figure 1

The detector assembly of the Philips SRI-100 imaging system on the gantry of the linear accelerator.

Images can be recorded with a minimum exposure of 4 cGy at dose maximum (0.7 seconds exposure time) and are displayed on the monitor. An automatic enhancement procedure, based on measurements of the mean and the standard deviation of the pixel grey value distribution, is applied. This procedure optimizes the setting of window and grey-scale level before final display. The images are automatically stored on hard disk or on floppy disk and hard copies are produced using a videographic printer.

On-line interpretation and comparison of the megavolt images are facilitated by the display of a thin wire mesh (with 4x4 cm squares at isocenter) over each image, allowing quick estimates of distances from anatomical structures to the field center and field edges and to the shielding blocks. Moreover, as the detector is at a fixed position with regard to the beam axis, a common coordinate system can be defined in the simulation images and in the MV

images. Thus, a method has been developed to select relevant points in the simulation image (e.g., field edges, anatomical structures or shielding blocks) with the cursor, after which the geometrically corresponding locations of these points in the MV image are calculated, and automatically displayed in the MV image. The position of anatomical structures, blocks, and field edges relative to these cursor marks can thus be quickly compared. A major advantage of this method is that the attention is focused on the position of a few clinically relevant points, enabling a quick decision whether or not a setup is acceptable.

Patient positioning in breast cancer

From November 1989 until June 1990, 31 consecutive patients treated with radiotherapy to the breast using tangential beams were entered into the study. The group comprised four patients who received radiotherapy to the axillary and supraclavicular nodal regions as well. Seventeen patients were positioned according to the technique traditionally applied in our department, that is, in the supine position on a flat board with an arm support (Fig. 2A). An individual plastic fixation mask was used to immobilize the chest and neck onto the treatment couch. Alignment was carried out using wall pointers. Field centers and field edges were marked on the mask. A lung shielding block was used to make the posterior edge of the field follow the chest wall contour (Fig. 3A). Thus the superior edge of the tangential beam remained in the true vertical in order to match with the inferior edge of a concurrent or future supraclavicular field.

When treating patients through the plastic fixation masks, the skin receives a significantly higher radiation dose. This results in enhanced acute skin reactions, notably a higher incidence of moist desquamation. For this reason, most radiation oncologists presently prefer positioning of the patients without fixation masks. At first patients were positioned without masks on the flat board as described above. In November 1989 a wedge-shaped board with an adjustable slope angle was introduced (Fig. 2B). As the slope angle can be adjusted to the contour of the patient's chest wall, the use of a lung shielding block is avoided while keeping the superior field edge vertical (Fig. 3B). Field markings are drawn on the skin. Fourteen patients were positioned without masks, five of which were positioned on the flat board and nine on the wedge-shaped board.

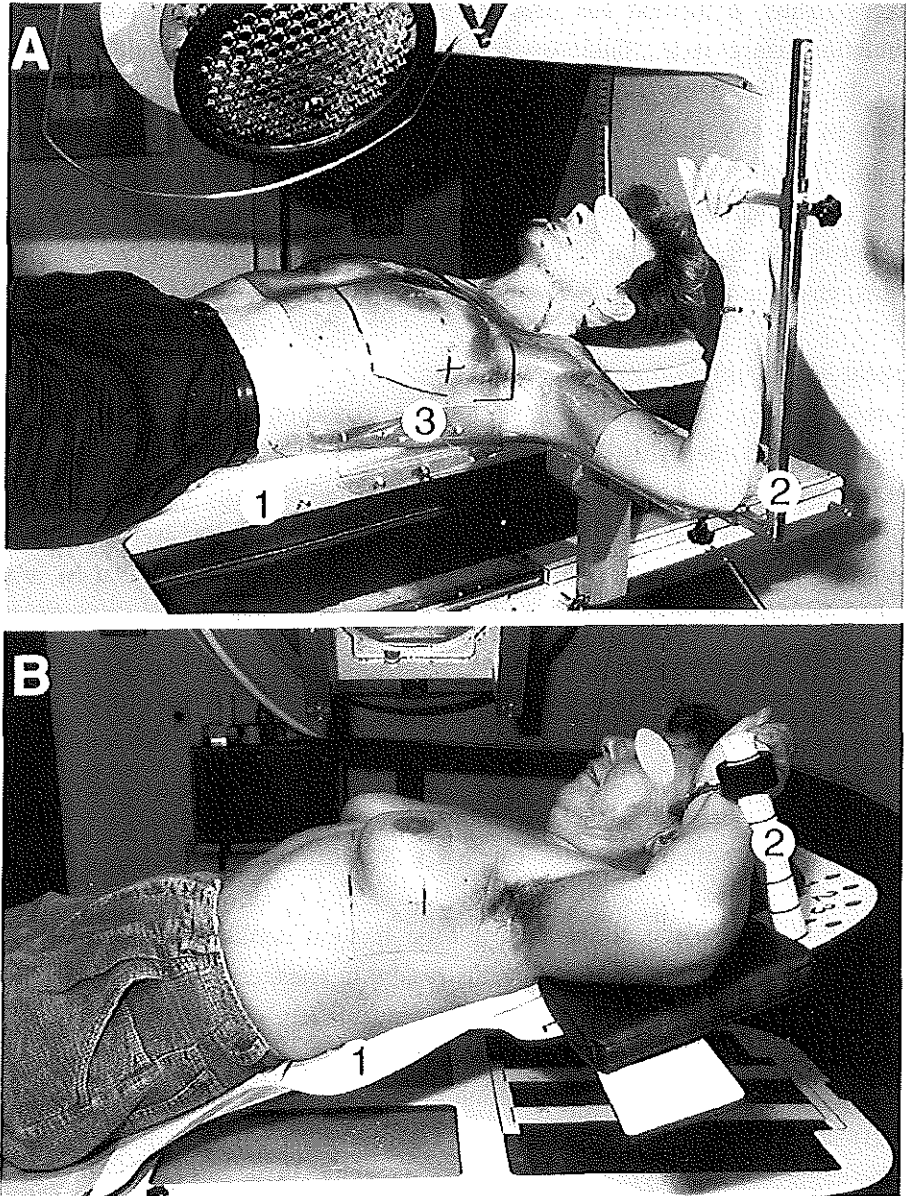


Figure 2

- 2A: Patient positioned with fixation mask on the flat board. (1) treatment couch with board; (2) arm support; (3) mask.
2B: Patient positioned without a mask on the wedge-shaped board. (1) wedge-shaped board; (2) arm support.

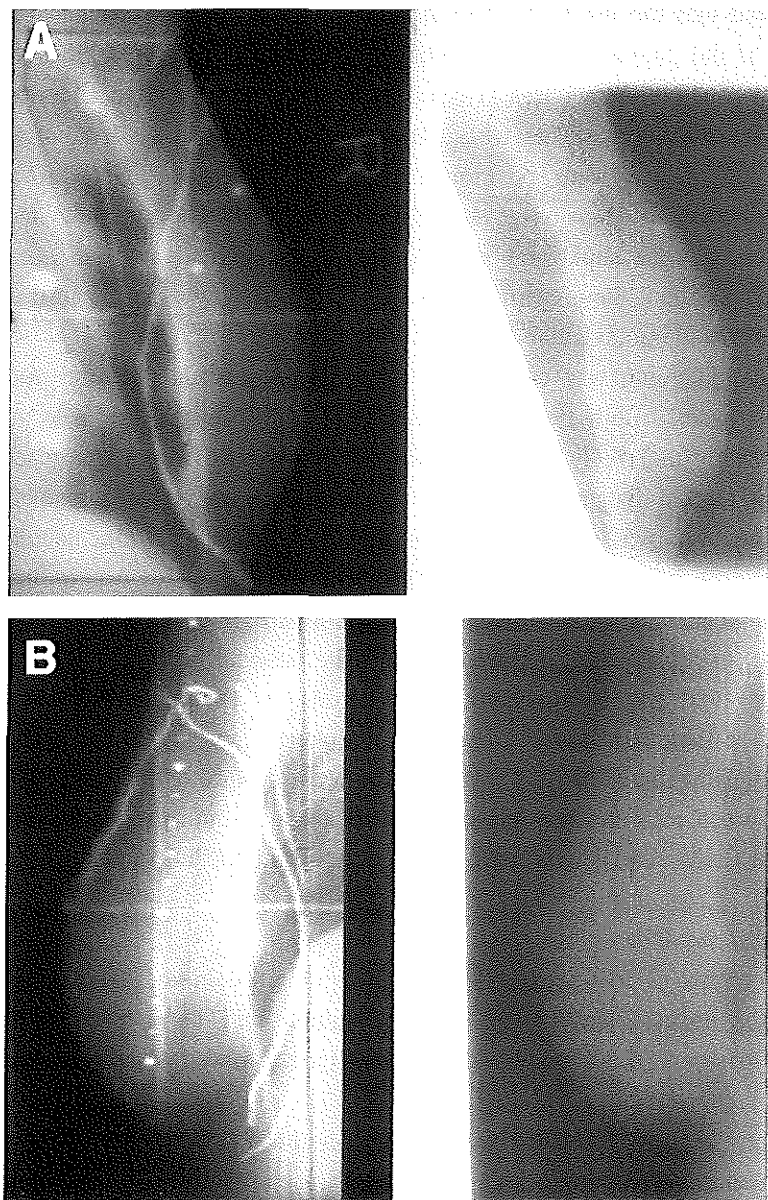


Figure 3

- 3A: Simulation image and corresponding megavolt image of a treatment field for a patient positioned on the flat board (as in Fig. 2A).
3B: Simulation image and corresponding megavolt image of a treatment field for a patient positioned on the wedge-shaped board (as in Fig. 2B).

It was felt that the use of a fixation mask might be more exact because of the fixation of the patient to the treatment couch, and because markings might be more reproducible, being less affected by movements of the shoulder and arm. For this reason, all patients whose treatment was to include irradiation to the regional lymphatics were positioned with fixation masks in order to avoid potential under- or overdosage at the field junctions. The supraclavicular field was matched to the superior border of the tangential fields and shielding blocks were used to block the area of divergence of the tangential beams in the inferior border of the supraclavicular field.

Treatment planning was carried out using opposed wedged lateral and medial tangential beams. Both fields were treated daily, five times a week, to a total dose of 45 Gy in 1.8 Gy fractions using 6 MV photons from a linear accelerator at a focus-to-skin distance of 100 cm. After this, an additional dose of 20 Gy in 2.5 Gy fractions was delivered to the site of the tumor excision, usually with a single electron beam. If irradiation of the regional lymphatics was indicated, this area was treated to a total dose of 40.5 Gy in 2.25 Gy fractions specified at 3 cm depth, using an anterior photon beam. The dose to the midplane of the axilla from this field was calculated and this dose was supplemented with a small posterior axillary field to 40.5 Gy at the midplane.

Megavolt imaging was performed twice a week throughout the radiotherapy series of each patient. MV images were obtained of both the medial and lateral treatment fields and, if irradiated, of the anterior supraclavicular field as well.

Analysis of the data

A total number of 510 megavolt images was obtained in addition to 66 digitized simulation images. Except for the recognition and correction of occasional striking errors (e.g., a misplaced shielding block or wedge), on-line assessment of the images was not performed.

To determine differences between simulation and treatment setup and treatment-to-treatment variations, the megavolt images were compared to the corresponding simulation image and to the first megavolt image, respectively. In earlier studies (26,56) this comparison was accomplished by measuring corresponding distances or by matching of anatomical structures and/or field edges. Using these methods it was difficult to accurately separate variations in patient position from variations in field size and shape. An important advantage

of the present method is the fact that the position of anatomical structures and of field edges can be determined independently.

The rigid design of the detector assembly ensures a fixed position of the beam axis with regard to the detector, as well as a fixed focus-detector distance. Tests of detector movements at different gantry positions have shown an excellent stability, reproducible within 1 mm at the isocenter for all gantry angles. Thus, a fixed coordinate system could be defined in the megavolt images with the origin at the beam center, and the orientation of the axes determined by the collimator angle. A similar coordinate system could be defined in the simulation image by careful alignment of the simulation film on the view box of the simulator work station during digitization (1). As a result, the position of anatomical landmarks and of shielding blocks and field edges could be determined in coordinates relative to a common origin. Thus, variations in the position of the patient in the treatment field and of field size, field shape and position of shielding blocks could be determined independently.

To compare MV images both to the corresponding SIM images and to the first MV image, relevant anatomical points and points on the field edges and shielding blocks were identified (Fig. 4). In each image these points were indicated on the video monitor with a mouse. Using simple mathematics with known translation, rotation, and scaling parameters, the coordinates of the points were calculated in millimeters and were loaded in a spread sheet. The reproducibility of the indication of the points on the video monitor was checked. For repeated indications of the points in the same image the reproducibility turned out to be excellent (1 standard deviation = 0.5 mm).

Special care was taken to detect the field edges in the megavolt images. Due to the strong image enhancement, the visible field edges have been shifted a few millimeters inwards relative to the true field edges. For this reason, detection of the field edges was performed in the raw, unprocessed images. A maximum gradient method (Sobel filter) was applied to determine those pixels in the field edges of the MV images which correspond to the region with the highest dose gradient in the penumbra of the radiation beam. The use of this filter as a method to detect the field edges has been described by Meertens *et al.* (79). In the method used in the present study, this filter was applied twice to each image in four orthogonal directions, resulting in a small black envelope between two white bars, the black envelope representing the true field edge. Tests performed

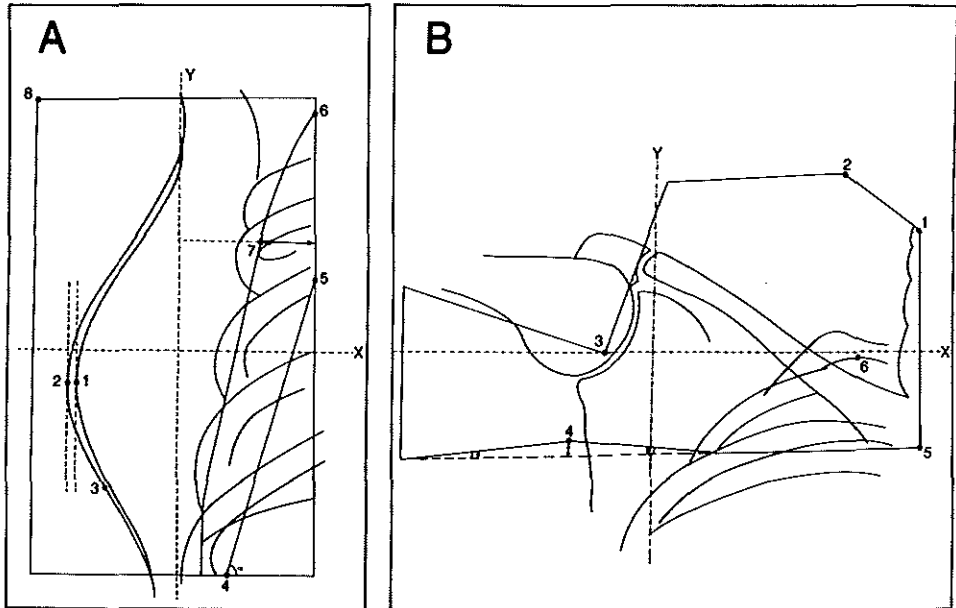


Figure 4

- 4A: Diagram of a tangential breast field showing the points indicated in the simulation images and megavolt images. 1: ventral border of the breast. 2: ventral border of the mask. 3: lead grain marker on the mask. 4: intersection of the lung shielding block with the caudal field edge. 5: intersection of the lung shielding block with the dorsal field edge. 6: intersection of the lung contour with the dorsal field edge. 7: point on the lung contour at a fixed vertical distance from the isocenter. 8: intersection of the ventral and cranial field edges. α : slope of lung block.
- 4B: Diagram of a supraclavicular field. 1,2: intersection of the laryngeal shielding block with the medial and cranial field edges. 3: humerus block. 4: intersection of the two blocks shielding the divergence of the tangential beams. 5: intersection of the medial and caudal field edges. 6: lung top.

earlier had shown the congruity of this envelope with the field edge (by definition the 50% isodose) to be very exact with $1 \text{ SD} = 0.7 \text{ mm}$.

After storage of the data in a spreadsheet, further analysis was performed using a statistical analysis software package. In order to compare treatment setup to simulation setup and to assess treatment-to-treatment variations, the coordinates of the points indicated in the megavolt images were subtracted from those in the simulation image and from those in the first megavolt image, respectively. Thus, SIM-MV differences and MV-MV differences were obtained. The mean SIM-

MV and MV-MV differences for the patient groups with masks and without masks were calculated, along with the standard deviation of the mean and range of extremes. Whenever a SIM-MV difference exceeded 1 standard deviation of the mean, the indication of the points and the storage of the patient data was checked and corrections were applied if required.

Results

The results are presented with emphasis on the potential differences in accuracy between positioning with and without a fixation mask. Mean SIM-MV and MV-MV differences are presented with standard deviations (SD) and range of extremes. For most points, values for medial and lateral fields could be presented together as differences were minimal. Whenever a difference between medial and lateral fields was observed, this is stated in the text.

Position of the patient in the treatment field

Analysis of the position of the ventral border of the breast in the ventral-dorsal direction yielded variations of 3.2 mm (1 SD) and 4.6 mm (1 SD) for positioning with a mask (WM) and without mask (no mask, NM), respectively (Table 1). The position of the lead grain marker on the mask varied 4 mm (1 SD) in the ventral-dorsal (x) direction and 2.7 mm (1 SD) in the cranio-caudal (y) direction (Fig. 5). As a measure of rotation of the patient in the field, the slope of the distal part of breast contour was calculated by drawing a line between a point on the breast contour at a fixed distance from the lead grain marker and the lead grain marker itself, and calculating the angle between this line and the ventral-dorsal (x) axis. The standard deviation of this angle was 3.7° . Most variations appeared to be randomly distributed, as reflected by the fact that mean SIM-MV differences were close to zero. However, for some individual patients systematic differences could be found.

Variations in field size and collimator rotation

A substantial amount of variations in field size was observed. As shown in Table 1, the field width varied with standard deviations of 5.4 mm (WM) and 5.7 mm (NM) and extreme values of up to 20 mm. Field length varied with

standard deviations of 6.9 mm (WM) and 6.5 mm (NM) and extreme values exceeding 20 mm. With regard to variations in field size, no significant differences were observed between positioning with or without a mask, or between medial and lateral treatment fields. On the average, variations were randomly distributed. For some individual patients, however, systematic errors were found (Fig. 6).

Another striking source of SIM-MV differences was observed: compared to the situation at simulation (collimator angle = 0 degrees), rotation of the collimator $> 3^\circ$ was found in 14% (WM) and 21% (NM) of megavolt images. Standard deviations of collimator rotation were 1.5° (WM) and 2° (NM). The two largest rotations (6° and 8°) were observed for lateral treatment fields in positioning without a mask.

Table 1. Mean values, standard deviations, and range of extremes for the differences SIM-MV^a; medial and lateral fields combined

Patient points and field size (Fig. 4A)	Mask (WM) ^b or no mask (NM) ^b	Mean SIM-MV mm	SD mm	range SIM-MV min-max
ventral border of breast (1,2); x	WM	1.1	3.2	-6.9 +9.5
	NM	2.8	4.6	-9.9 +14.2
lead grain on mask (3); x and y	WM,x	0.7	4.0	-11.5 +11.7
	WM,y	-1.3	2.7	-11.1 +4.9
field width (x)	WM	0.7	5.4	-17.6 +20.3
	NM	-1.5	5.7	-20.0 +11.9
field length (y)	WM	-2.3	6.9	-23.1 +16.7
	NM	-1.7	6.5	-18.6 +20.9

^a A negative value of a SIM-MV difference represents a mean shift of a certain point in the megavolt image in the dorsal (x) or cranial (y) direction when compared to the position of that point in the corresponding simulation image.

^b Patients positioned with a fixation mask on the flat board (17 patients) *versus* patients positioned without fixation mask (14 patients) on either the wedge-shaped board (nine patients) or the flat board (five patients).

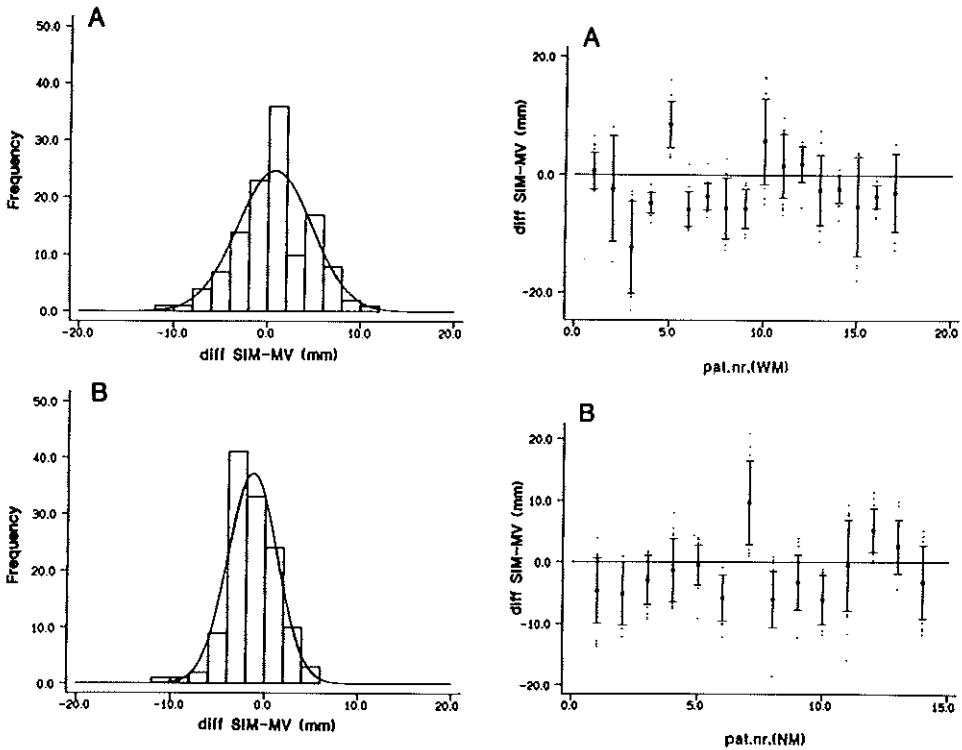


Figure 5 (left)

Histograms of the SIM-MV differences for the position of the lead grain marker on the mask in (A) the ventral-dorsal direction and (B) the cranio-caudal direction for patients positioned with a mask. The curve shows a Gaussian profile fitted to the data.

Figure 6 (right)

Diagrams of the SIM-MV differences for the field length per patient for (A) patients positioned with a mask and (B) patients positioned without a mask: mean differences and standard deviations of the mean. Note the systematic difference for some individual patients.

Position of the lung shielding block

When patients were positioned on the flat board (with or without masks), a lung shielding block was used to align the dorsal field border to the patient's chest contour. Analysis of the position of the lung block was performed using various parameters (Fig. 4). The results are presented in Table 2. Large variations in block position were observed, with standard deviations ranging from 10 mm to 16 mm and an isolated extreme difference of 64 mm. Standard deviations and range of extremes were largest for lateral treatment fields, especially in positioning without a mask.

The distance between the ventral lung border and the dorsal edge of the treatment field was calculated for all patients (Table 2). The distance varied from 0 (no visible lung tissue in the field) to 2.5 times the distance in the simulation image. Obviously, this was in part due to the variations in the position of the lung block and to the variations in field width. For patients positioned with a mask, a trend towards a systematic smaller distance was found. Errors resulting in the absence of any visible lung tissue in the treatment field were found for lateral fields, both in patients positioned with a mask (two patients, for the greater part of the treatment images) and in patients positioned without a mask (three patients, for 1-3 treatment images).

Flat board versus wedge-shaped board

A comparison of the accuracy of patient positioning without a mask on either the flat board (five patients) or the wedge-shaped board (nine patients) was made (not shown). For all parameters, standard deviations and error rates were virtually similar.

Supraclavicular fields

The accuracy of patient positioning in supraclavicular irradiation was studied in four patients. All patients were positioned with a mask on the flat board. The position of the patient, as determined by analysis of the position of the lung top, was more accurate in the transverse (x) direction (SD = 3.9 mm) than in the cranio-caudal (y) direction (SD = 8.0 mm). This appeared to be mainly due to an extreme cranial displacement of one patient. The SD for differences in field size was 5 mm. As for the shielding blocks, the position of the humerus block varied 2.5 mm and 3.5 mm (1 SD) for the x- and y-direction, respectively. The

position of the intersection of the two blocks shielding the divergence of the tangential beams in the inferior edge of the supraclavicular field, however, was found to be very unreliable. Especially in the transverse direction variations were large with a standard deviation of 27.4 mm.

Table 2. Mean values, standard deviations, and range of extremes for the differences SIM-MV^a; medial and lateral fields combined

Patient points and distances (Fig. 4A)	mask (WM) ^b or no mask (NM) ^b	Mean SIM-MV (mm)	SD mm	range SIM-MV mm
intersection lung block-field edge (5)	WM	-3.5	10.2	-42.0 +20.5
	NM	-0.1	14.0	-19.9 +41.6
slope α of lung block (degrees)	WM	0.2°	2.3°	-6.6° +6.1°
	NM	1.4°	5.4°	-6.2° +16.2
vert. distance lung block- lung (5-6)	WM	4.4	16.2	-63.6 +49.5
	NM	5.0	15.8	-47.8 +29.3
hor. distance dorsal field edge-lung (7)	WM	0.3	7.4	-16.7 +27.6
	NM ^c	0.1	5.8	-21.0 +12.1

^a A negative value of a SIM-MV difference represents a mean shift of a certain point in the megavolt image in the dorsal (x) or cranial (y) direction when compared to the position of that point in the corresponding simulation image.

^b Patients positioned on the flat board with a fixation mask (17 patients) *versus* without a mask (five patients).

^c All 14 NM patients.

Treatment-to-treatment variations

The variations in patient positioning in day-to-day treatment setup were analyzed by comparison of the MV-images to the MV image obtained at the first treatment. In general, MV-MV differences turned out to be somewhat smaller than SIM-MV differences, while the overall pattern of differences was essentially similar (Table 3).

Table 3. SIM-MV differences *versus* MV-MV differences: comparison of standard deviations; medial and lateral fields combined

Patient points and distances (Fig. 4A)	Mask (WM) or no mask (NM)	SIM-MV SD mm	MV-MV SD mm
ventral border of breast (1,2); x	WM NM	3.2 4.6	2.1 4.4
lead grain on mask (3); x and y	WM, x WM, y	4.0 2.7	3.1 2.5
field width (x)	WM NM	5.4 5.7	5.5 6.7
field length (y)	WM NM	6.9 6.5	3.6 4.9
intersection lung block-field edge (5)	WM NM	10.2 14.0	12.0 12.9
slope α of lung block (degrees)	WM NM	2.3° 5.4°	2.6° 5.9°
vert. distance lung block- lung (5-6)	WM NM	16.2 15.8	16.4 17.9
hor. distance dorsal field edge-lung (7)	WM NM	7.6 5.8	5.8 5.8

Discussion

The present focus on the accuracy of patient positioning has led to the development of various electronic portal imaging devices (5,80,123,132) and to a recent increase in studies on the accuracy of patient positioning for various tumor sites and positioning techniques. Especially complex fields (26,47,57,64,77,78,112) and head and neck fields -being a treatment site where dose-response curves are considered to be steep (44) and in which the presence of a critical organ close to the high-dose region makes precision imperative- (50,56,76,86) have been the subject of investigation. The earliest studies resulted in an increased attention of radiation oncologists to leaving adequate margins around the target volume and in a more regular use of verification films. As a result, in follow-up investigations a reduction of error rates was found (78,112).

Theoretical considerations (44), as well as clinical studies have shown that an underdosage in the field margins, due either to uncaredful planning of radiotherapy setup or to localization errors, can result in an increase in recurrence rates (64) and even in decreased survival rates (130). These findings have alerted radiation oncologists and physicists to the possible clinical impact of setup inaccuracies.

Field placement error rates reported in the literature vary for the several treatment sites (20,97). A uniform observation of many authors is that, even when mean deviations appear to be small, substantial inaccuracies for individual patients occur. This is also true for treatment setups where immobilization devices are used (50,56). Very little information is available regarding the accuracy of patient positioning in breast cancer. Rabinowitz *et al.* (97) did include two breast cancer patients, positioned with an arm support, in their study of the accuracy of radiation field alignment for a wide range of treatment sites. In the so-called daily study of seven patients who were selected to have daily portal films taken of one field, one breast cancer patient was included. The treatment-to-treatment variation, as reflected by the SD of all measurements performed on these portal films, was 3 mm (left oblique) and 3.8 mm (right oblique) for this patient. The average treatment-to-treatment variation (1 SD) for all patients in the daily study was 3.3 mm. The comparison of the last available portal film of each field with their corresponding simulation films yielded larger variations: a mean average discrepancy of 5.1 mm and a mean worst case discrepancy of 7.7 mm for all sites combined (71 patients). Regrettably, no separate reference to the breast cancer patients is made; probably these patients were included in the group of patients irradiated to thorax sites. For the subset of patients irradiated to the thorax, the mean average SIM-MV discrepancy was 5.8 mm, the mean worst case discrepancy was 9.2 mm and in 15% of patients the worst case discrepancy exceeded 15 mm. The thorax was the site with the highest error rates. Rabinowitz *et al.* (97) concluded that the discrepancies between simulation and treatment were significantly larger than treatment-to-treatment variations at most sites.

Another study referring to setup of breast cancer patients is that by Jakobsen *et al.* (62). They analyzed the setup accuracy of 29 breast cancer patients immobilized on either a foam cast or a new system consisting of an airtight plastic bag containing polystyrol microspheres. On all patients a mastectomy had

been performed and they received postoperative irradiation to the chest wall and the regional lymphatics. Jakobsen *et al.* (62) analyzed the anterior supra-clavicular/axillary fields by comparing the position of the center cross of the treatment field on the portal films to that on the simulation films. Standard deviations of displacement using the new system were 3 mm and 2.9 mm for the transversal and longitudinal direction and 1.4° for rotation of the field center. Displacements ≥ 1 cm occurred in 0.9% of treatments using the new system compared to 3.4% using the old system.

As stated by many authors (20,46,78,97), it is essential to know the accuracy of patient positioning for each treatment site to determine the amount of margin that should be left around the target volume. If reasons for inaccuracies can be identified, positioning techniques can be improved, enabling the use of small but reliable margins. For this reason, a series of prospective studies of the accuracy of patient positioning techniques for the various tumor sites is being carried out in the DDHCC. In earlier surveys the accuracy of patient positioning in the head and neck region (56) and in mantle field irradiation (26) were analyzed. Error rates were relatively modest as compared to the literature. When starting the analysis of the patient positioning in breast cancer, it was expected to find minor inaccuracies, as these treatments form a large part of the daily work load and the technique has been routinely used for over ten years. The position of the patient in the field as such turned out to be acceptable (standard deviations < 5 mm). However, relatively large variations were found for field size (SD 5-7 mm), collimator angle (SD $1.5\text{--}2^\circ$) and block position (SD 10-16 mm). It appeared that the technicians had become used to slightly adjusting the field size and/or collimator rotation in order to obtain a seemingly better congruity of the light beam with the skin or mask markings. As the study was performed shortly before the introduction of a record-and-verify system on this accelerator, these slight adjustments could go unnoticed. As a test, the congruity of some "adjusted" fields with their corresponding simulation images was compared to that of the same "unadjusted" fields (that is, with the field size as prescribed at simulation). As SDs for the "unadjusted" fields were smaller, it appeared that the adjustments had worsened rather than improved positioning accuracy. As adjusting the field size and/or collimator rotation on the basis of external landmarks results in a change in the parameters set at simulation, it cannot be predicted how the adjustments work out relative to the patient's internal

anatomy. Under- or overdosing could occur, especially at the field edges and field junctions. If congruity of the light beam with the skin or mask markings cannot be obtained, the set up should be checked by megavolt imaging and/or by repeating the simulation procedure.

A cause for concern was the large amount of variations in position of the lung shielding block. The alignment of the block to the skin or mask markings was found to be a source of errors, especially in lateral treatment fields. It had been expected that alignment would be more accurate in positioning with a mask, as the markings on the skin might fade with time. Although the standard deviations of the slope of the lung block and of the intersection of the block with the dorsal field edge (point 5 in Fig. 4) were slightly larger in positioning without a mask, this was not the case for the vertical distance between the lung block and the lung contour (Table 2). A possible explanation for the larger variations in lateral fields could be the fact that, to align a block to the skin or mask markings with the gantry at a rotation of $\pm 55^\circ$, the technicians have to bend far down to fix the heavy shielding block to the tray on the collimator. It could be that in this position alignment of the block is more difficult and is carried out as quickly as possible. The pins fixing the block to the tray might not have been fastened precisely at the center of the block, thus allowing the block to tilt somewhat to one side. It should be kept in mind that the tray with the shielding block is at close distance to the focus and thus small inaccuracies in block alignment can result in large deviations. Moreover, as the variations in field width and collimator angle influenced the position of the intersection of the lung block with the dorsal field edge, these variations contributed to the errors in block position.

It has been shown (76,122) that fixation devices can enhance positioning reproducibility. In this study, one of the major questions was if the use of a mask did improve accuracy when compared to positioning without a mask. As can be concluded from the data presented in Tables 1 and 2, no major differences were found. For positioning without a mask, most standard deviations and extreme values tended to be slightly larger than in positioning with a mask. However, variations in the distance between the dorsal field edge and the ventral border of the lung contour (point 7 in Fig. 4) were larger in patients positioned with a mask. No difference was found in the frequency of field "adjustments". Although ideally a precisely fitting mask would be expected to ensure exact repositioning of a patient, it seemed that in daily practice the

intended position could not be easily reproduced, and sometimes the mask appeared to have been put onto the patient with too much pressure. This might have caused a displacement of the breast relative to the markings on the mask, resulting in positioning errors especially for the position of anatomical structures relative to the field edge.

A comparison of the accuracy of patient positioning on the flat board to the wedge-shaped board yielded similar results. However, in positioning of patients on the wedge-shaped board no lung shielding block is used, thus ruling out a source of considerable errors, which seems to be an advantage of this technique. Other advantages of the wedge-shaped board are the ease and speed of patient positioning.

The accuracy of patient positioning for the supraclavicular fields was studied in only four patients. The most striking finding was the inaccuracy of the positioning of the blocks shielding the area of the divergence of the medial and lateral beams at the inferior edge of the field. The angle between these blocks and the inferior field border is small and the points of intersection of the blocks with the field edge might thus be difficult to discern (see Fig. 4B). These substantial variations in block position, together with the malrotations of the tangential fields result in an unintended zone of potential over- or underdosage at the junction of the fields. Elimination of the superior divergence of the tangential beams by rotating the couch 5° , instead of using shielding blocks in the supraclavicular field, might result in a sharper matchline between the fields. However, with the present inaccuracies it can be doubted if a better alignment would have been obtained. Recently, two accelerators with independent collimators have been installed in our institute. In the future these will be used to produce half beam blocking of the tangential and supraclavicular fields, thus removing the divergence in the field junction.

Treatment-to-treatment variations were analyzed by comparison of the MV images to the first MV image. MV-MV differences turned out to be somewhat smaller than SIM-MV differences, indicating that the transition from simulation to treatment yielded larger deviations than repeated treatment setups. This is in agreement with several other reports (46,97). The SDs for variation in position of the patient in the field (Table 3) correspond with the SD for treatment-to-treatment variations of 3 mm as reported by several authors (56,86,97).

However, treatment-to-treatment variations for field size and block positioning were obviously larger.

The findings of this study were presented to the technicians and the radiation oncologists, which resulted in recommendations for improvements which have been implemented in daily practice. Adapting the parameters set at simulation is strongly discouraged and is precluded by the use of record-and-verify systems on all accelerators. Megavolt imaging is now being performed for all the linac's patients at the first treatment, after each setup change and whenever a setup appears to be difficult to reproduce. Check images are obtained at 4 cGy, after which the treatment is interrupted for visual judgement of congruity with the simulation image. If by visual comparison of the megavolt image with the simulation image a relevant inaccuracy is found, the patient is repositioned. If the positioning of the patient cannot be reproduced as determined on the simulator, the simulation procedure is to be repeated before the next treatment. This has resulted in an early recognition and regular checking of setups which can only be reproduced with difficulty. A follow-up study is planned to check if the expected improvements in precision have indeed been achieved.

In conclusion, continuous attention to the accuracy of positioning techniques routinely employed is of utmost importance to achieve maximal precision in radiotherapy. This analysis of the accuracy of a "routine" technique has been shown to result in larger error rates than was expected. The SDs for the position of the patient in the field were comparable to the scarce data reported in literature, but error rates for field size and block positioning were found to be unacceptable. The use of a mask did not seem to improve positioning accuracy. The use of the wedge-shaped board is preferred because of the ease of patient positioning and because the use of a lung block is avoided. The electronic portal imaging device enables both a quick visual on-line comparison of the treatment image to the corresponding simulation image and extensive off-line analyses, thus contributing to precision of patient positioning.

The results of this study and of subsequent studies will be used to improve positioning techniques, and to determine the remaining unavoidable random positioning inaccuracies. It is intended to establish positioning tolerance tables and define critical margins for the various treatment sites in order to use these tables in further projects to develop computer aided on-line setup verification procedures with semi-automatic go/no go decisions.

Acknowledgements

The authors wish to thank D. Binnekamp, the technician of the megavolt imaging project group, for preparing the imaging sessions and for his assistance in the indication of the points in the images and storage of the data. The manuscript was skillfully prepared by Ms. I. Dijkstra. The invaluable assistance of J. Koffijberg and the cooperation of the radiation oncologists of the breast cancer board and of the technicians at the linac is gratefully acknowledged. This project was supported by the Dutch Cancer Society (grant no. DDHK 88-2).

CHAPTER 4

A QUALITY CONTROL STUDY OF THE ACCURACY OF PATIENT POSITIONING IN IRRADIATION OF PELVIC FIELDS

Carien L. Creutzberg, M.D., Vincent G.M. Althof, M.Sc.,
Marjan de Hoog, B.Sc., Andries G. Visser, Ph.D., Henk Huizenga, Ph.D.,
Arendjan Wijnmaalen, M.D., Peter C. Levendag, M.D., Ph.D.

International Journal of Radiation Oncology, Biology, Physics 34: 697-708, 1996

Abstract

Purpose Determining and improving the accuracy of patient positioning in pelvic fields.

Methods and Materials Small pelvic fields were studied in 16 patients treated for urological cancers using a three-field isocentric technique. Large pelvic fields were studied in 17 gynecological cancer patients treated with anterior and posterior (AP-PA) parallel opposed fields. Quantitative analysis of 645 megavolt images and comparison to 82 simulation images were carried out.

Results Small pelvic fields: For the position of the patient in the field, standard deviations of the difference between simulation (SIM) and treatment (MV) images were 3.4 mm in the lateral direction, 5.3 mm in the cranio-caudal direction, and 4.8 mm in the ventro-dorsal direction. Alterations in the positioning technique were made and tested. Large pelvic fields: Differences between simulation and treatment images for the position of the patient in the field were 4 mm (1 standard deviation) in the lateral direction and 6.5 mm in the cranio-caudal direction. A systematic shift of the treatment field in the cranial direction had occurred in the majority of patients. A positioning technique using laser lines and marking of the caudal field border was shown to be more accurate.

Conclusion Studies of positioning accuracy in routine irradiation techniques are needed to obtain data for definition of the margins for each treatment site at each institution. Random variations should be kept at a minimum by monitoring and improving positioning techniques. Treatment verification by megavolt imaging or film should be used to detect and correct systematic variations early in the treatment series.

Introduction

The introduction of highly sophisticated radiotherapy treatment equipment with multi-leaf collimators and of three-dimensional (3D) planning systems with Beam's Eye View facilities allows for high precision therapy to be delivered to the target volume with optimal sparing of normal tissues. As described in the International Commission on Radiation Units and Measurements (ICRU) 50

report (61), the planning target volume (PTV) is defined as the clinical target volume (CTV, i.e. gross tumor volume (GTV) and the region of subclinical disease) with an added margin to compensate for the effects of organ and patient movement and inaccuracies in beam and patient setup. The definition of this margin is essential, as it should be small enough to spare normal tissues and large enough to ensure irradiation of the CTV to the prescribed dose. The reproducibility of day-to-day patient setup might well be the crucial factor for determination of the size of the margins for each treatment technique at each individual institution.

In the Daniel den Hoed Cancer Center (DDHCC), a series of prospective quality control studies is being carried out to determine the accuracy of current positioning techniques. If the technique studied is shown to be reliable and reproducible within acceptable limits, small and safe margins can be defined around the CTV involved. If the study yields higher error rates than expected, the technique should be altered to improve its accuracy, after which the reproducibility should again be checked to ascertain the size of margins to be used.

In earlier studies the accuracy of patient positioning was evaluated in mantle field irradiation (26), in head and neck cancer (56) and in irradiation of breast cancer (24). The studies of head and neck cancer and of mantle fields showed modest error rates as compared to literature data. However, the study of patient positioning in breast cancer yielded larger error rates than was expected, stressing the importance of continuous attention to the accuracy of "routine" irradiation techniques. The present study was carried out to evaluate the accuracy of patient positioning in irradiation of pelvic fields. The study consisted of two parts, investigating treatment setup accuracy in small and large pelvic fields, respectively.

Methods and Materials

Two separate studies were carried out. In the first study, the accuracy of patient positioning in irradiation of small pelvic fields for urological cancers was investigated. The study group consisted of 16 patients treated for bladder or prostate cancer between October 1989 and June 1990. In the second study,

carried out between July 1990 and March 1991, large pelvic fields were investigated in 17 patients treated for cancer of the cervix or endometrium. In addition to both studies, follow-up studies were done to check if alterations, made as a result of the studies, had indeed improved positioning accuracy. The design and the results of the studies will be described separately.

Treatment technique in urological cancer

All patients were treated using computerized tomography (CT) planning. The patient was positioned for CT scanning in the supine treatment position on a flat couch. Using alignment lasers, a cranio-caudal midline reference line and two lateral lines were drawn on the patient's skin. Oral contrast was used for small bowel visualization and a radioopaque catheter was placed on the cranio-caudal reference line. The CT slice thickness and spacing were 10 mm. The CT information was sent to a planning system. The outlines of the target volume and of the organs at risk were drawn in every slice by the radiation oncologist responsible for the patient's treatment. The GTV was defined as the prostate gland (including, except for T1 tumors, the seminal vesicles) or the bladder, respectively. Usually, for the PTV a margin of 1.5 cm was added (0.5 cm for subclinical spread and an additional 1 cm to allow for patient movement and geometrical inaccuracies). A three-field isocentric technique with an anterior (AP) field and two wedged posterior oblique (PO) fields was used in all patients. The dose was specified at the isocenter. Simulation of the treatment plan was carried out. At simulation, a field center tattoo was placed, and two lateral skin markings were drawn at equal heights to minimize rotation of the pelvis. Treatment was carried out using 6 MV photons from a linear accelerator at a source-isocenter distance of 100 cm. All fields were treated daily, five times a week, to a total dose of 66 Gy using 2 Gy fractions. Prostate cancer patients were both CT scanned and treated with a full bladder to push the small bowel out of the field; patients with bladder cancer were asked to empty their bladder before scanning and treatment to keep the treatment volume as small as possible. The patients were positioned on the treatment couch in the same position as at CT scanning and simulation. Alignment was carried out using wall pointers. The source-skin distance (SSD) was calculated from the treatment plan and was used for patient setup. At the time of the study, no treatment verification/registration system was operational at the accelerator.

Follow-up studies

In 1991, alterations in the positioning technique were made which consisted of the use of a styrofoam table top to prevent sagging of the polycarbonate (mylar) film window, and the use of the isocenter-couch distance for patient setup. Furthermore, regular megavolt imaging was used at the first treatment fraction. A pilot study was carried out in August 1991 to check if positioning accuracy had been improved.

In 1992, a Netherlands collaborating group for Megavolt Imaging was started and a verification and correction procedure for small urological fields was designed and tested. As a pilot study, a series of 9 patients, treated December 1992 - January 1993, was studied to determine the feasibility of this procedure, and its effect on the incidence and magnitude of systematic errors.

Treatment technique in gynecological cancer

All patients were treated to the whole pelvis using anterior (AP) and posterior (PA) parallel-opposed fields encompassing the (site of the) uterus and adnexa, the parametria, the proximal two-thirds of the vagina, and the hypogastric and common iliac lymph node drainage areas. Patient positioning was carried out using a standardized technique developed in the DDHCC and in use since the early 1970s. This technique was designed at the time to avoid the use of skin markings on these often obese patients and use the pelvic bones for setup instead. The patient is positioned in the supine position on a special device consisting of a thin aluminium plate and two vertical hip supports with centimeter scales (Fig. 1A). Rotation of the pelvis is prevented by placing small metal plates over the hip supports and comparing the scales to ensure equal height on both sides. A so-called pair of compasses is used to ensure correct midline positioning of the patient (Fig. 1B). A vertical stand is fixed to the aluminium plate and a vertical pin is attached to the horizontal bar of the stand (Fig. 1C). The pin is then pushed against the pubic bone and the position of the pin on the horizontal bar is measured and noted for definition and daily reproduction of the cranio-caudal level of the field center. Using this technique, the positioning of the patient takes approximately 7 minutes.

At simulation, the cranial, caudal, and lateral edges of the treatment field are defined, and simulation films are taken. The radiation oncologist indicates the treatment field on the simulation films, after which a transparent sheet is

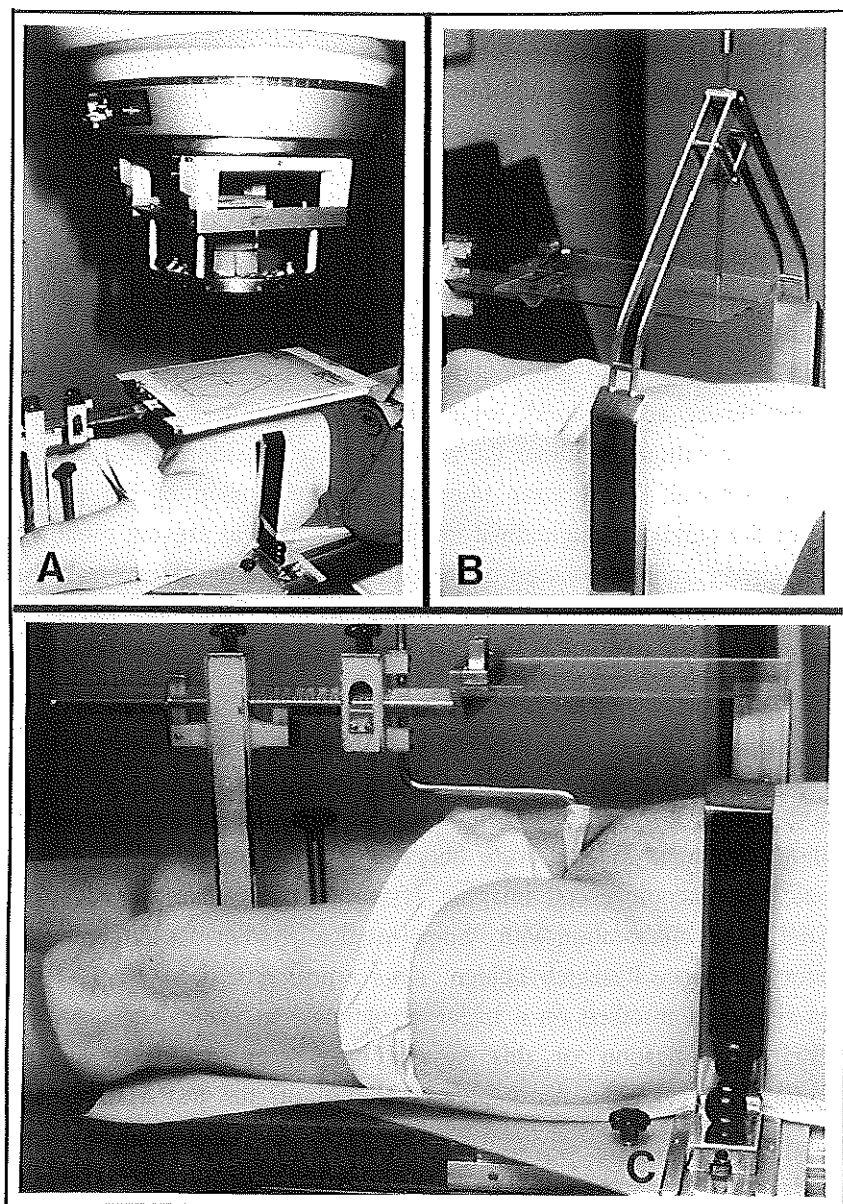


Figure 1

The positioning device for gynecological cancer patients. (A) Base plate, hip supports, and transparent sheet for block placement. (B) Midline positioning of the patient. (C) The vertical pin for cranio-caudal field orientation.

produced to be used for daily placement of the shielding blocks. Divergent shielding blocks are aligned to the markings on the transparent sheet and are fixed to a tray on the head of the linear accelerator. Both AP and PA fields are treated daily to a total dose of 46 Gy in 2 Gy fractions, using 6 MV photons at an SSD of 100 cm.

Follow-up study

In 1992, an alternative positioning technique using long laser lines was tested against the traditional technique in a small pilot study, and late 1993 a further series of 15 patients were positioned and treated using the new technique. On one of the newer accelerators³, which is equipped with alignment lasers, the patients were positioned without the special device. Positioning was carried out using long vertical lateral laser lines, to prevent torsion of the patient and rotation of the pelvis; a longitudinal midline laser line, to prevent torsion and to ensure a correct midline position of the patient; and a long transversal line with tattoos, for marking the caudal field border. In this positioning technique, the caudal field border and the transversal laser line are the main parameters for setup.

Megavolt imaging and analysis of the data

For both study groups, megavolt imaging was carried out twice a week throughout treatment. Images were obtained of all treatment fields using a fast electronic fluoroscopic portal imaging system⁴. This system was developed in the DDHCC in collaboration with Philips Medical Systems Radiotherapy and the Laboratory of Space Research Leiden. After a prototype phase (1985-1989), the product type was installed on a linear accelerator⁵ in 1989. The characteristics and clinical application of this system have been described in previous publications (1,2,24,123). An important feature of this fast on-line electronic

³ Siemens KD2, Siemens Medical Laboratories, Concord, California 94520, USA

⁴ Philips SRI-100 Radiotherapy Imaging System, Philips Medical Systems Radiotherapy, Crawley, West Sussex RH10 2RR, United Kingdom

⁵ Philips SL-75/10, Philips Medical Systems Radiotherapy, Crawley, West Sussex RH10 2RR, United Kingdom

imaging device is the fixed position of the detector with regard to the beam axis. This allows for the use of a common coordinate system in the digitized simulation (SIM) and megavolt (MV) images with the origin at the beam center and the orientation of the axes determined by the collimation system.

A total number of 645 MV images (406 and 239 images of the small and large pelvic fields, respectively) was obtained in addition to 82 (48 and 34) digitized SIM images. On-line assessment of the images was not performed. Relevant anatomical points and points on the field edges and shielding blocks were defined (Fig. 2) and indicated in each image on the video monitor with a mouse. The coordinates of these points were loaded in a spreadsheet and further analysis was performed using a statistical software package⁶. The reproducibility of the indication of the points on the video monitor was checked. The standard deviation of repeated indications of the points in the same image was 0.5 mm for both small and large pelvic fields. Field edge detection was carried out by applying the Sobel gradient operator twice to each unprocessed image in four orthogonal directions, resulting in a small black envelope between two white bars, the black envelope representing the true field edge (24). Earlier tests had shown the congruity of the field edges thus obtained with the true field edges (by definition the 50% isodose) to be accurate with 1 SD = 0.7 mm.

Differences between simulation and treatment setup were determined by comparison of the MV images with the corresponding SIM image. Differences between simulation and treatment images (SIM-MV) were calculated in mm at the isocenter. The position of the patient in the treatment field, the field size, and the position of shielding blocks were determined independently. This method of analysis was described in more detail in a previous publication (24).

The overall accuracy of a patient positioning technique is reflected by the standard deviations of the mean SIM-MV differences, averaged over all patients. If mean values of SIM-MV differences are close to zero, there are no *overall* systematic variations. However, for individual patients, systematic variations do occur. To separate random and systematic variations and to identify individual systematic variations, further analysis was carried out. To identify the *random* variation of a parameter, the spread of the SIM-MV differences around the

⁶ STATA, release 3.1; Stata Corporation, College Station, Texas 77840, USA

corresponding mean was calculated in each patient. For the total group of patients the average of these standard deviations for individual patients was taken as a measure for the random variations (defined as σ by Bijhold *et al.* (15)). It was verified that the average standard deviation was close to the result calculated by taking the "within patients" sum of squares divided by the number of degrees of freedom. The *systematic* variation of a parameter was calculated by determining the spread (1 SD) in the individual mean SIM-MV differences. The mean value of these individual mean SIM-MV differences represents the overall systematic variation, and the standard deviation of this distribution represents the magnitude of individual systematic variations (corresponding with Σ as defined by Bijhold *et al.* (15)). Thus, the *overall* accuracy is represented by the overall SD; the *random* variation by σ , the average SD of the SIM-MV differences per patient; and the systematic variation by Σ , the SD of the mean SIM-MV differences.

Results

Small pelvic fields for urological cancer

In AP fields, field size variations were surprisingly high (SD = 4.8 mm for both field width and length; extreme values of SIM-MV differences were 38 and 40 mm). This was found to be caused by the erroneous interchange of field width and length on three occasions (3 patients, for each patient at one fraction). A record-and-verify system was not yet operational at the time. Excluding these 3 patients, SDs for field width and length were 2.0 and 2.7 mm with extreme values of 3 and 10 mm. For PO fields, field size SDs were 3.0 (width) and 5.1 mm (length). The interchange of field width and length had been detected and corrected before irradiating the PO fields in 2 patients. Exclusion of the third patient yielded field size SDs for the PO fields of 2.8 mm (width) and 3.6 mm (length).

For AP fields, the position of the patient in the field was analyzed using four bony landmarks (Fig. 2A). The position of the patient in the field was more accurate in the medio-lateral (ML) direction (SD 3.3 - 3.8 mm) than in the cranio-caudal (CC) direction (SD 5.3 - 5.7 mm).

For PO fields, the femoral heads were used to analyze the position of the patient in the field (Fig. 2B, points 2 and 3 for the ventro-dorsal direction, and point 4 for the cranio-caudal direction). Rotation in the hip joint was measured by calculation of the angle between a line connecting points 2 and 5 and the caudal field border. The SD of this angle was 5.0° . As rotation in the hip joint does influence the position of point 2 in the ventro-dorsal direction, it was decided that point 3 be used for analysis of the position of the patient in the field for the ventro-dorsal direction.

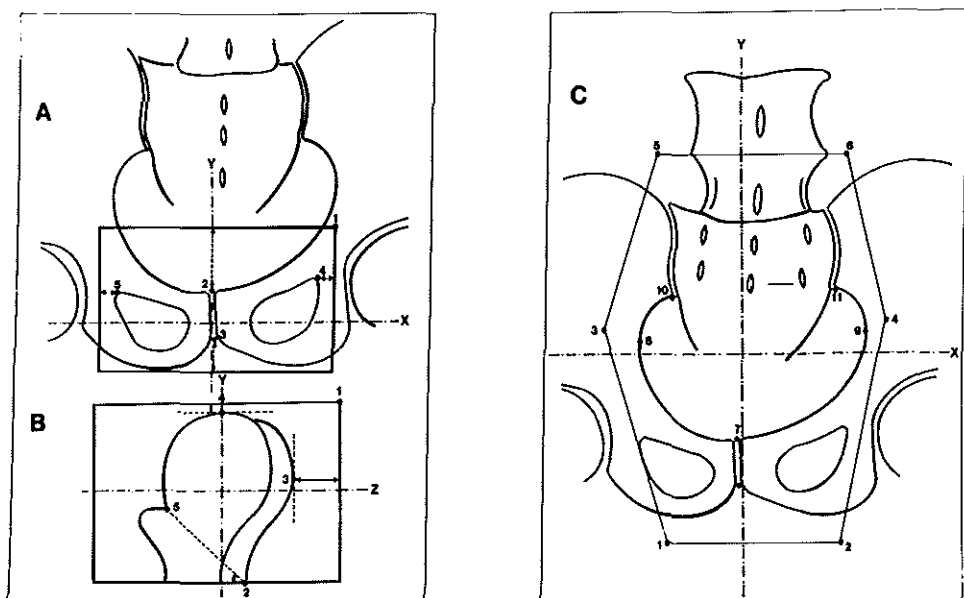


Figure 2

- 2(A): Diagram of a small pelvic field for urological cancer: AP field. 1: upper left field corner. 2: upper margin of pubic symphysis. 3: lower margin of pubic symphysis. 4: upper corner of left obturator foramen. 5: upper corner of right obturator foramen.
- 2(B): Diagram of a small pelvic field for urological cancer: PO field. 1: upper ventral field corner. 2: intersection of the femoral shaft with the caudal field border. 3: ventral border of the femoral head. 4: cranial border of the femoral head.
- 2(C): Diagram of a large pelvic field for gynecological cancer. 1-6: intersection of the shielding blocks with the field edges. 7: upper margin of pubic symphysis. 8: lateral edge of true pelvis, right. 9: lateral edge of true pelvis, left. 10: inferior aspect of sacroiliac joint, right. 11: inferior aspect of sacroiliac joint, left.

In Tables 1 and 2, the overall accuracy (SD) of patient positioning is presented, along with the systematic (Σ) and random (σ) components, for AP and PO fields respectively.

Table 1. Differences between simulation and treatment (SIM-MV^{*}): small pelvic fields (AP)

Patient points and field size [†] (Fig. 2B)		SD [*] mm	Systematic [*] Σ mm	Random [*] σ mm
field width	x	2.0	1.4	1.4
field length	y	2.7	1.7	1.8
Pubic symph (2)	x	3.4	2.3	2.5
range points 2-5	x	3.3-3.8	2.2-2.8	2.3-2.7
Pubic symph (2)	y	5.3	3.9	3.8
range points 2-5	y	5.3-5.7	3.9-4.6	3.7-4.0

* The standard deviation (SD) of the mean values of the difference between the position of the respective points, or of the field size, in the simulation and treatment images (SIM-MV), the systematic variations, and the random variations. For definition and calculation, see text.

† Field size after exclusion of three field width-length interchanges (see text).

Follow-up studies

In Fig. 3 the results of the study of 9 patients using the verification and correction rule are compared to those of the first study. Random errors were reduced to 2.7 mm (x), 2.5 mm (y) and 2.3 mm (z), and systematic errors to 1.3 mm (x), 2.0 mm (y) and 2.1 mm (z), respectively. This improvement

appeared to be statistically significant for the systematic errors in the lateral direction ($p = 0.04$ with the F-test, $p = 0.06$ with a nonparametric test [Wilcoxon Rank-Sum test]). The improvement in the cranio-caudal direction did not yet reach statistical significance ($p = 0.09$).

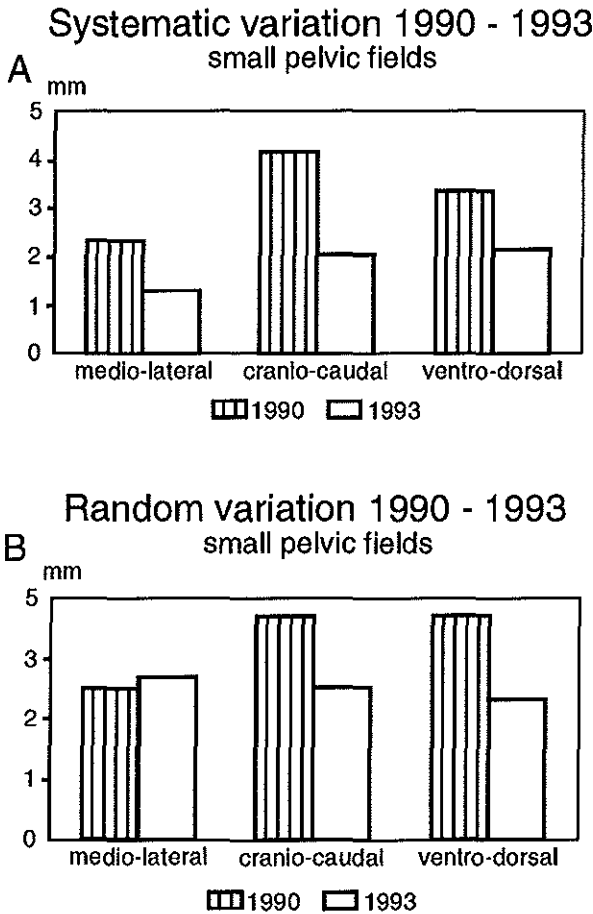


Figure 3

Histograms of (a) systematic and (b) random variations (1 SD) in the position of the patient in small pelvic fields in respectively, the medio-lateral, cranio-caudal, and ventro-dorsal directions. Comparison of the results of the 1990 study and the 1993 feasibility study using the verification and correction procedure. Note the reduction in systematic errors in the 1993 study.

Table 2. Differences between simulation and treatment (SIM-MV*): small pelvic fields (right and left oblique fields combined)

Patient points and field size [†] (Fig. 2B)	SD* mm	Systematic* Σ mm	Random* σ mm
field width (z)	2.8	2.2	1.9
field length (y)	3.6	3.0	2.0
Femoral head (3) (z)	4.8	3.3	3.7
Femoral head (4) (y)	5.7	4.2	3.6

* The standard deviation (SD) of the mean values of the difference between the position of the respective points, or of the field size, in the simulation and treatment images (SIM-MV), the systematic variations, and the random variations. For definition and calculation, see text.

[†] Field size after exclusion of the patient with a field width-length interchange (see text).

Large pelvic fields for gynecological cancer

In these fields, the field length is determined by the actual cranial and caudal field (collimator) edges, while the field width is determined by a combination of the field edges and the shielding blocks. In 13 patients, the field was too long with respect to the detector, so in these patients, the field length could not be measured. The results for field length are those of the remaining 4 patients (71 measurements). The other parameters could be measured in all patients. As the results for AP and PA fields differed only minimally, they were analyzed together.

The results are presented in Table 3. For representation of the position of the patient in the field, both the pubic symphysis (point 7) and a combination of points 7, 8, and 9 (x-direction) and 7, 10, and 11 (y-direction) were used (Fig. 2C and Table 3). Small differences between these values could be caused by a rotational component. For the position of the patient in the cranio-caudal

direction, mean SIM-MV differences were 2.3 mm (mean movement of the MV field in the cranial direction), with SD values of 6.3-7.3 mm and both random and systematic components of 4.5-5 mm. As illustrated in Fig. 4, systematic deviations occurred for most patients, with a field shift in the cranial direction in the majority of patients.

In-plane rotation of the patient was measured by calculating the slope of the lines connecting point 7 and points 8, 9, 10, and 11, respectively; the results were essentially the same, with 1 SD = 3° and extreme values up to 11°.

Table 3. Differences between simulation and treatment (SIM-MV): large pelvic fields (AP and PA combined)

Patient points and field size (Fig. 2C)	Mean SIM-MV* mm	SD* mm	Systematic* Σ mm	Random* σ mm
field width (x)	0.2	4.1	3.5	1.9
field length (y)	1.8	2.8	2.5	1.3
Pubic symphysis (7) x	0.7	4.4	3.1	3.4
Pubic symphysis (7) y	2.3	6.3	4.4	4.5
Patient position (x) range points 7-9	0.7-0.7	3.6-4.4	2.5-3.1	2.7-3.4
Patient position (y) range 7, 10, and 11	1.8-3.3	6.3-7.3	4.4-5.1	4.5-5.3
Rotation along z-axis (7-8;7-9)	1.0°	3.1°	2.2°	2.2°

* The mean values of the differences between the position of the respective points, or of the field size, in the simulation and treatment images (SIM-MV), the standard deviation (SD) of the mean, the systematic variations, and the random variations. A negative value of a mean SIM-MV difference represents a mean shift of that point in the MV images in the right lateral (x) or cranial (y) direction.

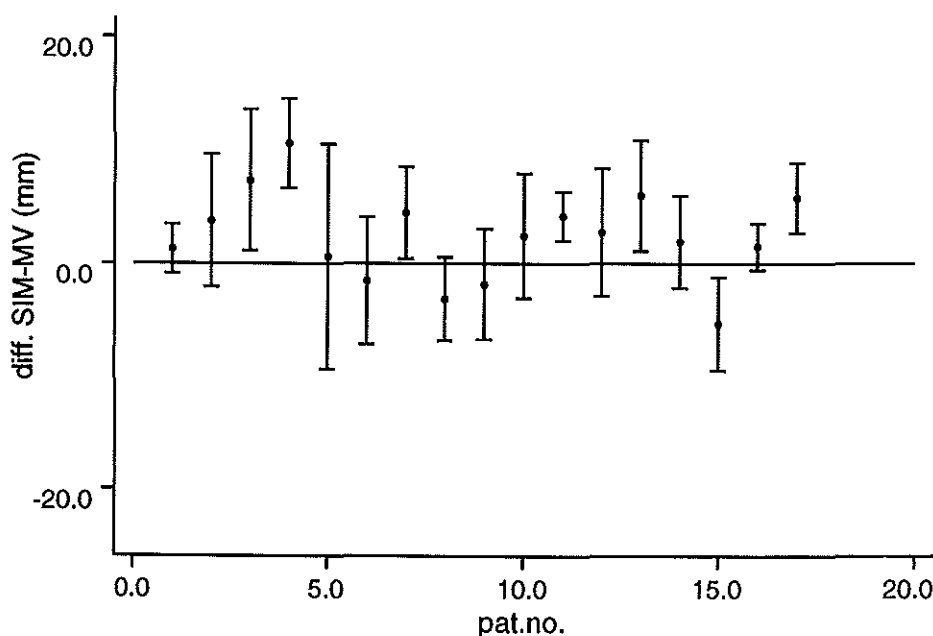


Figure 4

Large pelvic fields for gynecological cancer. Diagram of the SIM-MV differences for the position of the pubic symphysis (point 7 in Fig. 2C) in the cranio-caudal direction: mean differences and standard deviations of the mean per patient. Note the systematic shift of various patients in the caudal direction (field moving in the cranial direction).

Follow-up study

Table 4 summarizes the positioning accuracy of the 15 patients positioned using the technique with long laser lines and marking of the caudal field border. As this study had been carried out with megavolt films, the possibilities for contrast enhancement were more limited than in the previous study. As a result, the presence of the shielding block tray in the images often impaired the assessment

of the exact location of the pubic symphysis in the x-direction and of the sacro-iliac joints in both the x- and y-directions. Thus, the pubic symphysis was used to represent the position of the patient in the y-direction and the points on the lateral pelvic edges (points 8 and 9 in Fig. 2C) to represent the position in the x-direction. The results for the medio-lateral direction turned out to be essentially the same as those from the traditional technique (Tables 3 and 4). For the cranio-caudal direction, however, positioning accuracy was improved (Σ 3.1 mm vs. 4.4 mm; σ 3.0 mm vs. 4.5 mm); this difference was statistically significant for σ ($p < 0.01$ using the Student T-test (mean comparison test)). For Σ , the difference was not statistically significant ($p = 0.45$ according to the F-test and according to a nonparametric test (Wilcoxon Rank Sum test)).

To determine if the position of the pubic symphysis was indeed representative of the cranio-caudal position of the patient in the treatment field (rotational influences could cause differences between the position of this point and the points on the sacro-iliac joints) we determined the position of the patient using an anatomical match in a subset of 5 patients. The pelvic rim was indicated in the treatment images, and by matching this contour with that in the simulation image, SIM-MV differences for the medio-lateral and cranio-caudal directions could be calculated, as well as the in-plane rotation. The SDs for both directions turned out to be similar to those determined by analyzing the position of the pubic symphysis for the y-direction and the points on the pelvic rim for the x-direction. Rotations were shown to be modest: mean -0.5° , SD 1.6° , extremes -5° to $+3^\circ$.

Discussion

The recent literature has shown an increase in studies of the accuracy of patient positioning for various tumor sites and positioning techniques. Particularly reports on an increase in recurrence rates (64) and/or reduction in survival rates (130) caused by underdosage in the field margins, have alerted radiation oncologists to the possible clinical impact of positioning inaccuracies. Studies have demonstrated that attention to adequate margins around the target volume, and regular use of treatment verification, results in a reduction of error rates (48,78,112). These findings have led to an increased use of portal imaging, and

Table 4. Differences between simulation and treatment (SIM-MV): large pelvic fields (positioning technique with long laser lines and marking of the caudal field border; AP and PA combined)

Patient points and field size (Fig. 2C)	Mean SIM-MV* mm	SD* mm	Systematic* Σ mm	Random* σ mm
field width (x)	-0.1	3.6	3.1	1.7
field length (y)	-2.0	3.7	2.5	2.5
Patient position (8, 9); x	0.8-1.3	4.0-4.5	2.3-3.1	3.2-3.3
Patient position (7); y	-1.5	4.2	3.1	3.0
Rotation along z-axis (7-8;7-9)	-0.5	1.6	1.1	1.1

* The mean values of the differences between the position of the respective points, or of the field size, in the simulation and treatment images (SIM-MV), the standard deviation (SD), the systematic variations, and the random variations. A negative value of a mean SIM-MV difference represents a mean shift of that point in the MV images in the right lateral (x) or cranial (y) direction.

to the development of fast electronic portal imaging devices, allowing both quick on-line estimates of the setup accuracy and extensive off-line analyses. The present interest in conformal therapy has made exact knowledge of the accuracy of the positioning technique involved, and its verification, essential.

Pelvic fields have been the subject of several studies of positioning accuracy (15,28,32,46,99), since in general surveys of positioning accuracy (20,97) the pelvis was shown to be a site of relatively large errors, and because the pelvis is a site of high-dose curative treatment with the presence of critical, dose limiting normal tissues. Rabinowitz *et al.* (97) found for pelvic fields an average SIM-MV discrepancy of 5.6 mm and an average worst case discrepancy of 8.4 mm. Griffiths *et al.* (46) studied various setup methods in 20 patients treated to parallel opposed pelvic fields for gynecological cancers. Standard deviations for

lateral shift were 1.4 - 2.7 mm; for cranio-caudal shift, they were 2.9 - 4.5 mm. The use of alignment lasers reduced both the incidence and the maximum value of lateral shift errors. Errors were larger when a mattress was used and with increasing patient diameter. In a study of on-line portal imaging by De Neve *et al.* (28), 566 parallel opposed pelvic fields were evaluated in 13 patients. Portal images were immediately evaluated and, whenever a visible error was detected, corrective table adjustments were applied using a telecontrolled patient couch. In 54.5% of the fields, adjustments were performed. A setup method matching a longitudinal laser line and the caudal field border was shown to be more accurate in the cranio-caudal direction. Portal imaging and adjustments caused a 45% mean increase in treatment time. Balter *et al.* (6) performed simulations of on-line repositioning. He showed that repositioning of the field for those treatments in which an error of ≥ 1 cm is found, results in improvement in the cumulative dose distribution.

Bijhold *et al.* (15) developed a decision protocol for correction of systematic errors in patients receiving three-field pelvic irradiation for prostate cancer. A 3D displacement vector was calculated from the 2D vectors measured in the AP and lateral fields. Using a 99 or 95% confidence level based on the average value of the vectors measured, a decision rule was applied: a correction was performed if the deviation was outside the confidence region. On consecutive days additional images were taken, and the resulting displacement vectors were averaged with the previous vectors. Thus, by averaging, the influence of random variations on the displacement vector decreased, and the action level could be taken lower (i.e. at the 67% confidence level). The average systematic and random shifts for all patients were 1.2 mm and 1.7 mm in the lateral direction and 2 mm and 2.4 mm in the cranio-caudal direction, resulting in an overall SD of 3 mm.

In the present study, as in most of the other studies, the variations in patient position were larger in the cranio-caudal direction than in the lateral direction. Systematic and random components of the overall variations were similar, a finding which is in agreement with those of Bijhold *et al.* (15) and Huizenga *et al.* (56). As the study consisted of two separate patient groups, irradiated to different target volumes and using different positioning and treatment techniques, these will be discussed separately.

Small pelvic fields for urological cancer

The overall accuracy of patient position in the lateral direction was within acceptable limits (1 SD 3.4 mm), but for both the cranio-caudal and ventro-dorsal directions, the SDs were ≥ 5 mm. The variations in the cranio-caudal direction might be due to movement of the skin markings relative to the patient's anatomy. Respiration, weight loss, and possibly relaxation of the patient might be factors causing movement of the center tattoo, and rotation in the hip joints might result in movement of the lateral skin markings.

The variations in the ventro-dorsal direction were considered to be mainly due to two factors. First, the practice to calculate the SSD from the treatment plan and use this for patient setup, could be a source of errors, as the SSD is influenced by abdominal movement (respiration) and patient diameter (weight loss). Secondly, it was found that the polycarbonate (mylar) film window of the treatment couch was not rigid enough and tended to sag under the patients' weight, thus causing errors in the ventro-dorsal direction. It was subsequently decided that the isocenter-couch distance was to be used for patient setup instead of the SSD, and that a rigid styrofoam table top would be used to prevent sagging of the polycarbonate (mylar) film window. Furthermore, a verification protocol was started for all patients, in which on-line verification of the treatment field was carried out at the first or second treatment session. If, by on-line comparison of the treatment field with the simulation image, a relevant inaccuracy was found, the patient was repositioned. If this did not improve the accuracy, the simulation procedure was repeated before the next treatment fraction.

In 1993, a pilot study was carried out in a study group of 4 patients to check if the alterations had led to an improvement of accuracy. Standard deviations for patient position were 4.2 mm in the lateral direction, 2.9 mm in the cranio-caudal direction, and 4.5 mm in the ventro-dorsal direction. Standard deviations for field width and length were 2 mm, reflecting the present use of a verification system on the accelerator. As these results were from only a small group of patients, no tests for significance were performed. It was concluded that there was a trend of improved accuracy in the cranio-caudal and ventro-dorsal directions and this technique was subsequently used in the 1992-1993 study. This study, using a verification and correction protocol, did yield a statistically significant improvement in the systematic variations (Fig. 3).

Both in the present study and in the other studies of positioning accuracy in pelvic fields, the position of the pelvic bony structures in the field was used to ascertain the setup accuracy. However, the true accuracy of the treatment can only be judged in this way if the assumption, that the position of the prostate and/or the bladder within the pelvis is more or less fixed, is correct. The question of to what extent the bony structures of the pelvis represent the true position of the prostate or the bladder in the field, has been addressed by several authors (8,10,54,81,113), using ^{125}I seed implants or CT scans to compare the position of the prostate to that of the bony pelvis. Results of these studies have been summarized in Table 5.

Table 5. Displacement of the prostate gland within the bony pelvis: literature data on prostate motion

Author	Method	x*	SD* y*	z*
Hoekstra <i>et al.</i> (54)	I-seeds	1 mm	2 mm	1.5 mm
Balter <i>et al.</i> (8)	markers	0.8 mm	1.8 mm	2.2 mm
Ten Haken <i>et al.</i> (113)	I-seeds/CT	-	-	average 3 mm
Beard <i>et al.</i> (10)	CT scans supine	0-3 mm median 1	-	0-16 mm median 4.5
Melian <i>et al.</i> (81)	CT scans prone	0-15 mm	-	0-30 mm

* The standard deviations (SD) of displacement, or the range of absolute displacements, in the medio-lateral (x), cranio-caudal (y), and ventro-dorsal (z) directions.

It can be concluded from these studies that prostate motion within the bony pelvis is not insignificant, and that studies measuring the motion of the borders of the prostate gland on a series of CT scans yield larger shifts than studies measuring the motion of implanted ^{125}I seeds. Thus, prostate motion has to be taken into account when choosing the margin around the CTV for patient and/or

organ movement and geometrical inaccuracies. If values of 1 mm (1 SD) for the lateral direction, 2 mm for the cranio-caudal direction, and 5 mm for the ventro-dorsal direction are taken to represent the average prostate motion for the supine position as observed in these studies, then these data can be incorporated into the margin needed to account for positioning variations. In Table 6, an example of the calculation of margins is given: the SDs for prostate motion and those for positioning variations in the respective directions, as observed in the present study, have been added quadratically, and the 95% confidence interval (2 SD) was chosen to represent a safe margin. Table 6 shows margins to account for positioning inaccuracies as found in the present study, and the reduction of the size of margin which could be obtained in the "ideal" situation in which regular verification eliminates the systematic variations.

Table 6. Margins* calculated to account for geometrical inaccuracies in the treatment of pelvic fields for urological cancer

Direction	Margin based on overall accuracy of patient position	Margin based on overall accuracy and prostate motion	Margin based on random errors and prostate motion
cranio-caudal	10 mm	11 mm	9 mm
medio-lateral	7 mm	7 mm	6 mm
ventro-dorsal	10 mm	14 mm	12 mm

* The margin is defined as the 95% confidence interval (2 SD). Standard deviations (SD) for positioning accuracy and prostate motion have been added quadratically and rounded off to integral mm.

Roach *et al.* (100) calculated margins to account for setup variations and organ motion as well. In a theoretical patient, treated with a six-field conformal technique, margins for all six field directions were calculated using data on positioning variations, organ motion, and extracapsular extension in the respective directions. Using this sophisticated approach, margins ranging from 0.75 - 2.25 cm were required to ensure adequate coverage of the target volume while minimizing the volume of normal tissues irradiated. From studies as these

it is clear that in situations where the tightest possible margins are chosen (as in conformal therapy), the size of the margin should be based on positioning studies, performed in the same institution, to prevent marginal misses.

Large pelvic fields for gynecological cancer

The large SDs (6.3 and 6.9 mm) for patient position in the cranio-caudal direction were considered unacceptable. This finding, and the fact that systematic shifts of the treatment field had occurred mostly in the cranial direction, while the caudal field border is the most critical anatomical edge, prompted a search for the cause of these deviations. It was concluded that in this positioning technique the vertical pin (which is pushed against the pubic bone) was the only factor determining the cranio-caudal orientation of the patient. As this pushing of the pin is uncomfortable for the patients, especially in the second half of the treatment series, radiotherapy technicians may feel somewhat awkward using it. As a result, the pressure applied is susceptible to variations in use by different technicians and to variations over the treatment weeks. A pilot study was carried out to determine if the technique could be improved by drawing transverse skin markings over the iliac spine on both sides and placing a tattoo over the sternum, and using these markings for cranio-caudal field orientation instead of the pin. However, this pilot study yielded essentially the same results as the previous study (results not shown). Combining these findings and the results of De Neve *et al.* (28), who found a significantly higher accuracy for a positioning technique in which a longitudinal laser line and the lower field border were matched, a second pilot study was set up. Four patients were positioned without the special device using long laser lines and marking of the caudal field border. This study group was compared with a group of 4 patients treated on the same accelerator using the traditional positioning technique. Preliminary data of this study showed the new positioning technique to be much more reliable (results not shown). For this reason a larger follow-up study was carried out testing the accuracy of this new positioning technique. The position of the patients in the cranio-caudal direction was shown to be more accurate.

Immobilization

The question of to what extent immobilization of patients contributes to the setup accuracy has been addressed by several authors. Soffen *et al.* (107) compared

setup accuracy in 7 prostate cancer patients, immobilized with alpha cradle body casts, to that in a matched control group who were not casted. The median daily error for the casted group was 1 mm, while it was 3 mm for the noncasted group. The 10% largest daily variations were eliminated using the cast. Rosenthal *et al.* (102) compared two groups of 11 prostate cancer patients; one group was treated with alpha cradle immobilization, the other was not immobilized. The mean \pm 1 SD of the simulation to treatment variability was 4 mm \pm 2.6 mm using immobilization, compared to 6 mm \pm 4.5 mm without immobilization. Mitine *et al.* (87), however, comparing 6 patients treated without immobilization in the supine position to 12 patients in alpha cradle casts, 6 supine and 6 prone, observed a similar accuracy for the lateral direction and an improved accuracy for the cranio-caudal direction in the supine group when alpha cradle casts were used, but worse results in the group treated in the prone position in the alpha cradle cast as compared to the supine group without immobilization. It is extremely difficult to compare these results to each other and to our results. Different treatment techniques (six-field, four-field and three-field) have been used, often a single measurement has been performed in each direction, and results have been presented in very different ways. Taking the percentage of SIM-MV differences \leq 1 cm as a measure of setup accuracy, then alpha cradle casts seem to be increasing precision (98% vs. 85% in the study by Rosenthal *et al.* (102) and 100% vs. some 96% in the analysis of Soffen *et al.* (107)). In our study, 10% of urological cancer patients showed errors \geq 1 cm, which was reduced to a minimum of 1% using the verification and correction procedure on a routine basis. For the gynecological fields, accuracy obviously was worse, which is a common finding. Positioning accuracy diminishes with increasing patient weight (28,46,99). The field center is located in an area susceptible to movement (respiration, loose abdominal wall) and alignment often proves to be difficult. The immobilization system as traditionally used in our institute, using bony structures for set up, did not result in an acceptable setup accuracy. The use of the caudal field border as the most important parameter for alignment did result in an improvement in accuracy. This field border is located in the pubic area, which is much less susceptible to variations and is thus much easier to reproduce. Using alpha cradle casts in these patients might lead to further improvements in accuracy; this will be the subject of a future study.

The increased use of megavolt imaging and the results of positioning studies have focused attention on positioning accuracy and its relevance for the choice of margins. However, the studies have also raised the issue of how to implement their findings in clinical practice. Should we perform on-line verification of all fields on all patients and set limits of tolerance which technologists can use when deciding to irradiate or to adjust? Is it worthwhile to try and correct all random errors and accidental mistakes? At present, at most institutions, a verification system is operational on the accelerators which, if used with narrow tolerance settings, will prevent a large number of the accidental errors. For example, the interchanges of field length and width found in our study would have been prevented if the verification system had been operational at that time. Correction of all random errors would require continuous on-line verification. Setup corrections are time consuming and disturbing both for technologists and patients. In daily clinical practice, the number of corrections should be kept as small as possible. It seems therefore, to be far more efficient to obtain knowledge of the magnitude of random errors for the various treatment techniques at each institution by means of positioning studies like the present one, and to improve positioning techniques if large random errors are found. The margin to be added around the clinical target volume to compensate for inaccuracies in patient setup can thus be chosen on the basis of the magnitude of random variations observed. Then, efforts can be concentrated on detecting and correcting *systematic* errors early in the treatment series.

Through analysis of a number of megavolt images obtained during the first week(s) of treatment, it can be determined early in the treatment series whether a systematic error is present. Correction is then only applied if the displacement (averaged over the measurements made so far) exceeds an action level, which is decreased at each subsequent measurement. In this way, correction of random deviations, which would result in further errors, is prevented. A verification and correction procedure developed by Bijhold *et al.* (15) and Bel *et al.* (14) is presently being used by a Netherlands collaborating group for megavolt imaging, and tested in daily practice in three radiotherapy centers. Data from previous positioning studies in pelvic irradiation for urological cancer, carried out in each of the centers, have been used to choose the number of megavolt images to be taken and to set action levels for each center. The results of the first series of patients treated in our institution using this verification and

correction procedure shows promising results (Fig. 3). To determine if such a protocol does consistently reduce error rates and if the workload is acceptable in daily practice in busy radiotherapy departments, the combined results from a large number of patients will be presented in a joint publication.

In conclusion, the present study on positioning accuracy in irradiation of small and large pelvic fields showed larger errors than was expected. Positioning techniques were improved and checked again for their accuracy. Margins to be taken around the clinical target volume to account for geometrical inaccuracies should be based on the results of positioning studies carried out in the same institution. Verification and correction protocols will be increasingly important, especially in conformal therapy.

Acknowledgements

The authors wish to thank the radiation oncologists of the urological and gynecological cancer boards for their cooperation. The invaluable assistance of J. Koffijberg and the other radiotherapy technicians is gratefully acknowledged. The manuscript was skillfully prepared by Ms. I. Dijkstra. The DDHCC megavolt imaging project was supported by the Dutch Cancer Society (grant nos. 88-2 and 92-86).

CHAPTER 5

HIGH-PRECISION PROSTATE CANCER IRRADIATION BY CLINICAL APPLICATION OF AN OFFLINE PATIENT SETUP VERIFICATION PROCEDURE, USING PORTAL IMAGING

Arjan Bel, Ph.D., Pieter H. Vos, Ph.D., Patrick T.R. Rodrigus, M.D.,
Carien L. Creutzberg, M.D., Andries G. Visser, Ph.D., Joep C. Stroom, M.Sc.
and Joos V. Lebesque, M.D., Ph.D.

International Journal of Radiation Oncology, Biology, Physics 35: 321-332, 1996

Abstract

Purpose To investigate in three institutions, The Netherlands Cancer Institute (Antoni van Leeuwenhoek Huis [AvL]), Daniel den Hoed Cancer Center (DDHCC), and Dr. Bernard Verbeeten Institute (BVI), how much the patient setup accuracy for irradiation of prostate cancer can be improved by an offline setup verification and correction procedure, using portal imaging.

Methods and Materials The verification procedure consisted of two stages. During the first stage, setup deviations were measured during a number (N_{\max}) of consecutive initial treatment sessions. The length of the average three-dimensional (3D) setup deviation vector was compared with an action level for corrections, which shrunk with the number of setup measurements. After a correction was applied, N_{\max} measurements had to be performed again. Each institution chose different values for the initial action level (6, 9, and 10 mm) and N_{\max} (2 and 4). The choice of these parameters was based on a simulation of the procedure, using as input preestimated values of random and systematic deviations in each institution. During the second stage of the procedure, with weekly setup measurements, the AvL used a different criterion ("outlier detection") for corrective actions than the DDHCC and the BVI ("sliding average"). After each correction the first stage of the procedure was restarted. The procedure was tested for 151 patients (62 in the AvL, 47 in the DDHCC, and 42 in the BVI) treated for prostate carcinoma. Treatment techniques and portal image acquisition and analysis were different in each institution.

Results The actual distributions of random and systematic deviations without corrections were estimated by eliminating the effect of the corrections. The percentage of mean (systematic) 3D deviations larger than 5 mm was 26% for the AvL and the DDHCC, and 36% for the BVI. The setup accuracy after application of the procedure was considerably improved (percentage of mean 3D deviations larger than 5 mm was 1.6% in the AvL and 0% in the DDHCC and BVI), in agreement with the results of the simulation. The number of corrections (about 0.7 on the average per patient) was not larger than predicted.

Conclusion The verification procedure appeared to be feasible in the three institutions and enabled a significant reduction of mean 3D setup deviations. The computer simulation of the procedure proved to be a useful tool, because it enabled an accurate prediction of the setup accuracy and the required number of corrections.

Introduction

Electronic portal imaging devices (EPIDs) are increasingly used in clinical practice to improve setup accuracy. In comparison with portal films, acquisition is faster and the evaluation is greatly facilitated by using computerized analysis methods (40,41,118).

Portal image analysis has shown that both the systematic and the random component of the setup deviation during a treatment session are important (15,46,56,97). In principle, both components can be corrected by using online setup verification procedures with decisions on corrective actions taken during each treatment session. Recently, results of various online setup verification procedures were reported (29,35,38). These reports showed that online procedures would involve a considerable workload.

Online procedures are possibly not required when random deviations are small. In this case, an offline procedure can be used, to correct systematic deviations only. Random deviations can be incorporated as a small margin around the clinical target volume, with the magnitude of the margin depending on the standard deviation (SD) of the distribution of random deviations (115). A difficulty with offline procedures is, however, that each measured setup deviation is the sum of a random and the systematic deviation. When and how corrective actions should be performed is not obvious and criteria for performing corrections are still a subject of discussion (66,86,103,105). Recently, some theoretical procedures were proposed to deal with this problem (14,30,105,134), but until now there have been no reports available about the clinical results of one of these procedures.

In an earlier paper (14) we described an offline procedure, using a shrinking action level, which could be adapted to various clinical conditions. This procedure aimed at reducing systematic deviations as much as possible. A computer simulation of the procedure was performed, in which parameters of the procedure were varied. To enable the simulation, a preestimate of the distribution of systematic and random deviations was required. As output, the resulting setup accuracy was provided as a function of the required number of portal images and setup corrections. It turned out that, for a specific level of accuracy, a compromise had to be made between the number of portal images

and corrections. Hence, different institutions could make different choices for the parameters of the procedure depending on their specific demands.

The aim of this study was to investigate in three different institutions whether an offline three dimensional (3D) setup verification procedure is feasible in clinical practice, whether the procedure is efficient in reducing systematic deviations, and whether the improvement of patient setup accuracy could be predicted by a simulation of the setup verification procedure (14), using preestimated distributions of random and mean (systematic) deviations.

Methods and Materials

Three institutions in The Netherlands were involved in this study, i.e. The Netherlands Cancer Institute (Antoni van Leeuwenhoek Huis) in Amsterdam (AvL), the Daniel den Hoed Cancer Center in Rotterdam (DDHCC) and the Dr. Bernard Verbeeten Institute in Tilburg (BVI). Parameters will be labeled with AvL, DDHCC, or BVI for the corresponding institution. The study started January, 1993 in the AvL; December, 1993 in the DDHCC and January, 1994 in the BVI, and ended November, 1994.

Patients and treatment

The patients in this study were treated for prostate carcinoma. The total number of patients involved in the evaluation of the verification procedure was 151 with 62 patients in the AvL, 47 patients in the DDHCC, and 42 patients in the BVI.

Treatment preparation was similar in the three institutions. A computed tomography (CT) scan of the pelvic region was performed and the patient's skin was tattooed (marked in the DDHCC) to indicate a tentative isocenter. During treatment planning, a new isocenter was defined by a 3D shift with respect to the tentative isocenter, when necessary. In the BVI, the vertical position of the new isocenter was defined with respect to the treatment room coordinate system, taking into consideration the estimated bending of the treatment table.

During the subsequent treatment simulation, lines were drawn on the skin to mark the definitive isocenter, in the AvL and the DDHCC. In the BVI, asymmetric collimator settings and/or table shifts with respect to the tattooed tentative isocenter were used for correct positioning.

On the treatment machine, patients were positioned by aligning the lines, drawn during the simulation, with laser beams in the three main directions, in the AvL and the DDHCC. In the BVI, the tattoos (indicating the tentative isocenter) were aligned with laser beams in the horizontal plane only. Subsequently, the table height was adapted, using the calculated position of the isocenter with respect to the table, thus defining the origin for the subsequent procedure. In some patients, a change of the tentative isocenter was required in the horizontal plane; in these cases, a prescribed translation of the table was performed, relative to this origin.

The treatment techniques were different for the three institutions (Table 1). In the AvL, the conformal simultaneous boost technique (67) was applied with three orthogonal fields (8 MV). In the DDHCC, the gantry angle for the left lateral field ranged between 90° and 105° and for the right lateral field between 255° and 270° . In this institution, about half the number of patients were treated with rectangular fields (the majority with 25 MV), the other half treated with conformal fields (25 MV), defined by a multileaf collimator. In the BVI, a four-field box technique with rectangular fields was applied (10 MV). In the lateral fields, the collimator was rotated (collimator angle usually between 0° and 30°) to obtain a maximal sparing of the rectum.

Table 1. The treatment techniques, imaged fields and imaging systems of the three institutions

Institution	AvL	DDHCC	BVI
<i>Treatment technique</i>			
Fields	Three fields (AP and two lateral)	Three fields (AP and two lateral oblique)	Four fields (AP, PA and two lateral)
Wedges	Lateral fields	Lateral fields	Not used
Number of fractions	35	33	35
<i>Portal images</i>			
Imaged fields	All fields	All fields	AP and left lateral
Imaging system	Varian Portal Vision	Philips SRI 100	General Electric Target view

Portal image acquisition and analysis

In total, 4497 portal images were analyzed (2019 in the AvL, 1462 in the DDHCC and 1016 in the BVI). In the AvL and the DDHCC, all fields of a treatment session were imaged. In the BVI, portal images were made of the anterior-posterior (AP) and left lateral field only. The three institutions had different types of electronic portal imaging devices (Table 1) and used different methods of image analysis.

In the AvL, a portal imaging device⁷ was used which was based on a matrix of ionization chambers (120). Digitally reconstructed radiographs (DRRs) were made during the planning and used as reference images (12). The DRRs and the corresponding field outlines were imported into the portal image analysis system (118). On this reference image, a drawing of the bony anatomy was made. In the portal image, the field edges and the bony anatomy were detected and matched to the reference drawings automatically (40,41) and corrected manually when necessary. The accuracy of this method was estimated to be about 0.7 mm (1 SD) for the caudal-cranial direction in both the AP and lateral fields. For the left-right direction in the AP field and the ventro-dorsal direction in the lateral field, the accuracy was estimated to be 0.3 mm and 1.0 mm (1 SD), respectively (41).

In the DDHCC a camera based portal imaging device⁸ (123) was applied. The digitized simulator film was used as reference. Anatomical landmarks were indicated on the reference image and on the portal image and a landmark match of both images was performed. This match method was estimated to be accurate within 1 mm (1 SD).

A camera based portal imaging system⁹ (88) was also used in the BVI. The digitized simulator film served as reference image. The procedure for the analysis of portal images was very similar to the procedure used in the AvL; the only difference was that the anatomy in the portal image was delineated and matched by entirely manual techniques. The method was estimated to be equally accurate as in the AvL, with the exception of measurements in the lateral fields.

⁷ Varian Portal Vision, Varian Radiation Division, Palo Alto, CA.

⁸ Philips SRI 100, Philips Medical Systems Radiotherapy, Crawley, West Sussex, UK.

⁹ General Electric Targetview, General Electric, Benelux.

Due to the larger interobserver variability (almost all radiotherapy technicians performed the anatomy alignment), the accuracy of these measurements was estimated to be within 1 mm (1 SD) for both directions.

3D setup deviations

In a previous study, it was shown that for prostate treatments, deviations in a particular direction, as measured in more than one field of a treatment session, were sufficiently correlated to allow the calculation of one single 3D setup deviation vector (15). By computing the average deviation in a particular direction, the effect of the measurement error is reduced. The three main directions are denoted by X, Y, and Z, with the X axis corresponding to the left-right direction, the Y axis corresponding to the caudal-cranial direction, and the Z axis corresponding to the dorsal-ventral direction.

For the AvL, images were acquired for the three treatment fields: the AP, left lateral (LL), and right lateral (RL) field. For the X component of the 3D setup deviation vector, only the deviation from the AP field was available, X_{AP} . The deviation in the Y direction was taken to be equal to the average of the Y deviations in the three fields, $(Y_{AP} + Y_{RL} + Y_{LL})/3$. The deviation in the Z direction was taken from the deviations along this axis of the two lateral fields, $(Z_{RL} + Z_{LL})/2$. For the DDHCC, where three fields were also imaged, the same procedures were applied for the X and Y direction. The deviation in the Z direction was computed as $([Z \sin(-\gamma)]_{RL} + [Z \sin \gamma]_{LL})/2$, with γ being equal to the gantry angle of the lateral fields.

In the BVI, four fields were given but only portal images of the AP and the left lateral fields were acquired. The average of the deviations in the Y direction was calculated as $(2Y_{AP} + Y_{RL})/3$, thus taking the interobserver variability into account because the variability in the AP field was smaller than in the lateral field. The deviations along the X and Z directions were inferred from the AP and right lateral field, respectively, without calculation of an average.

First stage of the verification procedure

The first stage of the verification procedure was a 3D extension of the one dimensional (1D) verification procedure with a shrinking action level described previously (14). Only translational setup errors were considered. Rotational

errors were not considered in the procedure, because it has been shown in earlier studies that they are small for prostate treatments (15,119).

At the beginning of the treatment, during N_{\max} consecutive treatment sessions, portal images were obtained. Of each treatment session, the 3D setup deviation was calculated (a *measurement*). After each measurement, the length of the average vector of the 3D setup deviation vectors over the first N measurements, $|\bar{d}_{\text{avg}}| = |(\bar{x}, \bar{y}, \bar{z})|$, was calculated. The length of this average vector was tested against an action level α/\sqrt{N} , where α is the parameter indicating the initial action level. When $|\bar{d}_{\text{avg}}|$ was larger than the action level, a setup correction was performed (i.e., the patient was repositioned during the next treatment sessions by moving the isocenter over the average deviation in the three directions). After each correction, the calculation of the average vector was restarted and N_{\max} measurements had to be performed again. When a component of the required correction was smaller than a specific value, the correction was not applied in that direction. This value depended on the method of setup correction and was equal to 3 mm for the AvL and 2 mm for the DDHCC and the BVI.

To determine for each institution values for the parameters N_{\max} and α , a computer simulation of the procedure was performed, simulating the treatment of 10,000 patients. The simulation required as input a preestimate of the standard deviation σ_{pre} of the distribution of random deviations. Random deviations were assumed to be equal for different patients (15). A preestimate of the distribution of systematic deviations without corrections, with a standard deviation Σ_{pre} , was also needed to determine the expected workload. These data were obtained from earlier portal imaging studies in the three institutions (Table 2) (15,23,126). Both the systematic and random deviations were assumed to be normally distributed in the three directions. No correlations were assumed to exist between deviations in the three directions and the overall means were assumed to be equal to zero.

For each patient in the simulation, the vector length of the mean of the three directions, the *mean 3D deviation*, was calculated. All setup deviations were taken into account in this mean 3D deviation, irrespective of setup corrections. For each institution, the percentage of mean 3D deviations larger than 5 mm was plotted against the average number of measurements and corrections per patient (Fig. 1) for varying values of α and N_{\max} . All institutions aimed at a

reduction of mean 3D deviations larger than 5 mm to about 5% or less. To obtain this level of setup accuracy, a compromise had to be made between the number of measurements and corrections. The graphs of Fig. 1 enabled each institution to make a choice for the parameters which was optimal for their situation.

As can be seen in Fig. 1, the desired level of setup accuracy was preestimated for the AvL with the parameter values $N_{\max}^{\text{AvL}} = 2$ and $\alpha_{\text{AvL}} = 6$ mm, resulting in 1.2% of the mean 3D deviations larger than 5 mm (Table 3).

Table 2. Preestimates of the standard deviation of the distribution of random (σ_{pre}) and mean (systematic) (Σ_{pre}) deviations in each institution, which were used as input for the computer simulation of the verification procedure (Fig. 1)

Institution	AvL	DDHCC	BVI
<i>Preestimated distributions</i>			
Authors	Bijhold <i>et al.</i> (15)	Creutzberg <i>et al.</i> (23)	Vos <i>et al.</i> (126)
σ_{pre} (mm)	2	2	2.5
Σ_{pre} (mm)	2	3	3
<i>Verification procedure</i>			
<i>First stage</i>			
α (mm)	6	9	10
N_{\max}	2	4	4
<i>Second stage (weekly)</i>	Outlier detection	Sliding average	Sliding average

The standard deviations were assumed to be equal in the three directions. The overall mean was assumed to be zero for all distributions. The parameter values for the first stage of the procedure are the initial action level α and the number of measurements that had to be performed at the start of the treatment or after a setup correction, N_{\max} . During the second stage of the verification procedure, after finishing the first stage, different decision criteria were used in the three institutions.

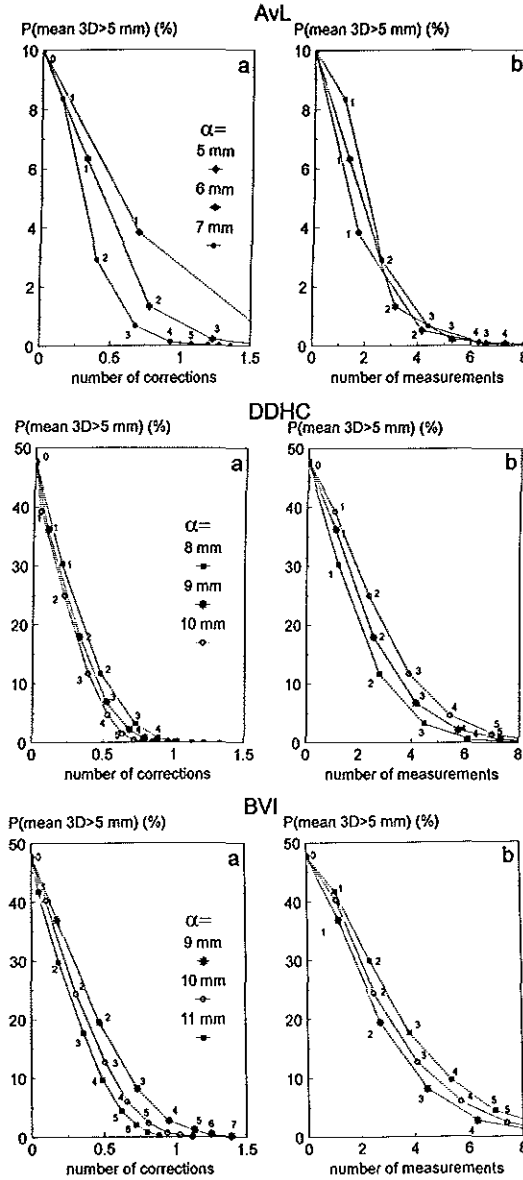


Fig. 1

Simulation of the first stage of the procedure. The setup accuracy, expressed as the percentage of mean 3D deviations larger than 5 mm, $P(\text{mean } 3D > 5 \text{ mm})$, is plotted against the average number of corrections (a) and measurements (b) per patient. The initial action level α and the number of measurements, N_{meas} , that had to be performed at the start of the treatment or after each correction, were varied. The value of N_{meas} is indicated near each point in the graph.

In the DDHCC and the BVI, the setup accuracy without corrections was estimated to be lower than in the AvL and more measurements had to be performed to obtain the desired level of setup accuracy. Parameter values $N_{\max}^{\text{DDHCC}} = N_{\max}^{\text{BVI}} = 4$ with initial action levels $\alpha_{\text{DDHCC}} = 9$ mm and $\alpha_{\text{BVI}} = 10$ mm were chosen in the DDHCC and the BVI, respectively, resulting in 2.4 and 5.6% of the mean 3D deviations larger than 5 mm (Fig. 1 and Table 3), respectively. For the three institutions, the number of measurements and corrections (Fig. 1 and Table 3) were acceptably low.

Table 3. The preestimated setup accuracy without corrections and the results of the simulation of both the first stage of the verification procedure and the total verification procedure

Institution	AvL	DDHCC	BVI
<i>Number of mean 3D deviations > 5 mm (%)</i>			
Without corrections	10.0	42.7	42.7
First stage of procedure	1.2	2.4	5.6
Total procedure	0.9	0.5	0.9
<i>Average number of measurements per patient</i>			
First stage of procedure	3.2	5.7	5.8
Total procedure	10.7	12.1	13.4
<i>Average number of corrections per patient</i>			
First stage of procedure	0.8	0.7	0.7
Total procedure	1.1	0.8	0.8

As input for this simulation, the preestimated distributions of random and mean (systematic) deviations were used (Table 2). As a measure of the setup accuracy, the percentage of mean 3D deviations larger than 5 mm was used. The resulting workload was quantified by the average number of measurements and corrections per patient.

Second stage of the verification procedure

When during N_{\max} consecutive treatment sessions no setup corrections were required, the first stage of the verification procedure was finished (14). This first stage was extended with a second stage to deal with large setup deviations that may arise during the course of the treatment. The cause of these deviations is yet unknown, but they can possibly be described as drifts, linear in time (34). Two different strategies for the second stage of the verification procedure were adopted. Both methods were based on a weekly check after the first stage of the procedure.

In the AvL, it was tested after each weekly measurement if the vector length was outside the initial action level ($\alpha_{\text{AvL}} = 6$ mm) and if one of the components of the vector was more than 5 mm different from the last calculated average. If both conditions were fulfilled, an "outlier" was detected and the calculation of $|\bar{d}_{\text{avg}}|$ was restarted. The next day, a new measurement was performed and the average of the last two measurements was tested against the corresponding action level ($\alpha_{\text{AvL}}/\sqrt{2} = 4.2$ mm).

For the DDHCC and the BVI, a sliding average method was used (105,126). After each weekly measurement, the vector length of the average of the last four measurements was calculated and tested against the lowest action level (i.e., 4.5 mm and 5 mm, respectively). Corrections were applied if this action level was exceeded. For all three institutions, the first stage of the verification procedure was restarted when a correction was required, otherwise the procedure continued with weekly measurements.

Both methods were also simulated with the corresponding preestimated data of the institutions as input and the already chosen parameter combinations for α and N_{\max} . Due to the lack of a model for gradual trends or sudden shifts in the setup during treatment, these errors could not be taken into account in the simulation. However, during the second stage of the verification procedure, random variations and remaining systematic deviations resulted in additional corrections in the simulation without occurrence of "real" gradual trends or sudden shifts of the setup. The simulation showed that these corrections resulted in a further substantial reduction of large mean 3D deviations (Table 3) compared with the first stage of the procedure.

Implementation of the procedure

In the three institutions, portal image acquisition and analysis were performed by the technicians. In the AvL and the DDHCC, the portal images were analyzed usually a few hours after the treatment session. In the BVI, the analysis was performed during the irradiation with the AP and RL fields, from which no portal images were acquired. The time required for analysis of the portal images of a treatment session was about 2-10 min. After matching the portal images with the reference images, the computer displayed decisions on corrective actions. In the AvL, the responsible physician checked and approved each setup correction. In the other two institutions, the DDHCC and the BVI, the technicians applied corrections of the patient setup, without consultation of a physician.

Setup corrections were implemented differently in the three institutions. In the AvL, new lines were drawn on the patient's skin and patients were aligned with these new lines. In the DDHCC, no new lines were drawn. When a correction was required, the patient was positioned using the original lines drawn during simulation and subsequently, the table was shifted according to the magnitude of the required correction. In the BVI, table shifts were already performed rather routinely during the treatment as a result of a change of the tentative isocenter during the planning. The overall correction was performed by moving the table over a distance equal to the sum of the setup correction and the already prescribed table movement. The setup correction procedure in the AvL resulted in a slight increase in the time (2-4 min) of that treatment session. In the two other institutions, the time of a treatment session was hardly prolonged due to setup corrections.

Analysis

An analysis of the data was performed to study the effect of the actual effectiveness of the verification procedure. The actual distribution of mean (systematic) deviations without corrections and the actual distributions of mean deviations after the first and second stage of the procedure were calculated. These last two distributions and the number of corrections and measurements were compared with the results of the simulation (using preestimated distributions) to evaluate the value of the simulation itself.

Structure of setup deviations without the verification procedure. To estimate the actual effect of the setup verification procedure, the setup deviations without the application of the verification procedure were estimated. The actual distribution of mean (systematic) deviations without corrections (SD denoted by Σ_{act}) was estimated for each direction by eliminating the effect of the setup corrections, both in the first and the second stage of the procedure. After each correction, the magnitude of that correction was added to the subsequent deviations. This distribution was tested for being normal, because a normal distribution was used in the simulation.

For a patient, for whom the setup was corrected, the variances of the distribution of random deviations before and after each correction were calculated for each direction. Subsequently, the weighted average of these variances was calculated for each direction, resulting in the variance of the distribution of random deviations for this patient, σ_i^2 . The variance of the distribution of random deviations for patients for which no corrections were applied, was defined in the usual way, $\sigma_i^2 = \sum_{j=1}^N (x_j - \bar{x})^2 / (N - 1)$, with x_j a measured setup deviation in one of the three directions. The variance of the actual distribution of random deviations of the whole patient group, σ_{act}^2 , was computed by subsequently taking the average of the variances of all patients. In the simulation, the preestimates of the distributions of random deviations were assumed to be normal with an SD which was assumed to be equal for each patient. Both assumptions were tested for all patients.

In the simulation, no time dependent gradual trends or sudden shifts of the setup during treatment were assumed. The occurrence of trends was studied by performing a linear fit of the deviations in three directions with time. Each slope was tested for being significantly different from zero. A detailed analysis of trends is presented in the appendix.

First stage of the verification procedure. The evaluation of the first stage of the procedure was confined to a test of the validity of the computer simulation, which served as a basis for the choice of the procedure parameters (Fig. 1). The effects of corrections during the second stage of the procedure were eliminated. The setup accuracy after application of the first stage of the procedure was subsequently determined by computing for each patient the mean 3D setup deviation. The resulting actual distribution of mean 3D deviations after the application of the first stage of the procedure was tested for being significantly

different from the corresponding preestimated distributions. Without corrections, these deviations are distributed as a χ^2 distribution and after the application of the procedure the tail of the distribution is cut off. In addition, the average number of measurements and corrections per patient during the first stage was determined and compared with the results of the simulation.

Total verification procedure. The total procedure, consisting of the first and second stage, was analyzed along the same lines as the first stage of the procedure. The actual distribution of mean 3D deviations and the average number of measurements and corrections per patient after application of the total procedure were calculated and compared with the results of the simulation.

An individual patient setup with an SD of the distribution of random deviations (α_i), which is larger than the standard deviation of the total group (σ_{act}) can lead to repeated setup corrections for this patient (14). Therefore, it was tested whether setups of individual patients with relatively large or small random deviations were significantly more or less corrected than the setups of the total group.

Statistical procedures. Several statistical tests were used to determine the significance of the difference between various quantities. The significance of the difference between the actual distribution of mean 3D deviations and the corresponding preestimated distribution, as derived from the simulation, was calculated by using the Kolmogorov-Smirnov (K-S) test (94). An F -test was used to determine whether the SD of the distribution of the random deviations of individual patients was significantly different from the SD of the actual distribution of the whole group.

A Monte Carlo simulation (94) was used to determine confidence levels of various quantities. This method is especially useful when a quantity is calculated from a distribution of measurements which is not normal, as with, for instance, the average of all setup deviations of all patients after application of corrections. The Monte Carlo simulation consists of the creation of an artificial "result", generated by randomly choosing data from the distribution of measurements. This procedure is repeated (10,000 times), resulting in a frequency distribution of the calculated quantity. Subsequently, the confidence levels of the calculated quantity can be determined.

This Monte Carlo simulation was used to determine whether the overall means (the average overall deviations of all patients) were significantly different from

zero and to test whether the preestimated and actual percentage of mean 3D deviations larger than 5 mm were significantly different. A Monte Carlo simulation was performed on the patient data to test the significance of differences between the average number of measurements and corrections per patient according to the actual patient data and the simulation. Finally, the method was used to test whether the slopes, after fitting the deviations with time (see appendix), were significantly different from zero.

Results

To enable evaluation of effectiveness of the verification procedure, results after elimination of the effect of corrections are presented first. Using these results, the validity of assumptions of setup deviations statistics, made for the computer simulation (Table 2) can also be tested. Subsequently, we present the evaluation of effectiveness of the first stage of the verification procedure in improving the setup accuracy, and a comparison with the outcomes of the simulation. Finally, such an evaluation and comparison are given for the total procedure, consisting of the first and second stages.

Structure of setup deviations without the verification procedure

The actual distributions of the mean (systematic) deviations (with SD Σ_{act}) without corrections were estimated (Table 4) by elimination of the effect of corrections. Only for the AvL, along the dorsal-ventral axis, was this distribution significantly ($p = 0.02$) different from a normal distribution. For none of the institutions were the differences between Σ_{act} and the corresponding preestimated values Σ_{pre} (Table 2) significant.

For the AvL and the BVI, the overall mean (i.e., the deviations averaged over all treatment setups of all patients), was significantly ($p < 0.001$) different from zero for the caudal-cranial and the dorsal-ventral direction (Table 4). For the DDHCC, the overall mean in the left-right direction was significantly ($p < 0.001$) different from zero. These overall means unequal to zero were most probably due to small systematic treatment machine inaccuracies.

Table 4. The actual distribution of mean (systematic) deviations without corrections, calculated by the elimination of the effect of the corrections, with the overall means and standard deviations (SDs)

Institution	AvL	DDHCC	BVI
Overall mean (mm)			
Left-right	0.3	-0.7	-0.3
Caudal-cranial	-0.9	-0.3	1.6
Dorsal-ventral	0.9	-0.4	-1.3
SD systematic (Σ_{act}) (mm)			
Left-right	2.4	2.9	2.2
Caudal-cranial	2.4	2.1	2.7
Dorsal-ventral	2.6	3.3	3.8
SD random (σ_{act}) (mm)			
Left-right	2.0	2.1	2.7
Caudal-cranial	1.8	2.1	2.1
Dorsal-ventral	1.7	2.1	2.3
Patients with σ_i significantly smaller than σ_{act} (%)			
Left-right	6	8	7
Caudal-cranial	10	6	2
Dorsal-ventral	5	4	2
For any direction	19	18	12
Patients with σ_i significantly larger than σ_{act} (%)			
Left-right	2	4	7
Caudal-cranial	6	4	2
Dorsal-ventral	5	4	0
For any direction	11	13	10

The standard deviation of the actual distribution of random deviations (σ_{act}) for all patients was calculated and subsequently, the percentage of patients with a standard deviation σ_i of the individual distribution of random deviations significantly ($p < 0.05$) larger or smaller than σ_{act} was determined.

As a result of the overall mean being unequal to zero and because of the differences between the preestimated and actual distribution of mean (systematic) deviations without corrections, the corresponding distributions of mean 3D deviations (Fig. 2) were significantly ($p < 0.01$) different for the AvL and the DDHCC. The differences at the level of 5 mm (Tables 3 and 5) were also substantial for the three institutions.

The SDs of the actual distribution of random deviations, σ_{act} (Table 4), for the three institutions were only slightly different from the SDs that were assumed in the simulation (Table 2). There were no patients with an actual distribution of random deviations significantly different from a normal distribution. It was tested whether the SD of the distribution of random deviations of individual patients (σ_i) along any direction was significantly ($p < 0.05$) different from σ_{act} (Table 4). For patients with σ_i significantly larger than σ_{act} , this SD was equal to 3.6 mm, 3.8 mm, and 4.4 mm for the AvL, the DDHCC, and the BVI, respectively. One patient (in the AvL) had a value of σ_i that was significantly larger than σ_{act} in more than one direction. There were no patients with σ_i significantly larger than σ_{act} in one direction and σ_i significantly smaller than σ_{act} in another direction.

Trends in time were analyzed by performing linear fits of the deviations, after the elimination of the effect of corrections. In about half the number of patients, a significant trend in time was observed (appendix Table A1). For about 20% of the patients in the AvL and the DDHCC and 5% of the patients in the BVI, these trends would have resulted in a drift of the length of the mean (systematic) 3D deviation vector of more than 5 mm during the course of the treatment.

First stage of the verification procedure

To test the validity of the simulation (using as input the preestimated distributions, Table 2), the actual and preestimated distributions of mean 3D deviations after application of the first stage of the procedure were compared. No significant differences between these distributions were found for any institution. However, at a particular level of the distributions (i.e., the probability of mean 3D deviations larger than 5 mm), a significant difference was found for the AvL between the actual value (11.3%, Table 5) and the preestimated value (1.2%, Table 3). This was probably caused by the underestimation of the actual number of mean (systematic) 3D deviations larger

than 5 mm (Table 4) without corrections with respect to the corresponding preestimated value (Table 2).

Table 5. The actual setup accuracy without corrections, after elimination of the effect of the corrections, and the results of the first stage of the verification procedure and the total verification procedure, consisting of the first and second stage

Institution	AvL	DDHCC	BVI
Number of patients	62	47	42
<i>Number of mean 3D deviations > 5 mm (%)</i>			
Without corrections	25.8	25.5	35.7
First stage of procedure	11.3	2.1	4.8
Total procedure	1.6	0	0
<i>Average number of measurements per patient</i>			
First stage of procedure	2.6	5.4	5.2
Total procedure	10.9	10.4	12.1
<i>Average number of corrections per patient</i>			
First stage of procedure	0.4	0.5	0.4
Total procedure	0.6	0.8	0.7
<i>Total procedure, subgroup with:</i>			
σ_i significantly smaller than σ_{act}	0.4	1.1	0.6
σ_i significantly larger than σ_{act}	1.4	1.5	1.5

The setup accuracy was quantified by the percentage of mean 3D deviations larger than 5 mm. The workload involved in the application of the procedure was quantified by the average number of measurements and corrections per patient. For the patients with a standard deviation of the individual distribution of random deviations σ_i in one or more of the directions significantly ($p < 0.05$) smaller or larger than the standard deviation of the total group σ_{act} , the average number of corrections per patient was determined.

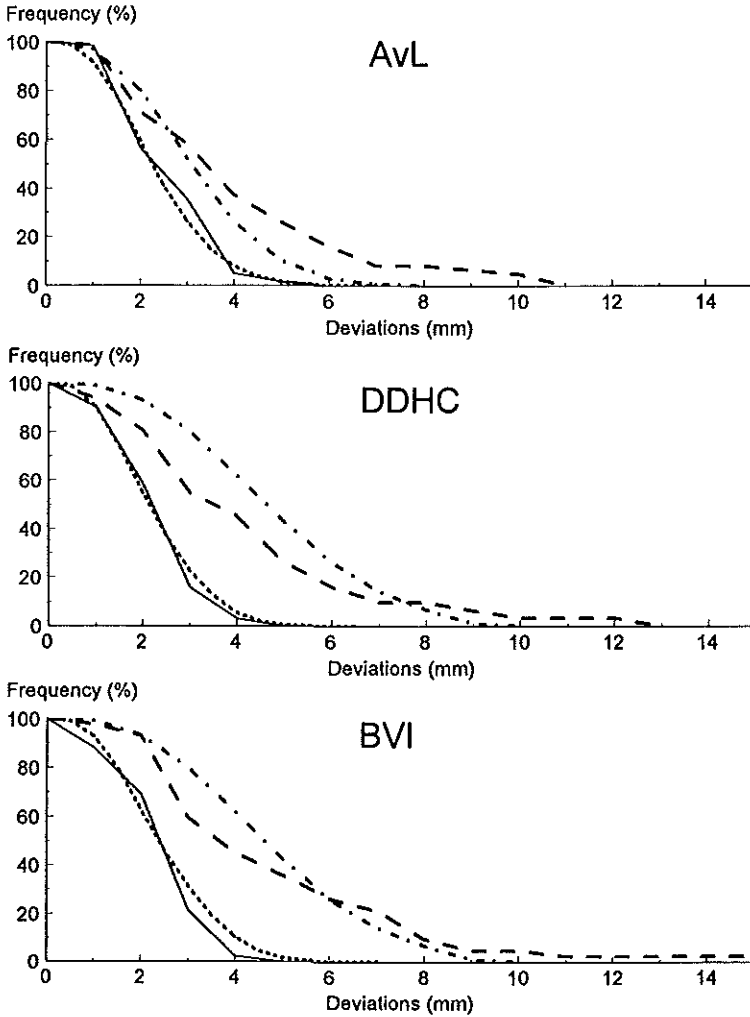


Fig. 2

Cumulative distributions of mean 3D deviations. Along the vertical axis, the percentage of deviations larger than a specific value is plotted against that value on the horizontal axis. Plotted are the preestimated distributions without corrections (dashed/dotted line) and the preestimated distributions after application of the total verification procedure (dotted line). The actual distributions without corrections and after application of the procedure are given by the dashed and solid line, respectively.

The workload of the first stage of the procedure was evaluated (Table 5). In the AvL, the average number of measurements and corrections per patient was significantly smaller than that estimated from the simulation (Table 3). For the two other institutions, the average number of measurements and corrections per patient was also lower than predicted, but only for the BVI the average number of corrections per patient was significantly smaller.

Total verification procedure

For each institution, the actual distribution of mean 3D deviations, after application of both the first and the second stage of the procedure, was calculated (Fig. 2, Table 5). For the three institutions there was a major improvement with respect to the actual and preestimated distribution of mean (systematic) 3D deviations without corrections. The actual distributions of mean 3D deviations after application of the total procedure did not differ significantly from the corresponding preestimated distributions. For the three institutions, the actual distributions of mean 3D deviations were similar. In comparison with the first stage of the procedure, the percentage of mean 3D deviations larger than 5 mm was further reduced. In the AvL, 1.6% of the mean 3D deviations was larger than 5 mm, and for the DDHCC and the BVI there were no more mean 3D deviations larger than 5 mm. These results were in agreement with the level of setup accuracy as preestimated by the simulation (Table 3).

The additional average number of corrections per patient during the second stage of the procedure (Table 5) agreed with the simulation (Table 3) for the three institutions. For the AvL, the total average number of measurements per patient during the first and the second stage of the procedure agreed with the simulation. In the DDHCC and the BVI, the total average number of measurements per patient was significantly smaller than was predicted. In the DDHCC, this was merely because the weekly check was not always performed consistently.

It was tested if the number of corrections of the subgroups of patients with relatively small or large standard deviations of the distribution of random deviations (σ_i) was different from the number of corrections of the total group. The average number of corrections per patient in the subgroup with a small σ_i (significantly smaller than the SD of the distribution of random deviations (σ_{ac}) of the whole group) was not significantly smaller than the average number of

corrections per patient of the total group (Table 5). On the other hand, for the subgroup of patients with a large σ_i (significantly larger than σ_{act}), more corrections were performed than in the total group (Table 5). For the three institutions together, this difference was significant, but for each particular institution, the difference could not prove to be significant.

The application of the procedure reduced the magnitudes of the overall means with respect to the calculated magnitudes of the overall means after the elimination of the effect of the corrections (Table 4). However, small overall means that were significantly different from zero were still present in the AvL in the ventral and the caudal direction with magnitudes equal to 0.6 mm and 0.5 mm, respectively. In the DDHCC, none of the overall means were significantly different from zero. In the BVI there was a significant overall mean different from zero in the cranial direction, with a magnitude equal to 0.8 mm.

Discussion

The offline setup verification procedure resulted in a major improvement of the setup accuracy in the three institutions involved in this study. Despite different treatment techniques, patient setup procedures, and portal imaging systems in the institutions, the same level of accuracy could be obtained by tailoring the procedure to the preestimated treatment accuracy without corrections in each institution, using a computer simulation.

By varying the parameters of the computer simulation procedure, each institution was able to balance the desired level of accuracy against the required number of portal images and setup corrections. The preestimated distributions of systematic and random deviations were not precisely equal to the actual distributions in the clinic. However, the resulting setup accuracy did not critically depend on such differences in input as discussed in an earlier report (14). The resulting setup accuracy was also not critically dependent on the occurrence of trends in time. For none of the institutions was the resulting setup accuracy significantly different from that expected.

In the three institutions, the procedure was mainly executed by technicians. Decisions on corrective actions were indicated by the computer. Technicians appreciated the availability of objective criteria, in contrast to old procedures in

which it was up to the subjective interpretation of the responsible physician to decide on setup corrections. Due to the computerized acquisition and (partly) computerized image analysis, the implementation could be performed without a large increase in workload. Especially in the BVI, image analysis was performed in a time efficient manner. The images were analyzed in the treatment control room after the acquisition of the portal images of two fields, while the patient was irradiated with the other fields from which no portal images were acquired.

In the simulation of the verification procedure it was assumed that the distributions of random deviations were equal for different patients. However, this study revealed that for about 11% of the patients the SD of the distribution of random deviations in one of the directions was larger than the SD of the whole group. Probably due to these large random deviations, the number of setup corrections for this subgroup was significantly larger than the number of setup corrections of the whole group. To deal with these large random deviations in the future, a new estimate of the SD of the random deviations of each individual patient (σ_i) can be made after each new setup measurement. Subsequently, it can be tested whether σ_i is significantly larger than the expected value. Possibly unnecessary setup corrections can be prevented by adapting the parameters of the verification procedure. For these patients, the procedure can be continued with a larger number of setup measurements and a larger initial action level (14). In addition, the treatment plan can be adapted. A new treatment plan can be made for the remaining treatment sessions, with an adapted margin around the clinical target volume. Moreover, the dosimetric consequences of the first part of the treatment (with a wrong estimate of the margin) should also be considered during such an adaption of the treatment plan.

A possible further improvement of setup accuracy can be obtained by "fine-tuning" the procedure. Because, in general, the random deviations are not equal in the three directions, the spherical action level can be replaced by an elliptical action level, with the main axis of the ellipsoid proportional to the variance of the distribution of random deviations in each direction. A further refinement can be obtained by performing corrections with a damping; overcorrection can be prevented as much as possible by performing a correction which is not equal to the average deviation but which is an optimal estimate of the systematic deviation (105).

Sudden shifts in the setup during the course of the treatment were not analyzed. Consequently, these errors were probably interpreted as trends in time. Although there is no clear explanation for these sudden shifts or gradual trends (34) in the setup, their occurrence clearly necessitates a verification procedure after the first stage of the procedure. Using the strategy in the second stage of the procedure of the AvL, with an "outlier" detection, sudden shifts in the setup can be detected quickly. On the other hand, gradual trends are better handled by the "sliding average" procedure of the DDHCC and the BVI. A promising, more general concept for a verification procedure during the second stage of the procedure can be derived from Yan *et al.* (134). In their approach, the setup deviation of the next treatment session was predicted. Corrective actions can be performed when this deviation is unacceptably large.

Conclusions

The offline setup verification procedure resulted in an improvement of patient setup accuracy by a major reduction of large systematic deviations, under different clinical conditions. The procedure could be implemented in the clinic with an acceptably small increase in workload. The resulting setup accuracy and the required workload could well be predicted by means of a computer simulation.

Appendix: Trends

Calculation of trends

The data after the elimination of the effect of corrections were used to determine the occurrence of trends. To study whether trends occurred at all, the deviations in each direction were linearly fitted with time, with the time expressed as the number of days since the start of treatment. It was tested whether slopes were significantly different from zero by means of a Monte Carlo simulation. The consequences of the trends were evaluated by calculating, for patients with a significant trend in one or more directions, the difference between the length of

the 3D setup deviation vector at the start and at the end of the treatment (3D drift).

The distribution of slopes, intersections (or: *initial systematic deviations*) and "time corrected" random deviations were calculated for each direction. For the calculation of the distribution of slopes, all slopes were taken into account, regardless of whether the slope was significantly different from zero or not. The distribution of time corrected random deviations was calculated by eliminating the trend (i.e., a factor equal to the slope multiplied by the time was subtracted from each setup deviation). The standard deviation of this distribution of time corrected random deviations will be smaller than the corresponding standard deviation of the actual distribution of random deviations, σ_{act} , without trends, because trends lead to an overestimate of the random deviations.

Results

In the three institutions, in about half the number of patients trends occurred in one or more directions, with a slope significantly ($p < 0.05$) different from zero (appendix Table 1). In the AvL, most trends were along the left-right axis, while in the BVI most trends were along the dorsal-ventral axis. In the DDHCC, the number of significant trends was about equally distributed over the three directions. In the AvL and the DDHCC, in about 20% of the patients a trend in one of the directions resulted in a drift of the length of the 3D vector that was larger than 5 mm (appendix Table 1). In the BVI, only 5% of the patients had such a drift.

The distributions of slopes had standard deviations that were on average equal to 0.07 mm/day in the AvL and the BVI. In the DDHCC, the SDs were slightly larger, about 0.12 mm/day. There were no preferences of the patients to move into a certain direction during the course of treatment, because none of the distributions of slopes had a mean that was significantly different from zero. The SDs of the distributions of initial systematic and time corrected random deviations were slightly smaller than the SDs of the corresponding actual distributions of the systematic and random deviations, σ_{act} and Σ_{act} , without taking trends into account (Table 4). The overall means of the distribution of initial systematic deviations were only slightly (less than 0.2 mm) different from the overall means calculated without taking trends into account.

Acknowledgements

The authors would like to thank the technicians who assisted in the implementation of the verification procedure. This study was supported by the Dutch Cancer Society, NKB grants NKI 91-01 and DDHK 92-86.

Table A1. Analysis of linear trends in time, with the number of significant ($p < 0.05$) trends and the resulting drift of the length of the 3D vector for patients with such a trend

Institution	AvL	DDHCC	BVI
<i>Number of significant ($p < 0.05$) trends (%)</i>			
<i>Left-right</i>	31	19	19
<i>Caudal-cranial</i>	27	21	17
<i>Dorsal-ventral</i>	11	19	31
<i>Any direction</i>	53	52	52
<i>Drift during treatment > 5 mm</i>	19	21	5
<i>SD all slopes (10^{-2} mm/day)</i>			
<i>Left-right</i>	7.1	12.1	7.5
<i>Caudal-cranial</i>	6.4	12.2	4.7
<i>Dorsal-ventral</i>	6.0	11.3	6.8
<i>SD initial systematic (mm)</i>			
<i>Left-right</i>	2.0	2.8	2.1
<i>Caudal-cranial</i>	2.0	2.6	2.6
<i>Dorsal-ventral</i>	2.5	2.8	3.6
<i>SD random (mm)</i>			
<i>Left-right</i>	1.9	2.1	2.6
<i>Caudal-cranial</i>	1.8	1.9	2.1
<i>Dorsal-ventral</i>	1.5	1.9	2.0

The standard deviation (SD) of the distribution of all slopes was calculated. The SD of the distribution of initial systematic and random deviations, was also calculated (comparable with the SD of the distribution of systematic and random deviations, Σ_{act} and σ_{act} , calculated without taking trends into account (Table 4)).

CHAPTER 6

GENERAL DISCUSSION, CONCLUSIONS AND IMPLICATIONS FOR FUTURE WORK

The past 10 years have shown a surge of activity and energy spent on developing and introducing the various electronic portal imaging devices (EPID) (18,104). The physical characterization of the EPIDs and the development of software tools for image acquisition, contrast enhancement and image comparison preceded their introduction into clinical practice. Studies on patient positioning for the various treatment sites were carried out in order to assess the accuracy achieved when using common positioning and fixation techniques in routine clinical practice. Sometimes, unexpected large variations were found, which necessitated a revision of the positioning technique used. Multiple factors acted together to cause an increasing number of patient positioning studies for various treatment sites: the fact that actual daily positioning could now be evaluated, the general interest in quality assurance, the growing awareness of the concepts of conformal therapy and of the rational basis of the choice of margin size, and the design of treatment schedules testing altered fractionation and/or dose escalation.

6.1. Patient positioning studies

6.1.1. Patient positioning in mantle fields

The first of the quality control studies described in this thesis was carried out using megavolt film, with its limitations in image enhancement and comparison tools. In this study on patient positioning in mantle field irradiation (Chapter 2), the irradiation of complex fields in patients positioned both supine (for the anterior field) and prone (for the posterior field) was analyzed. It was found that the prone position yielded larger errors than the supine position. The overall incidence of errors > 1 cm was 8%, which was modest in comparison to reported error rates for these complex treatment fields. However, for the prone treatment position (PA fields) the incidence of errors > 1 cm was 11%, in contrast to 2% and 5% for the supine treatment position (lateral and cranio-caudal directions, respectively). Moreover, for the prone position a mean 4-5 mm systematic cranial shift of the patients was found. As the prone position was a source of diminished positioning accuracy and was clearly less comfortable for the patients, a positioning technique has presently been introduced in which the patient is positioned in the supine position, and the PA

treatment field is delivered with the gantry rotating to the posterior position at a focus to skin distance of 115 cm. Cerrobend blocks, mounted on the head of the accelerator, are used for individual shielding. First experiences with this technique are satisfactory, both being more comfortable for the patient and more time efficient for the radiotherapy technicians.

6.1.2. Patient positioning in tangential breast irradiation

In the first study which was conducted using the newly developed electronic portal imaging device (EPID), the positioning accuracy in treatment of breast cancer patients using tangential fields was evaluated (Chapter 3). The aims were to check the accuracy of a common positioning technique, and to compare the positioning accuracy obtained with and without a fixation mask. This study yielded unexpected high error rates for field size, collimator rotation and block position. Whereas the positioning of the patient as such was acceptable, with variations of 3.2-4.6 mm (1 SD), the field width and length, the collimator rotation and the position of the lung shielding block varied widely. These findings provided valuable insight into the inaccuracies in treatment positioning which had been caused by the pressures of a very high daily workload on the technicians. In their attempts to rapidly position the patient and align the light field of the treatment unit to the patient's skin markings, they adjusted field width or length and/or rotated the collimator to obtain a visually correct alignment. Figure 1 shows an example of such an erroneous positioning. As a result of this study, the procedures for patient setup were revised: the treatment setup parameters as determined at the simulator were not to be altered at the treatment unit, and more extensive skin markings (especially long lateral reference lines to prevent rotation) were applied. At the same time, record and verify systems were rapidly made operational on all treatment units. One of the main conclusions of this study was, that continuous attention to routine, seemingly safe positioning techniques is of paramount importance to ensure quality control not only in sophisticated, high-dose tight-margin treatment techniques but also in the routine practice treating large numbers of patients.

After completion of this study, several other authors addressed the reproducibility of daily positioning in breast cancer. Similar positioning variations were found with deviations in the ventrodorsal (VD, or anterior-posterior) direction of 3-4 mm (1 SD) (21,36,73,85,121). Margins of 8-10 mm

were shown to be required to cover the breast in 95% of cases (36). The provision of additional arm support seemed to improve setup accuracy, especially in the cranio-caudal (CC) direction (85,121). Setup variations due to respiratory movement were studied by several authors (36,121,129). They found that respiration did not change the volume of irradiated breast and lung tissue within one treatment fraction significantly. The width of the lung tissue in the central plane of the field varied on average 1 mm (1 SD) with a maximum of less than 4 mm. Cranio-caudal movement never exceeded 4 mm during quiet respiration (121).

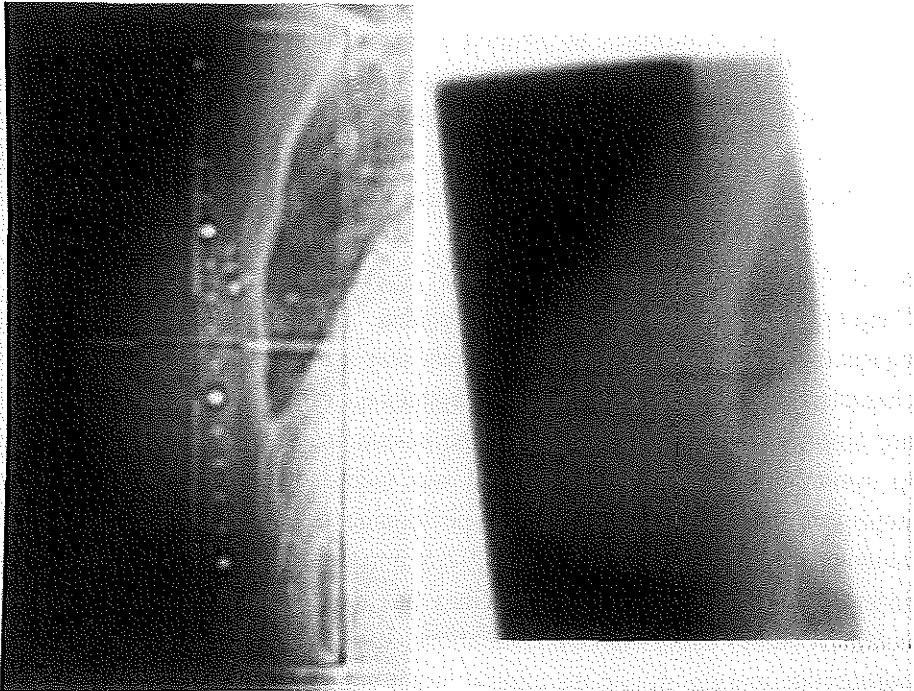


Figure 1

Simulation image and corresponding megavolt image of a tangential treatment field for breast cancer. This was the most extreme case of collimator rotation and increased field width.

After the protocol revision for patient setup and the introduction of record and verify systems on the linacs following the study described in Chapter 3, a follow-up study was conducted in 19 breast cancer patients to check if the variations for field size and collimator rotation had been reduced, and if the accuracy of patient positioning was consistent for the now routine treatment position without a mask on the wedge shaped board. Indeed the positioning accuracy turned out to be similar to that in the first study (SDs 3.8-4.4 mm for the VD direction and 3.1-4.1 mm for the CC direction), while SDs for field width and length were reduced and collimator rotation was eliminated. It appeared that SDs for the medio-lateral beam were on average 1 mm lower than for the latero-medial beam. Probably this reflects the major source of uncertainties in this positioning technique: the position of the ipsilateral arm. The lifting of the arm after axillary dissection is for some patients painful initially. Small differences in position of this arm may cause movement of the skin markings for the lateral beam, which influences field alignment, especially in the DDHCC¹⁰ treatment technique using a fixed source-skin distance. The use of an improved arm support (85,121), and of an isocentric technique, would probably eliminate this difference in accuracy between the beams.

6.1.3. Patient positioning in pelvic fields

Chapter 4 comprises studies on patient positioning in urological and gynecological pelvic fields. It was shown that a patient positioning technique is characterized both by its random and systematic variations. If *random* variations are large, as was initially the case, the positioning technique should be revised to minimize these daily variations. It was indeed demonstrated that the results improved following changes in the positioning techniques. A certain level of random variations (with a SD of 2-2.5 mm for urological fields) remained, inherent to the fact that human beings are daily being positioned by human beings. These small random variations can be dealt with by taking an appropriate margin around the clinical target volume (CTV). Thus, the definition of the margin to be taken around the CTV for each treatment site should be based on data from positioning studies for the specific site and treatment

¹⁰ University Hospital Rotterdam/Daniel den Hoed Cancer Center.

technique. In case of large *systematic* variations, the positioning technique should be reviewed in order to identify possible error sources. For example, the differences in pressure applied to the so-called pubic pin turned out to be a major cause of the systematic variations in the CC direction which had initially been found in gynecological cancer patients. More often, however, the systematic variations are small for some subsets of patients, and large for others. Then the question arises if further immobilization would be advisable, or if efforts should be directed towards early recognition and correction of these systematic errors.

6.1.4. Verification and correction procedure

In Chapter 5 the joint clinical testing by three large radiotherapy centers of a verification and correction procedure in the treatment of prostate cancer is described. It turned out to be feasible, and readily acceptable, to verify the position of the individual patient during four fractions early in the treatment series in order to ascertain the systematic setup deviation for that patient. At each of these fractions, the position of the patient was calculated off-line and the three-dimensional (3D) displacement vector of the isocenter was tested against a preset action level. The action level shrunk at each subsequent fraction: by averaging the new 3D displacement vector with the preceding vectors, the certainty that a displacement was (largely) systematic increased. In the DDHCC the action level diminished from 9 mm initially to 4.5 mm after 4 fractions. If at one of these initial four fractions the 3D displacement vector exceeded the action level for that fraction, the technicians corrected the isocenter position at the subsequent treatment fraction. In case of a correction, the verification and correction procedure was repeated. If after 4 fractions no correction had been applied, weekly checks were performed. This off-line verification and correction procedure was rapidly accepted. The incidence of mean (systematic) 3D deviations > 5 mm was reduced from 26% to 0%. Prerequisites for such a verification and correction procedure are a previously determined, acceptably low random error rate and a dedicated group of technicians performing the analyses and the corrections. Systematic errors can then be reduced to low levels (the magnitude of remaining errors depending on the action level chosen), ensuring a reproducible positioning within narrow and known limits. Especially

in conformal therapy such a verification and correction procedure has become an integral part of treatment protocols.

6.2. Implications for clinical practice

Some important questions remain to be resolved. To what extent are the findings of these and other studies representative for what can be implemented and expected in daily clinical practice? When should off-line verification and correction be chosen and when should this be performed on-line? What should be the frequency of portal imaging? What are its limitations and pitfalls?

The pelvis has been the site of study for the large majority of publications on portal imaging. The bony pelvis is easily recognizable on portal images, and after contrast enhancement, the quality of the images is virtually never a problem. Furthermore, it is a site of curative, high dose treatments, and the target volume is directly adjacent to sensitive organs (of which the rectum is the most important in terms of complication rates and its position close to, and partly in, the planning target volume). Prostate cancer is a commonly occurring tumor, so patient numbers are large enough to ensure rapid patient accrual into a study, and the benefits of improvement are applicable to many patients. Large numbers of studies have been carried out analyzing positioning accuracy in treatment of prostate cancer, which have been discussed in Chapters 4 and 5. This extensive studying of patient positioning in the pelvic region has led to various concepts of considerable importance.

6.2.1. *Organ motion*

The use of computed tomography (CT) scans for radiotherapy treatment planning enables accurate target volume delineation and tight beam planning. In the near future, the combination of CT with magnetic resonance imaging (MRI), with its superior ability to characterize soft tissues and delineate tumor extent, may provide further improvements in accuracy of target volume definition (63,98). However, during treatment the relative positions of the target (prostate gland) and the organs at risk (rectum and bladder) are variable, and susceptible to rectum and bladder filling. The more accurate the definition of the target volume becomes, and the tighter the margins are taken, the more important this

variability is. This stimulated studies on prostate motion. It was found (3,9,11,82,101,113,119) that movement of the prostate in the VD direction is larger than in the CC direction, whereas lateral movement is insignificant. The range of movements reported is 0-10 mm for the VD and CC directions (SDs 1-4.5 mm), and 0-2 mm for the medio-lateral (ML) direction. The movements are mainly limited to the superior part of the prostate and the seminal vesicles, and are clearly correlated with rectal filling. Rotations of the prostate around the ML axis also occur with rectal filling (119). Prostate movement is to a much lesser extent correlated with bladder filling (and then mainly in the prone treatment position). Movement of the prostate is also correlated with leg motions (119). Initial rectal volume or diameter does not correlate with the degree of prostate movement during treatment (11). As these movements can have a significant effect on target volume coverage, the findings resulted in recommendations for nonuniform margins to take around the prostate (92,100,101), in the use of prostate markers (7), and in the incorporation of motion uncertainties into the treatment plans (74). Pickett *et al.* (92) recommended that patients should be CT scanned and simulated with their rectum empty and their bladder full (most posterior position of the prostate). They applied nonuniform margins around the prostate, arguing that for the respective directions not only the range of prostate movement, but also the risk-benefit ratio is clearly different. Especially the posterior margin is critical, as enlargement results in an increased risk of rectal complications. They chose anterior and inferior margins of 2 cm, a posterior margin of only 0.5 mm and lateral and superior margins of 1.0 and 1.5 cm. Dose volume histograms showed that these nonuniform margins yielded equal sparing of rectum and bladder in comparison to an 1 centimeter uniform margin, whereas for the nonuniform margins the CTV coverage was adequate, in contrast to inadequate coverage of the CTV in 40% of cases for 1 cm uniform margins. Balter *et al.* (7) used an invasive method to account for organ motion: four radioopaque markers were implanted in the prostate and daily on-line verification and correction (VC) was carried out after analysis of the position of these markers, rather than of bony landmarks. Drawbacks of this approach are the time intensive daily on-line VC, the invasive nature of the intervention (each patient would need to have markers implanted) and the potential migration of markers, for example due to tumor regression.

6.2.2. Coverage probability

Mageras *et al.* (74) proposed a method to incorporate both systematic and random organ motion uncertainties into the treatment plan. Using data on prostate motion from an earlier study (82), they prospectively simulated organ motion effects during treatment planning of prostate cancer patients. Thus, a set of dose distributions was obtained, and ranked according to the mean CTV dose. Upper and lower confidence limit dose volume histograms (DVH) were generated, allowing the clinician to compare the coverage of target and nontarget organs to the DVH for the nominal plan.

The concept of incorporating both patient positioning variations and organ motion uncertainties into the treatment plan was explored in the DDHCC by Visser *et al.* (124,125) and Stroom *et al.* (109,111). The effects of the systematic and random variations determined in earlier studies (Chapters 4 and 5) were included in the treatment planning, yielding distributions of the so-called coverage probability (the probability of a point to be covered by the CTV). Dose probability histograms were calculated. For prostate cancer, literature data were used to incorporate the effects of organ motion as well. Figure 2 illustrates the effects of patient positioning variations and organ motion on the dose distribution for a prostate cancer case. Such a method of estimating the true dose distribution around the CTV provides an alternative approach to the more rigid use of CTV and PTV in the ICRU-50 report (61). It allows to individually choose the PTV as a volume corresponding to a high coverage probability level, and to calculate (nonuniform) optimized PTV margins based on the requirement that the CTV is irradiated to the specified dose with a high probability.

6.2.3. Digitally reconstructed radiographs versus simulation films

The fact that the positioning of the patient during CT scanning, which is the basis for the treatment plan and DVH calculations, is not exactly reproduced at simulation was explored by Bel *et al.* (12). In fact, the positioning at simulation represents one of the various treatment positions, with the difference that the setup at the simulator is checked using the CT data and planning information. From the CT data set a Digitally Reconstructed Radiograph (DRR) can be calculated, which represents a simulated X ray fluoroscopy image for the intended beam direction.

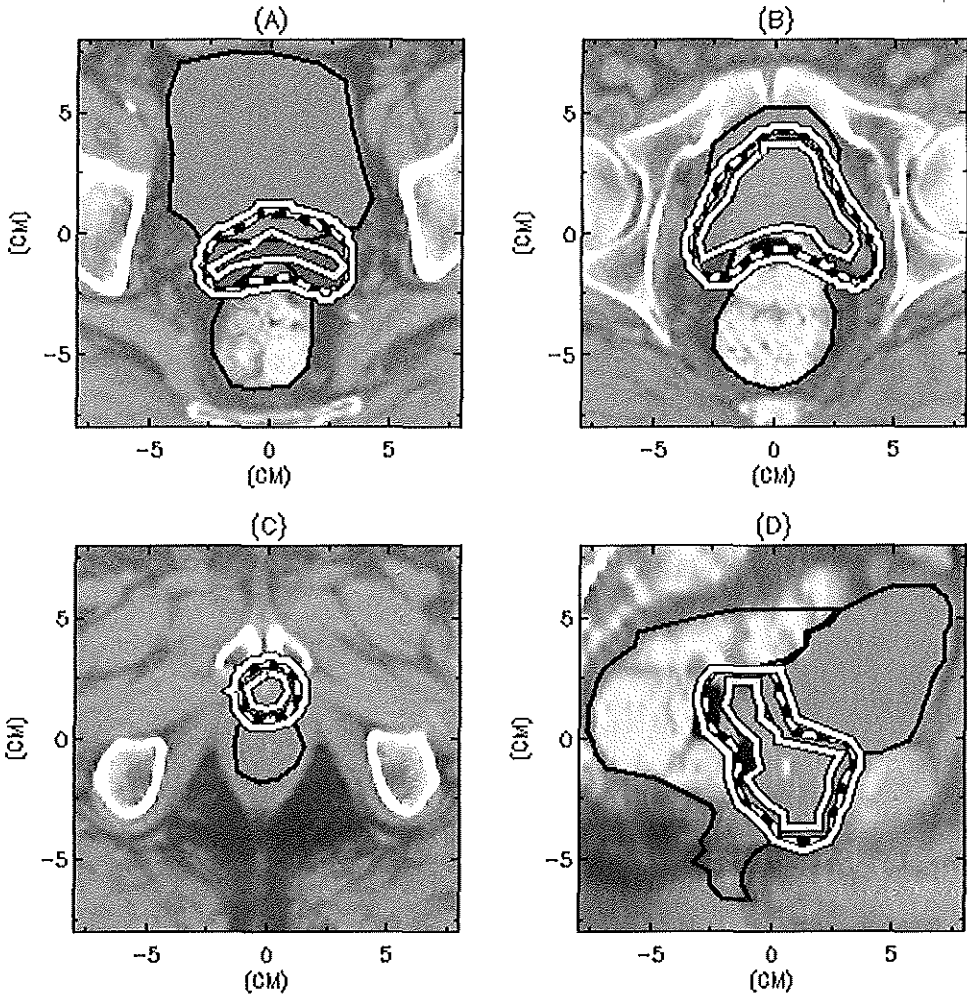


Figure 2

Treatment planning in prostate cancer using stepwise PTV calculation in a cranial transversal slice (A), a slice at the isocenter (B), a caudal slice (C), and a sagittal reconstruction (D). The CTV (inner grey contour) has been outlined by the radiation oncologist. This volume is subsequently expanded with a margin to account for the systematic setup variations and organ motion effects (PTV1, dotted line). The final PTV (outer white contour) results after the incorporation of random setup variations. Note that in the sagittal slice the influence of organ motion (especially rotation around the apex) can be clearly seen: the PTV margin is significantly larger in the cranial part of the target volume than in the caudal part. The contours of the rectum and bladder are depicted in black. Figure taken from ref. 109, with permission.

Bel *et al.* studied transfer errors by matching the simulation films with DRRs. Transfer errors were 1.5 mm (1 SD) for the ML direction and 4.5 mm (1 SD) for the CC direction in case of routine simulation. The use of DRRs at simulation (and the taking of extra simulation time) reduced these transfer errors to 1.4 mm and 1.5 mm (1 SD), respectively. The recommendation that DRRs be used for judgement of treatment setup rather than the simulation images, would reduce the role of the simulation procedure itself. Possibly, accurate checks of the patient setup at the treatment unit, using DRRs for comparison, could replace the simulation procedure completely. However, this would require high resolution DRRs (and thus the use of a very small CT slice distance), and MV imaging of sufficiently high quality and contrast.

6.2.4. Verification and correction procedures

The development and clinical testing of verification and correction (VC) procedures, both off-line (as described in Chapter 5) and on-line (6,28,35,38,83,117) showed that increased positioning accuracy can be attained and tight margins can be ensured, which make these procedures an indispensable part of conformal therapy, and a prerequisite especially in dose escalation protocols. It is clear that computer aided verification with actual measurement of the isocenter position yields much more improvement in accuracy than eye guided verification and correction (17,83,117). In the study by Michalski *et al.* (83) only 1.4% of the fields was corrected after visual judgement of an error > 1 cm. However, in 10% of the fields an error > 1 cm was present. Van den Heuvel *et al.* (117) showed that eye guided VC resulted in a reduction of the overall standard error from 5 mm to 2.5 mm for the ML direction, while for the CC direction there was only a marginal reduction of 5 to 4.5 mm. A computer aided VC procedure showed reduction of both systematic and random errors to SDs of ± 1 mm. Several authors (17,28,117) found that visual judgement is far more accurate in the ML than in the CC direction, due to more anatomical structures marking the ML direction (the pubic symphysis, the pelvic rim). Bissett *et al.* (17) conducted a study on quantitative vs. subjective (judgement by four radiation oncologists) verification of patient setup. While the translational error in the ML direction correlated with the oncologists' assessments, this was often not the case for CC translations. For rotational errors, there was no association between error size and clinical judgement. Gildersleve *et al.* (38)

randomized between intervention (eye guided VC supported by rapidly alternating display of the simulation and treatment images) and conventional treatment. In the intervention treatment, 71% of setups were corrected, reducing the error rate > 5 mm from 48% to 2%.

The improvements in setup accuracy by VC procedures are, however, made at the cost of increased treatment time (the reported increase in time spent at the treatment unit varied from 1 to 10 minutes for on-line VC, and usually some 1-2 minutes for off-line VC, in case of a correction). Most authors expected this extra time to reduce considerably with increasing experience with the protocol; indeed some reported an extra time of only 1 to 3 minutes. On-line VC is more time consuming than off-line VC, especially taking more time at the treatment unit itself, which is cumbersome for both the patients and the technicians. Moreover, the frequent treatment interruptions when using on-line VC may cause patient anxiety. These are some of the major drawbacks of on-line VC. Therefore, at the present time it seems advisable to use off-line VC whenever possible, and reserve on-line VC for selected cases with predominantly large random errors.

A computerized accept or reject strategy was described by Yan *et al.* (134) and Wong *et al.* (131). Using a software tool for off-line evaluation of portal images, the positioning accuracy is estimated for each patient after a number of initial portal images. The setup variation in the next treatment session is predicted by estimating a confidence region that should contain the next setup position. Then an accept or reject decision can be made by comparing this confidence region with a predefined allowance region of setup variation. As the confidence region is continuously updated during the course of treatment, the model adequately deals with time trends in patient setup. The retrospective simulation of such an accept or reject procedure showed that it correctly estimated the setup variations throughout the course of treatment, and that a 'reject' decision accurately predicted subsequent positioning outside the allowance region. Major drawbacks of such an approach are the facts that it is time consuming and that daily imaging is required. Yan *et al.* (133) further used this VC procedure in so-called adaptive radiation treatment (ART). After 8 initial treatment sessions, the confidence region of the current and subsequent setups is calculated. Based on this information, the margin around the CTV (and even, with a view to dose escalation, the prescribed dose) can be adaptively

modified. The field changes are applied by defining new multileaf collimator settings, instead of physical patient repositioning. This approach uses small margins for one patient, but larger margins for another, using initial treatment data to decide on margins on an individual basis. Simulation of the ART process for prostate cancer treatment demonstrated that for 64% of patients it would be possible to reduce the margins and, for the same NTCP, to increase the dose. It should be noted, however, that as the PTV is individually modified during treatment, the international guidelines to prescribe and report PTV doses (61) cannot be used.

6.2.5. Out-of-plane rotations

The value of (2D) VC procedures is limited when out-of-plane rotations are present. These out-of-plane rotations cause 3D anatomy displacements, which are seen in the 2D images as distortions. These can be wrongly interpreted as translations, and erroneous corrections can result. The problem of out-of-plane rotations was studied by Hanley *et al.* (51). If out-of-plane rotations occur, the matching of verification images with their reference image is impeded, leading to so-called misregistration errors: the difference between the calculated treatment position using the verification procedure, and the actual position. The magnitude of such misregistration errors was calculated, as well as their dosimetric effects. For pelvic treatments, the out-of-plane rotations comprised a pelvic 'roll' (rotation around the CC axis) or a pelvic 'tilt' (rotation around the ML axis). These were simulated in a phantom study. For out-of-plane rotations $> 2^\circ$ the misregistration errors were 2.3 ± 1.0 mm. As for prostate treatments the dose gradients are extremely steep in the VD direction, the misregistration errors in this direction dominated the dosimetric effects. They could result in an overdosing of the rectal wall: for example, an NTCP increase from 7.7 to 13.1% was calculated for a 2° rotation around a point on the abdominal skin. It was concluded that if out-of-plane rotations are ruled out, 2D image registration does not introduce errors > 1 mm or $> 1^\circ$ and can thus be confidently used to monitor and correct patient setup. Bijhold *et al.* (16) stated as well, that the magnitude of out-of-plane rotations should be less than 2° and that the displacements involved should be < 10 mm, for 2D VC to result in appropriate corrections. If these restrictions are violated, this is indicated by an imperfect

alignment of anatomical features. The displacement parameters then found may be erroneous and should not be used for a correction of the patient setup.

Although van Herk *et al.* (119) found only slight out-of-plane rotations of the pelvic bone in their analysis of prostate cancer treatments, for other sites out-of-plane rotations may be of clinical significance. In gynecological cancer patients treated to large pelvic fields, out-of-plane rotations of the pelvis (in particular pelvic tilt) are observed (25,110). Bel *et al.* (13) described a study on setup deviations in wedged pair irradiation of parotid gland and tonsillar tumors. Due to out-of-plane rotations (for example 'nodding' of the head), it was at first not possible to obtain consistent translational setup deviations. An improved fixation mask and the placement of a wax mould with metal markers in the external ear during portal imaging were required to obtain an adequate quantification of the setup deviations.

In cases where conventional 2D analysis produces inconsistent results, full 3D analysis based on DRRs could provide additional information (39). As DRRs can be computed for arbitrary angles, out-of-plane rotations can be accurately quantified. If persistent out-of-plane rotations are detected, they should be prevented by adjusting the positioning technique.

6.2.6. The frequency of portal imaging

Weekly portal filming, as traditional state-of-the-art practice, is not an adequate way of evaluating patient setup, as shown by Valicenti *et al.* (116). They performed daily EPI to evaluate the accuracy of weekly portal filming for various treatment sites. The displacements measured on the portal films frequently deviated from the corresponding portal image obtained in the same treatment setup. The respective frequencies of field placement errors exceeding tolerance limits of > 5 mm (for the head and neck region), > 7 mm (for the thorax) or > 10 mm (for the pelvis) were 11% for portal films and 14% for EPI in the ML direction (difference not significant). Surprisingly, for the CC direction the field placement error frequencies were 24% for portal films as compared to 13% for EPI ($p=0.0001$), mainly due to differences in the thorax and head and neck sites. The fact that portal films yielded more errors than EPI was considered to be mainly due to disruptions of the treatment procedure for the placing and removing of the films, causing movements of the patients. Interestingly, Hunt *et al.* (59) noted somewhat larger errors recorded by EPI

than by megavolt film. This was considered due to more care being taken by technicians on film days.

A single portal film is most likely to be of value if the systematic error component is much larger than the random error component. What, then, is the correct frequency of portal checks? Mitine *et al.* (86) and Denham *et al.* (30) both focused on the number of port films necessary to differentiate between random and systematic setup errors. This is essential, as an isocenter displacement on the basis of one (weekly or once only) portal film is not based on any insight into the nature of the displacement observed. Denham *et al.* argued that the larger the random error involved, the greater the number of films required before a systematic error can be reliably detected and quantified. For example, a random error as large as 10 mm would necessitate at least 7 films, whereas a random error of 4 mm would require 2-3 films, for detection of a systematic error of 5 mm. Mitine *et al.*, on the contrary, stated that for properly immobilized head and neck patients a single film check would be appropriate. As their comparison of simulation films to the first portal films yielded a positioning variation of 4 mm (1 SD) and the SD of subsequent films was 2.5 mm, they concluded that most errors were of systematic nature and therefore a single check would suffice. Using Mitine's data, Lebesque *et al.* (66) calculated that this policy of correcting an observed error on the single film check of > 5 mm, would cause 10% erroneous set up corrections and in 5% leave an undetected large systematic deviation (counteracted by a random variation in the opposite direction) uncorrected.

The computation of the number of portal images necessary to distinguish systematic and random variations, using predetermined random error rates for the same patient groups treated in the same institution as input, as described in Chapter 5, seems a reasonable and reliable alternative, while not causing too high a workload. For example, in the DDHCC at present three portal images are required for prostate cancer treatments, and four images for gynecological sites, to determine systematic errors and decide on corrections.

In general, once daily imaging for each treatment field is sufficient for the verification of patient positioning (36,114,121,129). Tinger *et al.* (114) determined intrafractional displacements in pelvic treatments (calculated from two images of each field). As the SDs of the interfractional displacements were more than 3 times as great as those of the intrafractional displacements for all

directions, intrafractional displacements were no significant factor in terms of positioning accuracy. Intrafractional displacements were also studied in breast cancer treatment (36,121,129). Intrafractional variation, being a reflection of both patient movement and normal respiration, was shown to be minor in comparison to interfractional variation. For example, Fein *et al.* (36) reported intrafractional variations of 0.9-2.1 mm (1 SD), contrasted to interfractional variations of 3.2-6.3 mm.

6.2.7. Patient positioning and immobilization

It can be learned from the studies cited above that first of all treatment accuracy is improved by the careful handling of patient positioning at the treatment unit itself. Positioning a patient is a tedious task, in which the technicians have to perform complicated setups using individual shielding and often asymmetrical fields, and have to deal with the patients themselves and inherent factors such as nervousness, their medical condition, etc. Kortmann *et al.* (65) analyzed positioning accuracy in difficult patient positioning (due to pain and reduced mobility of the patients' hips after operation). It was demonstrated that considerable variations occurred (SDs 4-8 mm for translations and 3.5-5° for rotations) in this difficult group. The inaccuracies mostly represented large random fluctuations. That high workloads and continuous time pressure result in less accurate setups was shown by Probst and Griffiths (95). In their study on the accuracy of a setup of a complex shaped cranial field, the technicians who had taken as much time as needed for patient setup, took on average 2 minutes extra and positioned the patient more accurately than a group of technicians who had performed the same setup at increased speed. Mean worst case discrepancies between simulation and treatment films were 5 mm for the increased speed setups, compared to 4 mm for the normal work speed. Thus, if a VC procedure were to be used in such setups, the extra time spent at careful positioning might be offset by the fact that less extra time would be needed for setup corrections. Motivating and educating technicians in these concepts is of great importance, as well as not increasing time pressure beyond limits.

When considering treatment accuracy, attention should be paid to immobilization. The advantages and disadvantages of immobilization devices should be weighed. In the head and neck area, fixation masks are obviously indispensable, as the range of complex movements in this area requires rigid

immobilization, and the patient is spared the nuisance of skin drawings and/or tattoos in this area. For breast treatment, the great disadvantage of increased skin reactions caused by the mask does not counterbalance the modest increase in positioning accuracy (Chapter 3). The large separation between the fixation points of these breast masks and the relatively wide range of possible movement within the mask made its role in preventing setup variations very limited. This can also be stated for the pelvic area, especially in cases where improved fixation would be most required (e.g., obese gynecological patients). Such pelvic masks do not improve positioning accuracy (27). Neither do vacuum mattresses seem to provide extra support (96). Only alpha cradles have been reported by some authors (102,107) to improve setup accuracy for pelvic treatments, however, others (87,108) did not find this improvement. Alpha cradles have the disadvantages of high cost (being used once and discarded after use) and the improvements in accuracy, if any, are modest. Song *et al.* (108) reported a comparative study in prostate irradiation using four different types of immobilization. The 62 patients were treated in the supine position using a four-field box technique. They were divided into five groups, with respectively no immobilization, an alpha cradle from the waist to the upper thigh or to below the knees, a styrofoam leg immobilizer, and an aquaplast cast encompassing the entire abdomen and pelvis with alpha cradle leg and feet immobilization. Overall, the maximum deviation was 2 cm and the median 1.2 cm. The probability of a deviation > 5 mm (called a 'movement') ranged from 0 to 76%, with a mean of 39%. There was no significant difference between the groups in the overall movement. The aquaplast immobilization had the smallest movement probability in the CC and VD directions, but had the largest movement probability in the ML direction. None of the immobilization devices produced a significant reduction in movement in obese patients compared to the setup without immobilization. Interestingly, in the group without immobilization, neither obesity nor increased pelvic circumference resulted in larger movement probability.

It can be concluded that careful daily positioning by motivated technicians potentially improves setup accuracy more than any immobilization device. The use of EPID at all treatment units would provide them with a tool to develop insight into the individual patient's setup, and into sources of inaccuracies. VC

tools which can independently be used, with predetermined action levels, will greatly enhance the responsible handling of daily patient treatment. As Ezz *et al.* (35) put it: "We envision the use of portal imaging in a way that may change the practice of radiation therapy. Rather than just use skin marks, the technicians will also use the internal bony anatomy, as seen in the portal image. However, this approach to radiation therapy will require considerable change in attitude by both radiation oncologists and technicians".

6.3. Recent developments and present EPI use in the DDHCC

The pelvic studies (Chapters 4 and 5) formed the basis for the present use of the off-line VC procedure for prostatic irradiation as a routine protocol. Furthermore, the VC procedure was also studied in a group of gynecological cancer patients. While the systematic errors (1 SD) were reduced from 2.4 mm (ML direction) and 4.2 mm (CC and VD directions) without the VC procedure, to 1.3 mm (ML) and 2.0 mm (CC and VD) using VC, the random error remained relatively large (3-4 mm). In some patients, the large random errors would cause too many corrections, which would not result in an improvement of setup accuracy, as they would involve the off-line correction of a setup error largely being caused by random variations. Therefore, the action level was taken higher in the patients which showed large random errors. The use of vacuum mattresses for immobilization did not improve these results (96). The larger random error rate in the gynecological patient group and the lack of improvement using immobilization led to the conclusion that on-line VC would be required for further reduction of setup errors. The study of on-line VC in the gynecological patient group (25,110) comprised 14 patients. After the acquisition of a 6 monitor unit (MU) image, the irradiation was interrupted to analyze the position of a set of anatomical landmarks in this AP image. In case of a (2D) setup deviation greater than 4 mm, a correction was applied by translating the patient couch. During the remaining treatment a 30 MU image was obtained for off-line analysis of both the AP and lateral fields to check the correction. With the use of this on-line procedure, the time spent at the treatment unit increased 1.5 minute. In case of a correction, a further 2.5 minutes were used. The time spent off-line to analyze the images was 10 minutes for an experienced

technician. The procedure was rapidly accepted by the technicians. In 57% of treatments a correction was applied. Both random and systematic errors were reduced to 1-2 mm, the limit of accuracy of the procedure itself. It appeared that in this patient group, consisting of females treated to the entire pelvis, out-of-plane rotations (especially rotation around the ML axis or 'tilting' of the pelvis) sometimes limited the value of the 2D analysis. This was met by choosing parts of the pelvis for contour matching which were least susceptible to these rotations (the pelvic rim). Figure 3 illustrates the on-line VC procedure.

Since 1994, the two DDHCC SRI-100 imaging devices have both been mounted on one of the most sophisticated linear accelerators, the dual gantry racetrack microtron (MM50), one on each gantry. In June 1997 one of these was replaced by an EPID with improved imaging characteristics, developed in the DDHCC. As many studies on conformal therapy are carried out at this treatment unit, the EPIDs are in continuous use. For all prostate treatments, the VC procedure is routinely used. This does require extra time investments, mainly off-line, as the technicians perform all analyses themselves. Because of the time pressure and in view of the low random error rate for prostate treatments, recently the number of initial portal images was reduced from 4 to 3. For gynecological patients a study on prone positioning in a so-called belly board (68,106), in order to reduce the volume of small bowel in the field, has recently been carried out. The positioning of these patients was monitored using the off-line VC procedure. Preliminary results show the random error rate to be relatively modest (1.6 - 2.6 mm), probably due to the facts that the board is in some respects an immobilization device, and that daily positioning is carried out with great care. Systematic errors are < 2 mm, reflecting the use of the VC procedure.

Apart from the use of EPI and of VC in pelvic treatments, conformal therapy studies have been started for treatment of lung cancer and of head and neck cancer, of which VC procedures are an integral part.

6.4. Drawbacks in the introduction and use of EPID

The introduction of fast electronic portal imaging has enabled the development of sophisticated procedures for patient setup verification and correction.

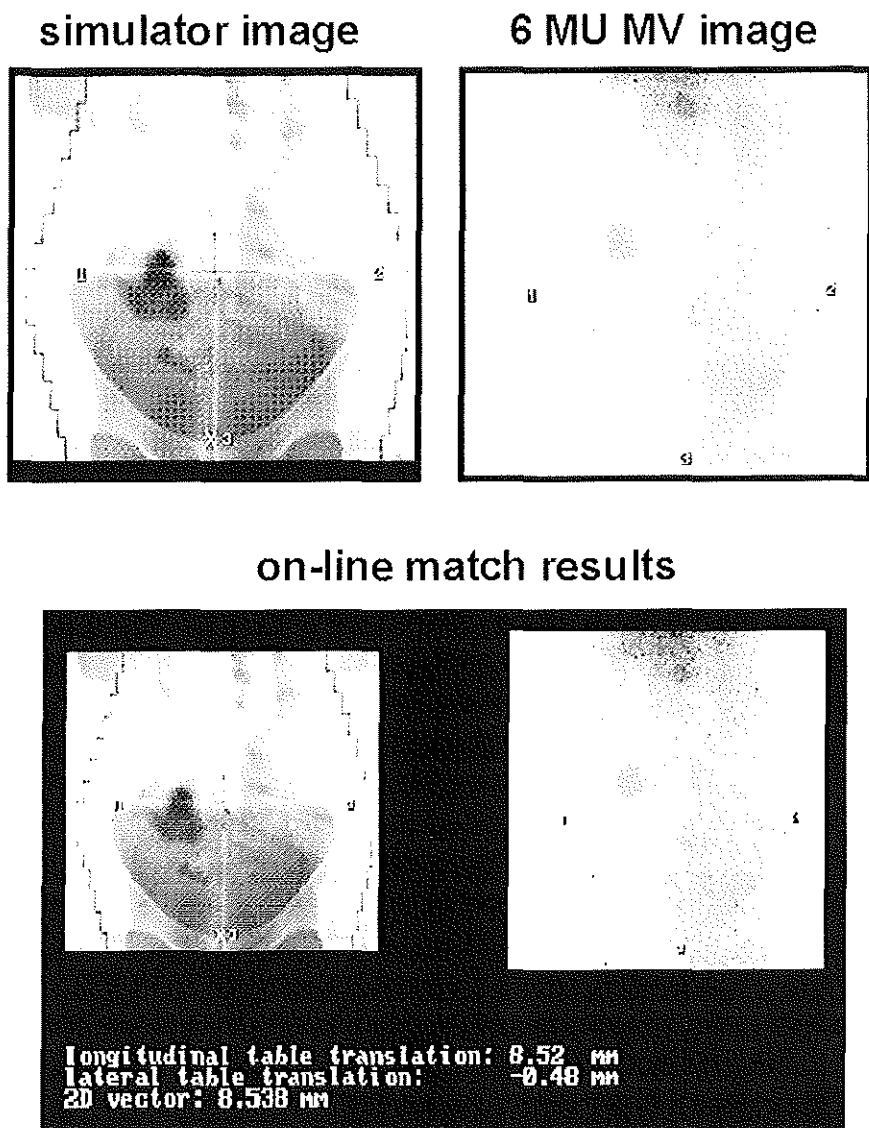


Figure 3A

On-line verification and correction procedure in gynecological cancer. (1) Display of the simulation image and selection of anatomical landmarks. (2) On-line 6 MU megavolt image of the AP field. The treatment is interrupted, and the position of the landmarks is indicated in the megavolt image. (3) The position of the patient is determined by comparison of the position of the landmarks in the simulation and the megavolt image. If the 2D setup deviation exceeds 4 mm, the patient couch is translated.

contour match 30 MU image



Figure 3B

During the remaining fraction dose, a 30 MU megavolt image is made. To determine the final patient setup, the 30 MU image is analyzed offline using a semiautomatic contour match procedure.

Moreover, it has stimulated awareness of and attention to the presence of daily variations in positioning, causes of imprecise treatment setup and methods to improve positioning accuracy. This does, however, not mean that these principles are nowadays fully integrated in daily routine practice. EPIDs are being acquired by many radiotherapy departments with the purpose of improving quality control and ensuring positioning accuracy. However, in practice, the actual use of the EPID depends on the availability of software tools for rapid image analysis and interpretation. Often the commercially available EPIDs come with insufficient software for practical use. Much effort of the department staff is required before efficient use of the EPID can be made and the device becomes fully integrated in clinical practice. Several factors strongly influence the acceptance and integration of an EPID in a radiotherapy department. The fact that the physicians and the technicians are not familiar with the new tool plays a role, as well as some undefined feeling that one's expertise at daily treating patients is being questioned. Furthermore, the accessibility of the software to not too experienced users and the speed at which analyses can be done determine the acceptance of the EPI procedures in a busy practice.

Of paramount importance are the consequences of the acquisition of portal images and the detection of positioning variations. If requirements are met as to the quality of the images and software tools, and if clear procedures are designed by which technicians can perform setup verification themselves and act according to the level of positioning variations found, EPI helps them to gain valuable insight into individual treatment accuracy and will act to emancipate them. Thorough training of the technicians in use of the EPI and its software for image analysis and comparison, and in the use of VC procedures is indispensable, as the precision of a VC procedure is dependent on the reproducibility of the image analysis.

When introducing an EPID into clinical practice, education of the physicians and technicians is needed in order to inform and motivate them and demonstrate the scope of possible applications. Smoothly functioning software is required to obtain easy acceptance, as time pressures are high. But first of all should the physicians come to an agreement as to what is considered a relevant variation. To draw arbitrary lines, such as considering a deviation > 5 mm unacceptable and ≤ 5 mm within limits, is not clinically justified in this era of conformal therapy, dose escalation and reduction of normal tissue complications. Each

treatment site, each technique, and each treatment intention requires dedicated verification procedures. If clear decisions are made for each site and technique, then appropriate VC procedures and tolerance limits can be designed. Choices should be made as to which techniques require very precise monitoring (as in high-dose, high-precision therapy) and which allow a more relaxed approach, never forgetting that most of the impact of quality control is obtained in improving the treatment quality of the large majority of routine treatments.

6.5. Conclusions and recommendations

Quality control of the accuracy of patient positioning is required not only in sophisticated treatment techniques, but also in routine clinical practice. Error rates should be minimized by optimizing treatment techniques and by careful daily patient positioning by motivated technicians, routinely using electronic portal imaging.

Verification and correction procedures are essential to recognize and correct systematic errors early in the course of treatment. Visual comparison of the simulation and portal images is of limited value. A computer aided analysis and quantification of the differences between simulation and portal images for all directions is indispensable. Before a VC procedure is integrated in patient setup protocols, it is required that the random error rate is small and reliably known, and no major out-of-plane rotations are present.

An off-line VC protocol as described in Chapter 5 seems to be an ideal compromise between the limited value of weekly portal imaging, and the very time consuming use of daily on-line VC procedures. However, the number of corrections carried out on the basis of an off-line VC protocol should be limited: for individual patients with large random errors, multiple setup corrections could result which would hardly improve the setup accuracy. For such patients an early switch to on-line VC should be made. It seems a reasonable approach to limit the number of off-line corrections in each patient to a maximum of two, and to switch to on-line VC if the setup is still not satisfactory. This would prevent the labor intensive and time consuming use of on-line VC in the large majority of the patients, but make selective use of it as required.

The use of data on systematic and random setup variations and organ motion during treatment planning enables the calculation of dose distributions and/or dose volume histograms which show the clinician what target coverage and normal tissue dose realistically to expect. Optimized PTV margins can be defined and individual treatment choices can be made.

EPI and VC procedures of such speed, ease, and automation level that imaging each treatment fraction can be considered a routine procedure, seem realistically to be within reach in the near future. Such a practice would allow the technicians to deal with gross errors and accidental mistakes (such as the misplacement of a block or wedge) by on-line correction. Off-line VC procedures could then be used to monitor treatment accuracy for all patients, intervening off-line when required, or switching to on-line VC in cases with predominantly random errors. Such routine EPI use requires dedicated protocols and tolerance limits for each treatment site and technique.

Finally, it should be kept in mind that no VC procedure does provide insight into the sources of the errors recorded. Probably, these are mostly due to the infinite number of possible movements and distortions in the human body, and are most effectively reduced not by ever tighter immobilization, but by giving the patients proper information, understanding and reassurance as well as time to settle down. This remains the professional skill of the technicians, which no EPI procedure could or should ever replace.

Bibliography

1. Althof VGM, Creutzberg CL, Huizenga H, Visser AG, Swanenburg BN. On the clinical use and characteristics of the first Philips radiotherapy imaging system. In: Hukku S, Iyer PS, eds. *Proceedings 10th International Conference on the Use of Computers in Radiation Therapy*. Lucknow, India: Sanjay Gandhi Post Graduate Institute of Medical Sciences, 107-110, 1990.
2. Althof VGM, De Boer JCJ, Huizenga H, Stroom JC, Visser AG, Swanenburg BN. Physical characteristics of a commercial electronic portal imaging device. *Med Phys* 23: 1845-1855, 1996.
3. Althof VGM, Hoekstra CJM, Te Loo HJ. Variation in prostate position relative to adjacent bony anatomy. *Int J Radiat Oncol Biol Phys* 34: 709-715, 1996.
4. Ågren Cronqvist A, Källman P, Turesson I, Brahme A. Volume and heterogeneity dependence of the dose-response relationship for head and neck tumours. *Acta Oncol* 34: 851-860, 1995.
5. Baily NA, Horn RA, Kampp TD. Fluoroscopic visualization of megavoltage therapeutic X-ray beams. *Int J Radiat Oncol Biol Phys* 6: 935-939, 1980.
6. Balter JM, Chen GTY, Pelizzari CA, Krishnasamy S, Rubin S, Vijayakumar S. Online repositioning during treatment of the prostate: A study of potential limits and gains. *Int J Radiat Oncol Biol Phys* 27: 137-143, 1993.
7. Balter JM, Lam KL, Sandler HM, Littles JF, Bree RL, Ten Haken RK. Automated localization of the prostate at the time of treatment using implanted radiopaque markers: technical feasibility. *Int J Radiat Oncol Biol Phys* 33: 1281-1286, 1995.
8. Balter JM, Sandler HM, Lam KH, Bree RL, Lichter AS, Ten Haken RK. Measurement of prostate motion over the course of radiotherapy. *Int J Radiat Oncol Biol Phys* 27 (Suppl. 1): 223, 1993.

9. Balter JM, Sandler HM, Lam KL, Bree RL, Lichter AS, Ten Haken RK. Measurement of prostate movement over the course of routine radiotherapy using implanted markers. *Int J Radiat Oncol Biol Phys* 31: 113-118, 1995.
10. Beard CJ, Bussiere MR, Plunkett ME, Coleman CN, Kijewski PK. Analysis of prostate and seminal vesicle motion. *Int J Radiat Oncol Biol Phys* 27 (Suppl. 1): 136 (abstract), 1993.
11. Beard CJ, Kijewski PK, Bussière M, Gelman R, Gladstone D, Shaffer K, Plunkett M, Costello P, Coleman N. Analysis of prostate and seminal vesicle motion: implications for treatment planning. *Int J Radiat Oncol Biol Phys* 34: 451-458, 1996.
12. Bel A, Bartelink H, Vijlbrief RE, Lebesque JV. Transfer errors of planning CT to simulator: A possible source of setup inaccuracies? *Radiother Oncol* 31: 176-180, 1994.
13. Bel A, Keus RB, Vijlbrief RE, Lebesque JV. Setup deviations in wedged pair irradiation of parotid gland and tonsillar tumors, measured with an electronic portal imaging device. *Radiother Oncol* 37: 153-159, 1995.
14. Bel A, Van Herk M, Bartelink H, Lebesque JV. A verification procedure to improve patient setup accuracy using portal images. *Radiother Oncol* 29: 253-260, 1993.
15. Bijhold J, Lebesque JV, Hart AAM, Vijlbrief RE. Maximizing setup accuracy using portal images as applied to a conformal boost technique for prostatic cancer. *Radiother Oncol* 24: 261-271, 1992.
16. Bijhold J, Van Herk M, Vijlbrief RE, Lebesque JV. Fast evaluation of patient setup during radiotherapy by aligning features in portal and simulator images. *Phys Med Biol* 36: 1665-1679, 1991.
17. Bissett R, Leszczynski K, Loose S, Boyko S, Dunscombe PB. Quantitative vs. subjective portal verification using digital portal images. *Int J Radiat Oncol Biol Phys* 34: 489-495, 1996.
18. Boyer AL, Antonuk L, Fenster A, Van Herk M, Meertens H, Munro P, Reinstein LE, Wong J. A review of electronic portal imaging devices (EPIDs). *Med Phys* 19: 1-16, 1992.

19. Brahme A. Dosimetric precision requirements in radiation therapy. *Acta Radiol Oncol* 23 (Fasc. 5): 379-391, 1984.
20. Byhardt RW, Cox JD, Hornburg A, Liermann G. Weekly localisation films and detection of field placement errors. *Int J Radiat Oncol Biol Phys* 4: 881-887, 1978.
21. Carter DL, Marks LB, Bentel GC. Impact of setup variability on incidental lung irradiation during tangential breast treatment. *Int J Radiat Oncol Biol Phys* 38: 109-115, 1997.
22. Chassagne DJ, Dutreix J, Dutreix A. *Report on a systematic overdosage of patients in 1970 and 1971. Internal report, Institut Gustave Roussy, Villejuif.* 1976.
23. Creutzberg CL, Althof VGM, De Hoog M, Visser AG, Huizenga H, Wijnmaalen AJ, Levendag PC. Consequences of variations in patient positioning for clinical practice. *Radiother Oncol* 32 (Suppl. 1): 117, 1994.
24. Creutzberg CL, Althof VGM, Huizenga H, Visser AG, Levendag PC. Quality assurance using portal imaging: the accuracy of patient positioning in irradiation of breast cancer. *Int J Radiat Oncol Biol Phys* 25: 529-539, 1993.
25. Creutzberg CL, Stroom JC, De Boer H, Visser AG, Quint S, Seven M, Olofsen-van Acht MJJ, Levendag PC. Improving set-up accuracy in treatment of gynaecological cancer. *Radiother Oncol* 40 (Suppl. 1): S116, 1996.
26. Creutzberg CL, Visser AG, De Porre PMZR, Meerwaldt JH, Althof VGM, Levendag PC. Accuracy of patient positioning in mantle field irradiation. *Radiother Oncol* 23: 257-264, 1992.
27. De Mol H, Van Aken H, Dom B, Meijnders P, Schaeken B, Vanregemorter J, Van den Weyngaert D. Pelvic immobilisation during irradiation of the prostate: a more accurate treatment? *Radiother Oncol* 40 (Suppl. 1): S228, 1996.

28. De Neve W, Van den Heuvel F, Coghe M, Verellen D, De Beukeleer M, Roelstraete A, De Roover P, Thon L, Storme G. Interactive use of on-line portal imaging in pelvic radiation. *Int J Radiat Oncol Biol Phys* **25**: 517-524, 1993.
29. De Neve W, Van den Heuvel F, De Beukeleer M, Coghe M, Thon L, De Roover P, Van Lancker M, Storme G. Routine clinical on-line portal imaging followed by immediate field adjustment using a tele-controlled patient couch. *Radiother Oncol* **24**: 45-54, 1992.
30. Denham JW, Dally MJ, Hunter K, Wheat J, Fahey PP, Hamilton CS. Objective decision-making following a portal film. The results of a pilot study. *Int J Radiat Oncol Biol Phys* **26**: 869-876, 1993.
31. Dunscombe PB, Fox K, Loose S, Leszczynski K. The investigation and rectification of field placement errors in the delivery of complex head and neck fields. *Int J Radiat Oncol Biol Phys* **26**: 155-161, 1993.
32. Dunscombe PB, Loose S, Leszczynski K. Sizes and sources of field placement error in routine irradiation for prostate cancer. *Radiother Oncol* **26**: 174-176, 1993.
33. Dutreix A. The third Klaas Breur Memorial Lecture, 1984. When and how can we improve precision in radiotherapy? *Radiother Oncol* **2**: 275-292, 1984.
34. El-Gayed AAH, Bel A, Vijlbrief RE, Bartelink H, Lebesque JV. Time trend of patient setup deviations during pelvic irradiation using electronic portal imaging. *Radiother Oncol* **26**: 162-171, 1993.
35. Ezz A, Munro P, Porter AT, Battista J, Jaffray DA, Fenster A, Osborne S. Daily monitoring and correction of radiation field placement using a video-based portal imaging system: a pilot study. *Int J Radiat Oncol Biol Phys* **22**: 159-165, 1992.
36. Fein DA, McGee KP, Schultheiss TE, Fowble BL, Hanks GE. Intra- and interfractional reproducibility of tangential breast fields: a prospective on-line portal imaging study. *Int J Radiat Oncol Biol Phys* **34**: 733-740, 1996.

37. Flamant R, Malaise EP, Dutreix J, Hayem M, Pierquin B, Tubiana M, Dutreix A. Un essai thérapeutique clinique sur l'irradiation des cancers amygdaliens par faisceaux de photons ou d'électrons de 20 MeV. *Eur J Cancer* 3: 169-181, 1967.
38. Gildersleve J, Dearnaley DP, Evans PM, Law M, Rawlings C, Swindell W. A randomised trial of patient repositioning during radiotherapy using a megavoltage imaging system. *Radiother Oncol* 31: 161-168, 1994.
39. Gilhuijs KGA, Drukker K, Touw A, Van de Ven PJH, Van Herk M. Interactive three dimensional inspection of patient setup in radiation therapy using digital portal images and computed tomography data. *Int J Radiat Oncol Biol Phys* 34: 873-885, 1996.
40. Gilhuijs KGA, Touw A, Van Herk M, Vijlbrief RE. Optimization of automatic portal image analysis. *Med Phys* 22: 1089-1099, 1995.
41. Gilhuijs KGA, Van Herk M. Automatic on-line inspection of patient setup from digital portal images. *Med Phys* 20: 667-677, 1993.
42. Glatstein E, Wasserman TH. Hodgkin's disease. In: Perez CA, Brady LW, eds. *Principles and practice of radiation oncology*. Ogunakadekogua: Lippincott Co, 1057-1072, 1987.
43. Goitein M. Causes and consequences of inhomogeneous dose distributions in radiation therapy. *Int J Radiat Oncol Biol Phys* 12: 701-704, 1986.
44. Goitein M, Busse J. Immobilization error: Some theoretical considerations. *Radiology* 117: 407-412, 1975.
45. Grant L, Jackson W, Isitt J. An investigation of the mantle technique. *Clin Radiol* 24: 254-262, 1973.
46. Griffiths SE, Khoury GG, Eddy A. Quality control of radiotherapy during pelvic irradiation. *Radiother Oncol* 20: 203-206, 1991.
47. Griffiths SE, Pearcey RG. The daily reproducibility of large, complex-shaped radiotherapy fields to the thorax and neck. *Clin Radiol* 37: 39-41, 1986.

48. Griffiths SE, Pearcey RG, Thorogood J. Quality control in radiotherapy: the reduction of field placement errors. *Int J Radiat Oncol Biol Phys* 13: 1583-1588, 1987.
49. Hall EJ. Time, Dose, and Fractionation in Radiotherapy. In: Hall EJ, ed. *Radiobiology for the Radiologist*. Philadelphia: J.B. Lippincott Company, 240-259, 1988.
50. Halverson KJ, Leung TC, Pellet JB, Gerber RL, Weinhaus MS, Wong JW. Study of treatment variation in the radiotherapy of head and neck tumors using a fiber-optic on-line radiotherapy imaging system. *Int J Radiat Oncol Biol Phys* 21: 1327-1336, 1991.
51. Hanley J, Mageras GS, Sun J, Kutcher GJ. The effects of out-of-plane rotations on two dimensional portal image registration in conformal radiotherapy of the prostate. *Int J Radiat Oncol Biol Phys* 33: 1331-1343, 1995.
52. Herring DF, Compton DMJ. The degree of precision required in the radiation dose delivered in cancer therapy. *Br J Radiol Suppl.* 5: 51, 1971.
53. Hess CF, Kortmann R, Jany R, Hamberger A, Bamberg M. Accuracy of field alignment in radiotherapy of head and neck cancer utilizing individualized face mask immobilization: a retrospective analysis of clinical practice. *Radiother Oncol* 34: 69-72, 1995.
54. Hoekstra CJM, Althof VGM, Te Loo HJ, Van 't Riet A, Mak ACA. Are set-up variations in bony structures equivalent with positional changes of the prostate in external radiotherapy? *Radiother Oncol* 24 (Suppl.): S45, 1992.
55. Hoekstra CJM, Levendag PC, Van Putten WLJ. Squamous cell carcinoma of the supraglottic larynx without clinically detectable lymph node metastases: problem of local relapse and influence of overall treatment time. *Int J Radiat Oncol Biol Phys* 18: 13-21, 1990.
56. Huizenga H, Levendag PC, De Porre PMZR, Visser AG. Accuracy in radiation field alignment in head and neck cancer: A prospective study. *Radiother Oncol* 11: 181-187, 1988.

57. Hulshof M, Vanuytsel L, Van den Bogaert W, Van der Schueren E. Localisation errors in mantle field irradiation for Hodgkin's disease. *Int J Radiat Oncol Biol Phys* 17: 679-683, 1989.
58. Hunt MA, Kutcher GJ, Burman CM, Fass DE, Harrison LB, Leibel SA, Fuks ZY. The effect of setup uncertainties on the treatment of nasopharynx cancer. *Int J Radiat Oncol Biol Phys* 27: 437-447, 1993.
59. Hunt MA, Schultheiss TE, Desobry GE, Hakki M, Hanks GE. An evaluation of setup uncertainties for patients treated to pelvic sites. *Int J Radiat Oncol Biol Phys* 32: 227-233, 1995.
60. International Commission on Radiation Units and Measurements. *ICRU Clinical dosimetry Report 10 d, National Bureau of Standards, Handbook 87*. Washington: 1962.
61. International Commission on Radiation Units and Measurements. *Prescribing, Recording, and Reporting Photon Beam Therapy (ICRU Report 50)*. 1993.
62. Jakobsen A, Iversen P, Gadeberg C, Lindberg Hansen J, Hjelm-Hansen M. A new system for patient fixation in radiotherapy. *Radiother Oncol* 8: 145-151, 1987.
63. Khoo VS, Dearnaley DP, Finnigan DJ, Padhani A, Tanner SF, Leach MO. Magnetic resonance imaging (MRI): considerations and applications in radiotherapy treatment planning. *Radiother Oncol* 42: 1-15, 1997.
64. Kinzie JJ, Hanks GE, Maclean CJ, Kramer S. Patterns of care study: Hodgkin's disease relapse rates and adequacy of portals. *Cancer* 52: 2223-2226, 1983.
65. Kortmann R, Hess CF, Jany R, Meisner C, Bamberg M. Reproducibility of field alignment in difficult patient positioning. *Int J Radiat Oncol Biol Phys* 29: 869-872, 1994.
66. Lebesque JV, Bel A, Bijhold J, Hart AAM. Detection of systematic patient setup errors by portal film analysis. *Radiother Oncol* 23: 198, 1992.
67. Lebesque JV, Keus RB. The simultaneous boost technique: The concept of relative normalized total dose. *Radiother Oncol* 22: 45-55, 1991.

68. Letschert JGJ, Lebesque JV, Aleman BMP, Bosset JF, Horiot JC, Bartelink H, Cionini L, Hamers JP, Leer JWH, Van Glabbeke M. The volume effect in radiation-related late small bowel complications: results of a clinical study of the EORTC Radiotherapy Cooperative Group in patients treated for rectal carcinoma. *Radiother Oncol* 32: 116-123, 1994.
69. Levendag PC, Nowak PJCM, Van der Sagen MJC, Jansen PP, Eijkenboom WMH, Planting AST, Meeuwis CA, Van Putten WLJ. Local tumor control in radiation therapy of cancers in the head and neck. *Am J Clin Oncol* 19: 469-477, 1996.
70. Levendag PC, Ravasz LA, Terhaard CHJ, Hordijk GJ. T3 squamous cell carcinoma of the larynx treated by a split-course radiation protocol. A multiinstitutional study. *Am J Clin Oncol* 16: 509-518, 1993.
71. Levendag PC, Schmitz PIM, Jansen PP, et al. Fractionated high-dose-rate brachytherapy in primary carcinoma of the nasopharynx. *J Clin Oncol* 16: 2213-2220, 1998.
72. Levendag PC, Schmitz PIM, Jansen PP, Senan S, Eijkenboom WMH, Sipkema DJ, Meeuwis CA, Kolkman-Deurloo IKK, Visser AG. Fractionated high-dose-rate and pulsed-dose-rate brachytherapy: First clinical experience in squamous cell carcinoma of the tonsillar fossa and soft palate. *Int J Radiat Oncol Biol Phys* 38: 497-506, 1997.
73. Lirette A, Pouliot J, Aubin M, Larochelle M. The role of electronic portal imaging in tangential breast irradiation: a prospective study. *Radiother Oncol* 37: 241-245, 1995.
74. Mageras GS, Kutcher GJ, Leibel SA, Zelefsky MJ, Melian E, Mohan R, Fuks ZY. A method of incorporating organ motion uncertainties into three-dimensional conformal treatment plans. *Int J Radiat Oncol Biol Phys* 35: 333-342, 1996.
75. Marks JE, Davis MK, Haus AG. Anatomic and geometric precision in radiotherapy. *Radiol Clin Biol* 43: 1-20, 1974.
76. Marks JE, Haus AG. The effect of immobilisation on localisation error in the radiotherapy of head and neck cancer. *Clin Radiol* 27: 175-177, 1976.

77. Marks JE, Haus AG, Sutton HH, Griem ML. Localisation error in the radiotherapy of Hodgkin's disease and malignant lymphoma with extended mantle fields. *Cancer* 34: 83-90, 1974.
78. Marks JE, Haus AG, Sutton HH, Griem ML. The value of frequent treatment verification films in reducing localization error in the irradiation of complex fields. *Cancer* 37: 2755-2761, 1976.
79. Meertens H, Bijhold J, Strackee J. A method for the measurement of field placement errors in digital portal images. *Phys Med Biol* 35: 299-324, 1990.
80. Meertens H, Van Herk M, Bijhold J, Bartelink H. First clinical experience with a newly developed electronic portal imaging device. *Int J Radiat Oncol Biol Phys* 18: 1173-1181, 1990.
81. Melian E, Kutcher GJ, Leibel SA, Zelefsky MJ, Baldwin B, Fuks ZY. Variation in prostate position: quantitation and implications for three-dimensional conformal radiation therapy. *Int J Radiat Oncol Biol Phys* 27 (Suppl. 1): 137 (abstract), 1993.
82. Melian E, Mageras GS, Fuks ZY, Leibel SA, Niehaus A, Lorant H, Zelefsky MJ, Baldwin B, Kutcher GJ. Variation in prostate position quantitation and implications for three-dimensional conformal treatment planning. *Int J Radiat Oncol Biol Phys* 38: 73-81, 1997.
83. Michalski JM, Graham MV, Bosch WR, Wong J, Gerber RL, Cheng A, Tinger A, Valicenti RK. Prospective clinical evaluation of an electronic portal imaging device. *Int J Radiat Oncol Biol Phys* 34: 943-951, 1996.
84. Mijnheer BJ, Battermann JJ, Wambersie A. What degree of accuracy is required and can be achieved in photon and neutron therapy? *Radiother Oncol* 8: 237-252, 1987.
85. Mitine C, Dutreix A, Van der Schueren E. Tangential breast irradiation: influence of technique of set-up on transfer errors and reproducibility. *Radiother Oncol* 22: 308-310, 1991.
86. Mitine C, Leunens G, Verstraete J, Blanckaert N, Van Dam J, Dutreix A, Van der Schueren E. Is it necessary to repeat quality control procedures for head and neck patients? *Radiother Oncol* 21: 201-210, 1991.

87. Mitine C, Van Eycken E, Nickers P, Delcoigne B, Hoornaert M, Beauduin M. Pelvic irradiation: influence of technique of set-up on the accuracy of field alignment. *Radiother Oncol* 32 (Suppl. 1): S146, 1994.
88. Munro P, Rawlinson JA, Fenster A. A digital fluoroscopic imaging device for radiotherapy localization. *Int J Radiat Oncol Biol Phys* 18: 641-649, 1990.
89. Niemierko A. Reporting and analyzing dose distributions: A concept of equivalent uniform dose. *Med Phys* 24: 103-110, 1997.
90. Okunieff P, Morgan D, Niemierko A, Suit HD. Radiation dose-response of human tumors. *Int J Radiat Oncol Biol Phys* 32: 1227-1237, 1995.
91. Perez CA, Stanley KE, Grundy G, Hanson W, Rubin P, Kramer S, Brady LW, Marks JE, Perez-Tamayo R, Brown GS, Concannon JP, Rotman M. Impact of irradiation technique and tumor extent in tumor control and survival of patients with unresectable non-oat cell carcinoma of the lung. *Cancer* 50: 1091-1099, 1982.
92. Pickett B, Roach III M, Verhey LJ, Horine P, Malfatti C, Akazawa C, Dea D, Varad B, Rathbun C, Phillips TL. The value of nonuniform margins for six-field conformal irradiation of localized prostate cancer. *Int J Radiat Oncol Biol Phys* 32: 211-218, 1995.
93. Pötter R, Haverkamp U. Quality assurance based on portal imaging in malignant lymphoma. *Proc 9th Annual Meeting of the ESTRO* 54, 1990.
94. Press WH, Flannery BP, Teukolsky SA, Vetterling WT. *Numerical recipes in C*. Cambridge: Cambridge University Press, 471-565, 1991.
95. Probst H, Griffiths S. Increasing the work speed of radiographers: the effect on the accuracy of a set-up of a complex shaped cranial field, part of a matched cranio spinal junction. *Radiother Oncol* 38: 241-245, 1996.
96. Quint S, Seven M, De Hoog M, Olofsen-van Acht MJJ, Creutzberg CL. Positioning gynaecological patients for conformal radiotherapy using vacuum mattresses. *Abstract book 4th International Workshop on Electronic Portal Imaging* 18, 1996.

97. Rabinowitz I, Broomberg J, Goitein M, McCarthy K, Leong J. Accuracy of radiation field alignment in clinical practice. *Int J Radiat Oncol Biol Phys* 11: 1857-1867, 1985.
98. Rasch C, Keus RB, Pameijer FA, Koops W, De Ru VJ, Muller S, Touw A, Bartelink H, Van Herk M, Lebesque JV. The potential impact of CT-MRI matching on tumor volume delineation in advanced head and neck cancer. *Int J Radiat Oncol Biol Phys* 39: 841-848, 1997.
99. Richards MJS, Buchler DA. Errors in reproducing pelvic radiation portals. *Int J Radiat Oncol Biol Phys* 2: 1017-1019, 1977.
100. Roach M, Pickett B, Rosenthal SA, Verhey LJ, Phillips TL. Defining treatment margins for six field conformal irradiation of localized prostate cancer. *Int J Radiat Oncol Biol Phys* 28: 267-275, 1994.
101. Roeske JC, Forman JD, Mesina CF, He T, Pelizzari CA, Fontenla E, Vijayakumar S, Chen GTY. Evaluation of changes in the size and location of the prostate, seminal vesicles, bladder, and rectum during a course of external beam radiation therapy. *Int J Radiat Oncol Biol Phys* 33: 1321-1329, 1995.
102. Rosenthal SA, Roach III M, Goldsmith BJ, Doggett EC, Pickett B, Yuo H, Soffen EM, Stern RL, Ryu JK. Immobilization improves the reproducibility of patient positioning during six-field conformal radiation therapy for prostate carcinoma. *Int J Radiat Oncol Biol Phys* 27: 921-926, 1993.
103. Shalev S. Progress in the evaluation of electronic portal imaging - Taking one step at a time. *Int J Radiat Oncol Biol Phys* 28: 1043-1045, 1994.
104. Shalev S. Treatment Verification Using Digital Imaging. In: Smith AR, ed. *Radiation Therapy Physics*. Berlin-Heidelberg: Springer-Verlag, 155-173, 1995.
105. Shalev S, Glutchev G. Decision rules for the correction of field set-up parameters. *Med Phys* 21: 952, 1994.

106. Shanahan TG, Mehta MP, Bertelrud KL, Buchler DA, Frank LE, Gehring MA, Kubsad SS, Utrie PC, Kinsella TJ. Minimization of small bowel volume within treatment fields utilizing customized "belly boards". *Int J Radiat Oncol Biol Phys* 19: 469-476, 1990.
107. Soffen EM, Hanks GE, Hwang CC, Chu JCH. Conformal static field therapy for low volume low grade prostate cancer with rigid immobilization. *Int J Radiat Oncol Biol Phys* 20: 141-146, 1991.
108. Song PY, Washington M, Vaida F, Hamilton R, Spelbring D, Wyman B, Harrison J, Chen GTY, Vijayakumar S. A comparison of four patient immobilization devices in the treatment of prostate cancer patients with three dimensional conformal radiotherapy. *Int J Radiat Oncol Biol Phys* 34: 213-219, 1996.
109. Stroom JC, De Boer JCJ, Huizenga H, Visser AG. Implementation of geometrical inaccuracies in radiotherapy treatment planning by means of coverage probability. *Int J Radiat Oncol Biol Phys* submitted: 1998.
110. Stroom JC, Quint S, Seven M, Olofsen-van Acht MJJ, De Hoog M, Creutzberg CL, De Boer H, Visser AG. The need for on-line set-up corrections of patients with gynaecological tumors. *Med Phys* 23: 1083, 1996.
111. Stroom JC, Visser AG, De Boer JCJ, Huizenga H. Use of coverage probability to quantify results of clinical positioning studies in radiotherapy planning. In: Hounsell AR, Wilkinson JM, Williams PC, eds. *Proceedings of the XIth International Conference on The Use of Computers in Radiation Therapy. 20-24 March 1994, Manchester, UK*. Manchester: Christie Hospital NHS Trust, 264-265, 1994.
112. Taylor BW, Price Mendenhall N, Million RR. Reproducibility of mantle irradiation with daily imaging films. *Int J Radiat Oncol Biol Phys* 19: 149-151, 1990.
113. Ten Haken RK, Forman JD, Heimbürger DK, Gerhardsson A, McShan DL, Perez-Tamayo C, Schoeppe SL, Lichter AS. Treatment planning issues related to prostate movement in response to differential filling of the rectum and bladder. *Int J Radiat Oncol Biol Phys* 20: 1317-1324, 1991.

114. Tinger A, Michalski JM, Bosch WR, Valicenti RK, Low DA, Myerson RJ. An analysis of intratreatment and intertreatment displacements in pelvic radiotherapy using electronic portal imaging. *Int J Radiat Oncol Biol Phys* 34: 683-690, 1996.
115. Urie MM, Goitein M, Doppke KP, Kutcher GJ, Lo-Sasso T, Mohan R, Munzenrider JE, Sontag M, Wong JW. The role of uncertainty analysis in treatment planning. *Int J Radiat Oncol Biol Phys* 21: 91-107, 1991.
116. Valicenti RK, Michalski JM, Bosch WR, Gerber R, Graham MV, Cheng A, Purdy JA, Perez CA. Is weekly port filming adequate for verifying patient position in modern radiation therapy? *Int J Radiat Oncol Biol Phys* 30: 431-438, 1994.
117. Van den Heuvel F, De Neve W, Verellen D, Coghe M, Coen V, Storme G. Clinical implementation of an objective computer-aided protocol for intervention in intra-treatment correction using electronic portal imaging. *Radiother Oncol* 35: 232-239, 1995.
118. Van Herk M, Bel A, Gilhuijs KGA, Vijlbrief RE. A comprehensive system for the analysis of portal images. *Radiother Oncol* 29: 221-229, 1993.
119. Van Herk M, Bruce A, Kroes G, Shouman T, Touw A, Lebesque JV. Quantification of organ motion during conformal radiotherapy of the prostate by three-dimensional image registration. *Int J Radiat Oncol Biol Phys* 33: 1311-1320, 1995.
120. Van Herk M, Meertens H. A matrix ionization chamber imaging device for on-line patient setup verification during radiotherapy. *Radiother Oncol* 11: 369-378, 1988.
121. Van Tienhoven G, Lanson JH, Crabeels D, Heukelom S, Mijnheer BJ. Accuracy in tangential breast treatment set-up: a portal imaging study. *Radiother Oncol* 22: 317-322, 1991.
122. Verhey LJ, Goitein M, McNulty P, Munzenrider JE, Suit HD. Precise positioning of patients for radiation therapy. *Int J Radiat Oncol Biol Phys* 8: 289-294, 1982.

123. Visser AG, Huizenga H, Althof VGM, Swanenburg BN. Performance of a prototype fluoroscopic radiotherapy imaging system. *Int J Radiat Oncol Biol Phys* 18: 43-50, 1990.
124. Visser AG, Stroom JC, De Boer JCJ, Creutzberg CL, Levendag PC, Huizenga H. Coverage probability: including effects of set-up variations or organ motion in RT treatment planning. *Radiother Oncol* 32 (Suppl. 1): S27, 1994.
125. Visser AG, Stroom JC, De Boer JCJ, Heijmen BJM. A software tool to include geometrical variations in radiotherapy planning by means of coverage probability. *Med Biol Eng Comput* 35 (Suppl. Part 2): 1068, 1997.
126. Vos PH, Bel A, Poortmans PMP, Vlaun V, Rodrigus PTR, Lebesque JV. Set-up accuracy for pelvic fields after application of a 3-D correction procedure using digital portal imaging. *Int J Radiat Oncol Biol Phys* 30 (Suppl. 1): 229, 1994.
127. Wambersie A. Quality assurance in radiation therapy with special reference to the situation in Europe. *Int J Radiat Oncol Biol Phys* 10 (Suppl. 1): 153-160, 1984.
128. Wambersie A, Dutreix J, Dutreix A. Precision dosimetrique requise en radiotherapie: conséquences concernant le choix et les performances exigées des détecteurs. *J Belge Radiol* 52: 2-11, 1969.
129. Westbrook C, Gildersleve J, Yarnold J. Quality assurance in daily treatment procedure: patient movement during tangential fields treatment. *Radiother Oncol* 22: 299-303, 1991.
130. White JE, Chen T, McCracken J, Kennedy P, Seydel HG, Hartman G, Mira J, Khan M, Durrance FY, Skinner O. The influence of radiation therapy quality control on survival, response and sites of relapse in oat cell carcinoma of the lung. *Cancer* 50: 1084-1090, 1982.
131. Wong J, Yan D, Michalski JM, Graham M, Halverson K, Harms W, Purdy J. The cumulative verification image analysis tool for offline evaluation of portal images. *Int J Radiat Oncol Biol Phys* 33: 1301-1310, 1995.

-
132. Wong JW, Binns WR, Cheng AY, Geer LY, Epstein JW, Klarmann J, Purdy JA. On-line radiotherapy imaging with an array of fiber-optic image reducers. *Int J Radiat Oncol Biol Phys* **18**: 1477-1484, 1990.
 133. Yan D, Wong J, Vicini F, Michalski JM, Pan C, Frazier A, Horwich E, Martinez A. Adaptive modification of treatment planning to minimize the deleterious effects of treatment setup errors. *Int J Radiat Oncol Biol Phys* **38**: 197-206, 1997.
 134. Yan D, Wong JW, Gustafson G, Martinez A. A new model for "accept or reject" strategies in off-line and on-line megavoltage treatment evaluation. *Int J Radiat Oncol Biol Phys* **31**: 943-952, 1995.

SUMMARY

As a result of the introduction of sophisticated techniques for radiotherapy planning and delivery, quality control of the accuracy of the daily positioning of the patient has become increasingly important. For high-precision therapy, exact patient positioning is an absolute prerequisite. Megavolt film has traditionally been used to verify the position of the patient during radiotherapy. More recently, electronic portal imaging devices (EPID) have been developed which enable fast, on-line acquisition and comparison of portal images. The development of the EPIDs and the concurrent introduction of conformal therapy have focused attention to the verification and the correction of daily patient setup. This thesis deals with the clinical introduction of portal imaging, the investigation and improvement of the accuracy of patient positioning in various treatment techniques, and the development of strategies for verification and correction of patient setup.

Chapter 1 discusses the clinical consequences that variations in patient positioning may have. Dose variations of about 5-10% over a significant part of the target volume and/or neighbouring organs at risk may have a clear impact on the tumor control probability and normal tissue complication probability. The impact of such dose variations depends, among others, on the steepness of the dose response curves for the tumor type and normal tissues involved. Underdosing in the field margins has in some studies been shown to lead to a clinically apparent decrease in local control rates and survival rates.

The series of studies on the accuracy of patient positioning started with a prospective analysis of mantle field irradiation in 13 lymphoma patients (Chapter 2). This study was carried out using megavolt films. Differences between simulation and treatment films were larger for posterior fields (with the patient positioned prone) than for anterior fields (supine position). Errors were modest as compared to reported error rates. The prone treatment position yielded larger errors than the supine position, as well as a systematic cranial shift of the patients. It was recommended that attention be paid to improving treatment accuracy in the prone position. At present, the introduction of more

sophisticated treatment units has enabled the use of the supine position for both anterior and posterior fields.

The positioning accuracy in the treatment of 31 breast cancer patients was studied using the newly developed EPID (Chapter 3), and differences between two positioning techniques were evaluated. Seventeen patients were immobilized with plastic fixation masks on a flat board, and 14 patients were positioned without a mask on either a flat or a wedge-shaped board. Comparison of these positioning techniques yielded a similar setup accuracy, while the standard deviations (SD) of the differences between simulation and megavolt images tended to be somewhat larger in positioning without a fixation mask. However, large SDs were found for field size, collimator rotation and for the position of the lung shielding block in patients positioned on the flat board. These appeared to be due to the technicians' inclination to slightly adapt the field size or rotate the collimator in order to obtain a seemingly better congruity of the field with the skin or mask markings. The wedge shaped board was preferred because of the ease of patient setup and because the use of the lung shielding block (being a source of treatment inaccuracies) is avoided. This study emphasized the importance of focusing attention to the accuracy of daily patient positioning, not only in new, sophisticated treatment techniques but also in the setups routinely used. As a result of this study, procedures for patient setup were revised and record-and-verify systems were made operational on all treatment units in our institute.

Chapter 4 comprises studies on the accuracy of patient positioning in urological and gynaecological pelvic fields. Small pelvic fields were studied in 16 patients treated for urological cancers using a CT-planned three-field isocentric technique, and large anterior and posterior parallel opposed pelvic fields were studied in 17 gynaecological cancer patients. For urological fields, random and systematic errors were shown to be larger in the cranio-caudal and ventro-dorsal directions than in the medio-lateral direction. These errors were reduced following changes in the positioning technique. In gynaecological fields, large random errors and, for the cranio-caudal direction, a systematic cranial shift of the patients were detected. The positioning technique which had been traditionally used was abandoned, and a new setup using long laser lines was tested and

found to be more accurate. Chapter 4 describes how patient positioning techniques can be optimized on the basis of portal imaging studies, resulting in the reduction of both random and systematic errors. Studies such as these can also be used to establish the level of random setup variations, to be used for the calculation of appropriate margins to take around the clinical target volume. In Chapter 4, examples are given of the calculation of margins for prostate cancer treatment, taking into account patient positioning variations as well as prostate motion. As both setup variations and prostate movements are different for the respective directions, nonuniform margins around the CTV are obtained, instead of the usual uniform margins. Such well established margins, based on actual treatment data, can then safely be used in radiotherapy planning for conformal techniques.

Usually, after optimizing a patient positioning technique, systematic variations remain that are small for some subsets of patients, but larger for others. In such cases, efforts should be directed towards an early recognition and correction of these systematic errors on an individual basis. This led to the development of verification and correction (VC) procedures. An (off-line) VC procedure was designed to determine and correct systematic setup errors in the treatment of prostate cancer, and was clinically introduced and tested in 151 patients in three radiation oncology centers (Chapter 5). During a few initial treatment fractions, portal images were obtained and the average 3D displacement vector was compared with an action level, which decreased with the number of measurements. If the length of the vector exceeded the action level, at the next treatment session an isocenter correction was applied at the treatment unit. After a correction, the VC procedure was repeated. Otherwise, weekly setup measurements were performed. The application of the procedure resulted in a major improvement of setup accuracy in all three centers. The rate of mean systematic 3D deviations > 5 mm decreased from 26-36% to 0-1.6%. The number of corrections was on average 0.7 per patient. The VC procedure was rapidly accepted by the technicians and clinicians, as 3D setup accuracy was significantly improved, while the increase in workload was modest.

In Chapter 6, the findings and conclusions of the studies are discussed and put into clinical perspective. The most recent developments in on-line and off-line

verification and correction are summarized, and reviewed together with related topics such as organ motion, the required frequency of portal imaging, the value of immobilization techniques, and the drawbacks in the introduction and application of portal imaging. Coverage probability, a concept to incorporate both the effects of systematic and random patient setup variations and organ motion uncertainties into the treatment planning, enables the calculation of dose distributions which show the clinician what target coverage and normal tissue dose realistically to expect. It is concluded that the verification of daily patient positioning is essential, both in high-precision treatments and in the routine clinical practice, and should be an integral part of (conformal) treatment protocols. Electronic portal imaging is an indispensable tool to minimize systematic and random errors, both by optimizing positioning techniques, and by the verification and correction of patient setup early in the treatment course. Verification and correction can be performed on-line (interrupting the treatment for the analysis of the portal image and, if required, a setup correction) or off-line (in which case the correction is applied at the next treatment fraction). On-line VC is more time consuming and, because of the frequent treatment interruptions, more bothersome for the patient, while its advantage is that random errors can be corrected as well. When random errors are established to be sufficiently small, off-line VC procedures are recommended to monitor treatment accuracy. On-line VC could then be selectively used in cases with large random errors.

SAMENVATTING

Door de introductie in de radiotherapie van geavanceerde bestralingsapparatuur en drie-dimensionale computer planningsystemen is het mogelijk geworden de bestralingsvelden het doelgebied zeer nauwkeurig te laten omvatten, waardoor de omgevende gezonde weefsels maximaal worden gespaard. Deze zgn. conformatie technieken worden gebruikt om de bijwerkingen van de radiotherapie te verminderen, en/of de dosis te verhogen zonder dat de kans op ernstige complicaties toeneemt, teneinde de kans op locale controle en mogelijk ook genezing te verbeteren. Bij een dergelijke techniek is een uiterst nauwkeurige positionering van de patient ten opzichte van de bestralingsbundel een absolute vereiste. Controle van de dagelijkse positionering van de patient gedurende de bestralingsserie is daarom van groot belang. Tot voor kort werden hiervoor megavoltfoto's (röntgendoorlichtingsfoto's, gemaakt met de megavolt-energie van de bestralingsbundel) gebruikt. Meer recent is electronische megavolt afbeeldingsapparatuur ontwikkeld, waarmee het mogelijk is om in enkele seconden na de start van een bestraling op een monitor een röntgendoorlichtingsbeeld te krijgen van het deel van de patient dat in het bestralingsveld ligt. Nog tijdens de bestraling kan vergelijking met de simulatiefoto (de geplande positie van de patient) plaatsvinden. De ontwikkeling van deze electronische megavolt-afbeeldingssystemen (MVA) en de gelijktijdige introductie van conformatieradiotherapie technieken hebben de aandacht gevestigd op het belang van verificatie, en waar nodig correctie, van de dagelijkse patientpositionering. Dit proefschrift bevat een aantal studies naar de daadwerkelijke nauwkeurigheid van de dagelijkse instelling van de patient voor de bestraling bij een aantal verschillende tumorsoorten en bestralingstechnieken, zoals die gebruikt werden binnen de afdeling Radiotherapie van de Daniel den Hoed Kliniek. Op basis van deze studies werden de positioneringstechnieken verbeterd en de dagelijkse variaties geminimaliseerd. Tenslotte werd een verificatie en correctie procedure geïmplementeerd om tijdens een bestralings-serie de nauwkeurigheid van de patientpositionering te optimaliseren.

In hoofdstuk 1 worden de mogelijke klinische consequenties beschreven die onnauwkeurigheden in de dagelijkse positionering van de patient kunnen hebben. Dosisvariaties van 5-10% in een belangrijk deel van het doelvolumen kunnen een

duidelijke invloed hebben op de kans op het volledig vernietigen van de tumor en/of de kans op schade aan de gezonde weefsels. Hoe groot de invloed van dergelijke dosisvariaties kan zijn, hangt onder meer af van de steilheid van de dosis-effect relatie van de betreffende tumor en omringende organen. In sommige studies is aangetoond dat onderdosering in de randen van het doelvolumen kan leiden tot een klinisch aantoonbare vermindering van de kans op lokale tumorcontrole en overleving.

De serie studies naar de nauwkeurigheid van de patientpositionering startte met een analyse van zgn. mantelveldbestralingen bij 13 patienten met de ziekte van Hodgkin (hoofdstuk 2). Deze studie werd uitgevoerd met megavoltfoto's. De verschillen tussen de simulatiefoto's (als referentiewaarde) en de megavoltfoto's bleken groter in de achtervoorwaartse (PA) velden (met de patient in buikligging) dan in de voorachterwaartse (AP) velden (met de patient in rugligging). De gevonden onnauwkeurigheden waren geringer dan in de literatuur gerapporteerde afwijkingen. In buikligging was de positionering minder nauwkeurig dan in rugligging, en werd een verplaatsing naar craniaal gevonden. Tegenwoordig is het mogelijk de patient in rugligging te positioneren voor beide bestralingsbundels, hetgeen comfortabeler is en de nauwkeurigheid van de bestraling ten goede komt.

De nauwkeurigheid van de dagelijkse positionering bij de borstsparende behandeling van 31 patienten met borstkanker werd onderzocht met behulp van het recent geïntroduceerde MVA systeem (hoofdstuk 3). Twee verschillende positionerings- en fixatietechnieken werden vergeleken. Bij 17 patienten werden plastic fixatiemaskers gebruikt die aan een platte plank op de bestralingstafel werden vastgemaakt, en 14 patienten werden zonder masker op een platte of hellende plank (zgn. wigplank) gepositioneerd. Vergelijking van deze twee technieken gaf aan dat de nauwkeurigheid ongeveer gelijk was; de standaard deviaties (SD) van de verschillen tussen de simulatie- en megavoltbeelden waren iets groter bij de positionering zonder fixatiemasker. Er bleek echter, dat er onacceptabel grote variaties gevonden werden voor de veldgrootte, de collimator hoek, en voor de positie van de afdekblokken voor de long bij de ligging op de platte plank. Deze variaties bleken te zijn veroorzaakt door de neiging op het bestralingstoestel de veldgrootte aan te passen of de collimator soms iets te

roteren, teneinde een ogenschijnlijk betere overeenkomst tussen het lichtveld van het toestel en de huidmarkeringen op de patient te bereiken. De voorkeur werd gegeven aan de wigplank vanwege het gemak van positioneren, en omdat het gebruik van een longafdekblok (zoals gebleken een bron van onnauwkeurigheden) wordt vermeden. Deze studie onderstreepte het grote belang van kwaliteitscontrole van de dagelijkse patientpositionering, niet alleen voor nieuwe of ingewikkelde technieken, maar ook voor de routinematig gebruikte technieken. Als gevolg van deze studie werden de procedures voor het instellen van de bestralingsbundel herzien, en werden verificatiesystemen op alle bestralingsapparaten aangebracht.

Hoofdstuk 4 bevat studies naar de nauwkeurigheid van patientpositionering bij de bestraling van urologische en gynaecologische bekkenvelden. Bij 16 patienten met blaas- of prostaatacarcinoom werd de nauwkeurigheid van een CT-geplande drie-velden techniek onderzocht. Grotere AP-PA bekkenvelden werden geanalyseerd bij 17 gynaecologische patienten. Bij urologische velden bleken in de cranio-caudale en dorso-ventrale richtingen grotere onnauwkeurigheden op te treden dan in de medio-laterale richting. De positioneringstechniek werd veranderd, waarna de nauwkeurigheid toenam. Bij gynaecologische patienten werden grote random variaties gevonden, alsmede systematische verschuivingen in de cranio-caudale richting. De positioneringstechniek die van oudsher bij deze patienten werd gebruikt, werd verlaten en een nieuwe techniek met lange laserlijnen werd onderzocht en nauwkeuriger bevonden. In dit hoofdstuk wordt beschreven hoe positioneringstechnieken kunnen worden verbeterd op basis van MVA-studies, waarbij zowel random als systematische verschuivingen kunnen worden verminderd. Deze studies zijn ook zeer geschikt om vast te stellen welke variaties aanwezig blijven, ook na optimalisering van de gebruikte technieken. Deze onvermijdelijke onnauwkeurigheid kan dan worden gebruikt bij het definiëren van de marges die rond het doelvolumen moeten worden aangehouden om adequate bestraling van het doelgebied te verzekeren. In hoofdstuk 4 worden voorbeelden gegeven van het berekenen van deze marges voor bestraling van prostaatkanker, waarbij zowel rekening wordt gehouden met de variaties in patientpositionering als met verschillen in ligging van de prostaat. Aangezien deze variaties niet even groot zijn voor de verschillende richtingen, worden zo specifieke, anisotrope marges rond het doelvolumen verkregen in plaats van de

gewoonlijk toegepaste uniforme marges. Dergelijke specifieke marges, gebaseerd op werkelijk gemeten variaties, kunnen dan veilig worden toegepast bij de planning voor conformatieradiotherapie.

Na het optimaliseren van positioneringstechnieken blijven er systematische verschuivingen optreden, die voor sommige patienten zeer gering zijn, maar bij andere groter. In zulke gevallen is vroegtijdige herkenning en correctie van systematische variaties op individuele basis van groot belang. Om deze reden werden verificatie en correctie (VC) procedures ontwikkeld. In hoofdstuk 5 wordt de introductie en evaluatie van een dergelijke procedure bij de behandeling van patienten met prostaatkanker beschreven. De VC procedure werd getest bij 151 patienten in drie radiotherapeutische centra. Aan het begin van de bestralingsserie werden enkele megavoltafbeeldingen gemaakt, en werd de gemiddelde 3D verplaatsing berekend. De actiedrempel voor een correctie nam af met het aantal metingen. Als de verplaatsing groter was dan de actiedrempel, werd bij de volgende behandeling een isocentrum correctie toegepast. Na een correctie werd de VC procedure herhaald; in de andere gevallen werden wekelijks afbeeldingen gemaakt. De toepassing van de VC procedure resulteerde in een sterke verbetering van de nauwkeurigheid van positionering in alle centra. Het percentage systematische verschuivingen > 5 mm nam af van 26-36% tot 0-1.6%. Gemiddeld werd 0.7 correctie per patient toegepast. De VC procedure bleek snel en gemakkelijk te worden geaccepteerd door de laboranten en clinici, aangezien de nauwkeurigheid significant verbeterde, bij een relatief beperkte toename van de werklast.

In hoofdstuk 6 worden de bevindingen en conclusies van de studies besproken en in klinisch perspectief geplaatst. Hierbij worden de meest recente ontwikkelingen in verificatie en correctie van de patientpositionering samengevat, samen met onderwerpen zoals orgaanbeweging, de frequentie van megavoltafbeeldingen, de waarde van fixatietechnieken, en de valkuilen en beperkingen bij de klinische introductie en het gebruik van MVA. De integratie van de dagelijkse variaties in de patientpositionering en de orgaanbeweging in de planning voor radiotherapie maakt het mogelijk een inschatting te maken van de werkelijk te verwachten dosisverdeling in het doelvolumen en de normale weefsels. Geconcludeerd wordt dat de verificatie van de dagelijkse patientpositionering essentieel is, zowel bij

complexe precisietechnieken als bij de meer routinematige behandelingen, en een integraal deel zou moeten uitmaken van (conformatie)radiotherapieprotocollen. MVA is onmisbaar voor het minimaliseren van systematische en random fouten, zowel door het controleren en verbeteren van positioneringstechnieken, als door de verificatie en de correctie van de patientpositionering aan het begin van de behandelingsserie. Verificatie en correctie kan tijdens de bestralingsbehandeling zelf worden verricht (waarbij de bestraling na klein deel van de dagdosis onderbroken wordt voor het analyseren van het megavoltbeeld en de eventuele correctie van de patientpositionering, zgn. on-line VC), danwel na de behandeling (waarbij een eventuele correctie wordt toegepast bij de volgende bestraling, zgn. off-line VC). On-line VC kost meer tijd op het bestralingstoestel en is, door het onderbreken en zonodig corrigeren, meer belastend voor de patient, terwijl het voordeel ervan is dat ook random fouten kunnen worden gecorrigeerd. Als aangetoond is dat de random variaties van een bestalings-techniek voldoende klein zijn, is het aan te bevelen om off-line VC procedures te gebruiken om de nauwkeurigheid van behandeling te bewaken. In situaties met grotere random variaties kan dan selectief on-line VC worden toegepast.

DANKWOORD

Dit proefschrift zou nooit tot stand zijn gekomen zonder de inspiratie, steun, inspanningen en ideeën van heel veel mensen. Ik wil jullie allen daarvoor van harte danken.

Prof. Dr. P.C. Levendag, mijn promotor: beste Peter, dank je voor mijn introductie in de MVA werkgroep, je niet aflatende vertrouwen dat dat tot dit proefschrift zou leiden, en je enorme snelheid in het lezen van concepten: zaken die maanden (te) lang schrijfwerk kostten gaf je, voorzien van bondig advies en commentaar, binnen enkele dagen terug.

Dr. A.G. Visser, mijn co-promotor: beste Andries, je was al die jaren mijn steun en toeverlaat. Je enthousiasme en grote kennis van dit onderwerp vormen een solide basis voor de MVA werkgroep. Dank voor je nimmer aflatende geduld en begeleiding en de zeer prettige samenwerking.

Vincent Althof, Joep Stroom en Hans de Boer, de project-fysici: ik heb heel veel van jullie geleerd, en de samenwerking enorm gewaardeerd. Vincent als MVA-werker "van het eerste uur": dank voor de vele discussies, je inzet voor de klinische acceptatie en de nuttige uitwisseling van fysische en klinische kennis. Joep en Hans, dank ook voor het maken van de fraaie figuren.

Marjan de Hoog en Dirk Binnenkamp: wat een uren minutieus werk hebben jullie aan het opnemen van de beelden en uitvoeren van de analyses besteed. Marjan, je grote motivatie en toewijding, en de snelheid waarmee je je alles eigen maakte hebben op mij diepe indruk gemaakt. Je inzet voor de overdracht van MVA-kennis en -ervaring naar je collega's was onmisbaar voor de klinische integratie. Dank voor al je inzet en collegialiteit.

Sandra Quint, Merik Seven, John van Sörnsen de Koste, MM50-groep, en alle andere laboranten die bij de MVA-studies betrokken waren: dank voor jullie enthousiasme en jullie inzet voor de verschillende studieprotocollen, de veranderingen in de positioneringstechnieken en de implementatie van de verificatie- en correctieprocedure. Jullie motivatie was heel consequent gericht op het belangrijkste doel: het zo goed mogelijk behandelen van de patienten.

Joos Lebesque, stimulerende kracht in het landelijke MVA-netwerk en altijd belangstellende collega: ik heb je inzichten en nuttige adviezen enorm gewaardeerd.

Van de overige mede-auteurs van de artikelen in dit proefschrift dank ik vooral Henk Huizenga voor de samenwerking in de eerdere jaren van het MVA-project, en Arjan Bel voor zijn ontwerp van de verificatie- en correctieprocedure en de samenwerking daarbij in het MVA-netwerk.

Ineke van Mierlo, Arendjan Wijnmaalen en Véronique Coen, collega's van mijn waarneemteam: dank voor alle extra uren die jullie voor mij hebben waargenomen om de voor mij zo kostbare studieverlofweken te realiseren. Jullie betrokkenheid bij het welslagen daarvan waren een grote stimulans. Ineke, jouw spontane aanbod om je 'tempel van rust aan de Maas' hiervoor beschikbaar te stellen was van onschatbare waarde. De blik op de bruggen heeft inspiratie voor vele zinnen in dit proefschrift opgeleverd: heel veel dank daarvoor.

De medewerkers van de bibliotheek, met name mevr. M. Westerhout-Kersten: heel veel dank voor het met eindeloos geduld opzoeken van relevante literatuur en het attenderen op nieuwe publicaties.

De medewerkers van de audio-visuele dienst, met name Hans Vuik: dank voor de prachtige foto's, afbeeldingen en dia's, altijd snel en meer dan op tijd.

Carolien Bayards en Inge Dijkstra: dank voor jullie ondersteuning, de hulp met alle briefjes, stukken, herzieningen, referenties, printen, kopiëren, en jullie geduld: fantastisch! Inge, heel veel dank voor het verzorgen van de lay-out.

Mijn paranimfen Manouk Olofsen en Jacoline Bromberg: dank voor de vele gezellige uren bijpraten over dit en vele andere onderwerpen, jullie 'oor' voor alle wel en wee rond dit boekje in de loop der jaren, en jullie grote vriendschap. Jacoline, nu is wel afdoende aangetoond dat het bestuderen van kindersweetvoeten naast heel veel plezier, ook een solide wetenschappelijke basis geeft.

Mijn moeder: een beter voorbeeld van de succesvolle combinatie van liefdevol, creatief en stimulerend moederschap met eigen werk, identiteit en ontplooiing kan niemand zich wensen. Wat ben ik je daar dankbaar voor. Je grote steun en trouw bij het voor mij mogelijk maken van deze uitdagende, rijke en soms uitputtende combinatie is niet te beschrijven.

Rutger, Doortje en Paul: gelukkig is de 'last' van dit boekje voor jullie beperkt gebleven. De tijd met jullie is daar veel te kostbaar voor. Jullie zijn het geluk in mijn leven.

CURRICULUM VITAE

Carien Creutzberg werd op 11 maart 1961 geboren in Leiderdorp. In 1979 behaalde zij het VWO diploma aan het Haags Montessori Lyceum, waarna zij de studie Geneeskunde begon aan de Rijksuniversiteit Leiden. Tijdens die studie deed zij in 1982 een keuzepracticum Dermatologie in Londen ("sweat production in children's feet"), en in 1985 een co-assistentenschap Dermatologie en een stage Kindergeneeskunde in Londen. Van december 1982 tot juni 1985 was zij als student-assistent bij de vakgroep Endocrinologie van het Academisch Ziekenhuis Leiden betrokken bij onderzoek naar de behandelingsresultaten van het schildklier carcinoom (Dr B.M. Goslings, Dr L.D.J.M. Schelfhout). In 1987 behaalde zij haar artsexamen (cum laude).

Van februari 1987 tot oktober 1988 werkte zij als arts-assistent Chirurgie in het Bergwegziekenhuis te Rotterdam (Dr J.W. Merkelbach). Daarna volgde zij de opleiding tot radiotherapeut-oncoloog in de Daniel den Hoed Kliniek te Rotterdam. De vrije stage, met als onderwerp Palliative Medicine, volgde zij in Trinity Hospice te Londen (Dr G.B. Field).

In augustus 1993 werd de specialistenopleiding afgerond en sindsdien is zij werkzaam als staf lid radiotherapeut-oncoloog in de Daniel den Hoed Kliniek. Vanaf 1989 maakt zij deel uit van de projectgroep Megavolt afbeeldingen, in het kader waarvan de studies tot stand kwamen die resulteerden in dit proefschrift. Zij is getrouwd met Rutger Klei en is moeder van Dorine (1993) en Paul (1995).

